CRITICAL EVALUATION OF ITALIAN STRONG MOTION DATA AND COMPARISON TO NGA GROUND MOTION PREDICTION EQUATIONS

JONATHAN P. STEWART

UNIVERSITY OF CALIFORNIA, LOS ANGELES
DEPARTMENT OF CIVIL & ENVIRONMENTAL ENGINEERING

GIUSEPPE SCASSERRA, GIUSEPPE LANZO, AND
FABRIZIO MOLLAIOLI

UNIVERSITÀ DI ROMA LA SAPIENZA
DIPARTIMENTO DI INGEGNERIA STRUTTURALE E GEOTECNICA

PAOLO BAZZURRO

AIR WORLDWIDE CORPORATION
SAN FRANCISCO, CALIFORNIA

CRITICAL EVALUATION OF ITALIAN STRONG MOTION DATA AND COMPARISON TO NGA GROUND MOTION PREDICTION EQUATIONS

Jonathan P. Stewart

Department of Civil and Environmental Engineering

University of California, Los Angeles

Giuseppe scasserra, Giuseppe Lanzo, and Fabrizio Mollaioli

Università di Roma La Sapienza

Dipartimento di Ingegneria Strutturale e Geotecnica

and

Paolo Bazzurro

Air Worldwide Corp.

San Francisco, CA

ABSTRACT

We describe an Italian database of strong ground motion recordings and databanks delineating conditions at the instrument sites and characteristics of the seismic sources. The strong motion database consists of 236 corrected recordings from 86 earthquakes and 101 recording stations. Uncorrected recordings were drawn from public web sites and were processed on a record-by-record basis using a procedure utilized in the Next-Generation Attenuation (NGA) project to remove instrument resonances, minimize noise effects through low- and high-pass filtering, and baseline correction. The number of available uncorrected recordings was reduced by 52% (mostly because of s-triggers) to arrive at the 236 recordings in the database. The site databank includes for every recording site the surface geology, a measurement or estimate of average shear wave velocity in the upper 30 m (V_{s30}), and information on instrument housing. Of the 86 sites, 39 have on-site velocity measurements (17 of which were performed as part of this study using SASW techniques). For remaining sites, we estimate V_{s30} based on measurements on similar geologic conditions where available. Where no local velocity measurements are available, correlations with surface geology are used. Source parameters are drawn from databases maintained (and recently updated) by Istituto Nazionale di Geofisica e Vulcanologia and include hypocenter location and magnitude for small events (M < ~5.5) and finite source parameters for larger events.

Ground motion prediction equations (GMPEs) have recently been developed in NGA project that are intended for application to shallow crustal earthquakes in tectonically active regions. We investigate the compatibility of those models with respect to magnitude-, distance-, and site-scaling implied by Italian strong motion data. This is of interest because (1) the Italian data is principally from earthquakes in extensional regions that are poorly represented in the NGA dataset and (2) past practice in Italy has been to use local GMPEs based on limited data sets which cannot resolve many source, path, and site effects known to be significant. We find that the magnitude scaling implied by the Italian data is compatible with the NGA relations. However, the Italian data attenuate faster than implied by the NGA GMPEs at short periods, and the differences are statistically significant for three of four relations. Three regression coefficients are re-evaluated for the three affected NGA GMPEs to reflect the faster attenuation; a constant term, a geometric spreading and anelastic attenuation term, and a source depth term. The scaling of ground motion with respect to site shear wave velocity is consistent between the

NGA models and Italian data. Moreover, the presence of nonlinearity in the Italian data is confirmed and found to be generally compatible with what is provided by NGA site terms. The scatter of Italian data is much higher than in the NGA models, although only the intra-event error is sufficiently well established by the data to justify modification of NGA models. On the basis of these findings, we recommend that NGA relations, with the aforementioned minor modifications, be used to evaluate median ground motions for seismic hazard analysis in Italy.

ACKNOWLEDGMENTS

CONTENTS

LIST OF FIGURES

LIST OF TABLES

1 Introduction

1.1 MOTIVATION AND SCOPE

The characterization of earthquake ground motions for engineering applications generally involves the use of empirical models referred to as ground motion prediction equations (GMPEs) or attenuation relations. GMPEs describe the variation of particular intensity measures (such as peak acceleration, spectral acceleration, or duration) with magnitude, site-source distance, site condition, and other parameters.

Because most GMPEs are empirical, they are dependent on the databases utilized in their development. The development of GMPEs requires a database of strong motion accelerograms and their intensity measures, a databank of site conditions for accelerometers, and a databank of earthquake source parameters.

In Italy there has been a strong preference towards the use of local GMPEs derived solely from data in that region. The current national hazard map for Italy (Working Group, 2004) was developed using slightly modified versions of an Italian GMPEs (Sabetta and Pugliese, 1996), a European GMPE (Ambraseys et al., 1996), and GMPEs for particular regions within Italy (e.g., Malagnini and Montaldo, 2004). These relations are based on relatively small databases – for example the Sabetta and Pugliese (1996) GMPE was derived from an Italian database of 95 recordings from 17 earthquakes. Local databases such as this are naturally smaller than world-wide databases, meaning that error in individual data points have greater influence on the GMPE.

Many of these local European GMPEs suffer from other deficiencies as well. Because of the small size of the European database, earthquake effects that are well established in other areas are not represented in the European models. A prominent example of this is nonlinear site effects, which are well known to be particularly significant for soft soils at levels of ground motion with peak accelerations stronger than about 0.2 g (e.g., Choi and Stewart, 2005). European models use a linear site term, which is established from relatively weak motion data (i.e., average site-source distances that are relatively large). Since engineering design often involves relatively small site-source distances and strong levels of ground motion, application of those linear site terms for engineering design is expected to introduce significant levels of overconservatism. This is but one example of the types of problems encountered with current European GMPEs that can be addressed through a careful analysis of the data. Many other specific effects are described in the chapters that follow, especially Chapter 4.

The scope of this project involved two principal tasks. The first task concerned clean up and enhancement of the strong motion database and related metadata for Italian earthquakes. Our goal was to bring the Italian strong motion database and the site and source databanks to standards comparable to those established during the Next Generation Attenuation (NGA) project in California. That work is described in Chapter 2 of this report. The resulting database is freely accessible via the web. Chapter 3 describes the organization of the web site.

The second principal task involved analysis of the data relative to the NGA GMPEs, which is described in Chapter 4. Our goal was to evaluate whether the magnitude-scaling, distance-scaling, and site effects implied by the Italian data are consistent with the respective aspects of the NGA models. This then allows us to define the over-arching project vision. Those aspects of the NGA models found to be consistent with the Italian data are retained for use in

Italy, while any aspects found to be deficient are corrected relative to the Italian data. In this way, modified GMPEs applicable to Italy are developed. This is extremely useful, because many of the relatively sophisticated source-, path-, and site effects inherent to the NGA models can then be applied with confidence for the Italian region.

1.2   PROJECT ORGANIZATION

This was a highly collaborative project involving U.S. and Italian investigators from multiple institutions. The work described here represents the principal findings of the doctoral research of the second author, who worked under the technical direction of the first author. The data collection involved assistance from many individuals, as noted in the Acknowledgments. In particular, the strong motion data processing was performed under the direction of Dr. Walter Silva at Pacific Engineering and Analysis, who also performed the data processing for the NGA project. Secondly, site-specific shear wave velocity profiling was performed by Dr. Robert Kayen of USGS in collaboration with the first and second authors. That work is described in detail in Kayen et al. (2008) and in Chapter 2.

The data analysis described in Chapter 4 benefitted significantly from technical discussions between the first author and numerous individuals with related expertise, such as Brian Chiou, Robert Graves, and Julian Bommer.

2 Database for Earthquake Strong Motion Studies in Italy

2.1 INTRODUCTION

The characterization of earthquake ground motions for engineering applications generally involves the use of empirical models referred to as ground motion prediction equations (GMPEs) or attenuation relations. GMPEs describe the variation of particular intensity measures (such as peak acceleration, spectral acceleration, or duration) with magnitude, site-source distance, site condition, and other parameters. A review of GMPEs for peak acceleration and spectral acceleration available in the literature prior to 2006 is presented by Douglas (2003a, 2006). The most recent GMPEs for crustal earthquakes in active regions were developed as part of the Next Generation Attenuation (NGA) project (http://peer.berkeley.edu/products/nga_project.html).

Because most GMPEs are empirical, they are dependent on the databases utilized in their development. The development of GMPEs requires a database of strong motion accelerograms and their intensity measures, a databank of site conditions for accelerometers, and a databank of earthquake source parameters. Most of the available GMPEs utilize *inconsistent* databases and databanks, in the sense that the data are derived from different sources of variable quality. One of the major thrusts of the NGA project was to compile consistent strong motion, site, and source databases for the development of GMPEs applicable to shallow crustal earthquakes in tectonically active regions. This consistency took the form, for example, of consistent

processing of all recordings, classification of geologic site conditions in uniform formats, and the compilation of source parameters developed in a uniform format by a single agency.

The NGA GMPEs (Abrahamson and Silva, 2008; Boore and Atkinson, 2008; Campbell and Bozorgnia, 2008; Chiou and Youngs, 2008; Idriss, 2008) are intended to be applicable to geographically diverse regions – the only constraint being that the region is tectonically active and the earthquake hypocentral depth is relatively shallow. The database involved is therefore large, consisting of 3551 recordings from 173 earthquakes (Chiou et al., 2008). In some regions, there has been a preference towards the use of local GMPEs derived solely from data in that region. This practice has been particularly common in Europe (Bommer, 2006), with Italy and Greece being prominent examples. The current national hazard map for Italy (Working Group, 2004) was developed using slightly modified versions of an Italian GMPEs (Sabetta and Pugliese, 1996), a European GMPE (Ambraseys et al., 1996), and GMPEs for particular regions within Italy (e.g., Malagnini and Montaldo, 2004). These relations are based on relatively small databases – for example the Sabetta and Pugliese (1996) GMPE was derived from an Italian database of 95 recordings from 17 earthquakes. Local databases such as this are naturally smaller than world-wide databases, meaning that error in individual data points have greater influence on the GMPE.

A second major application of ground motion databases linked to site/source databanks (beyond the development of GMPEs) is for dynamic analyses of structural and geotechnical systems. Major recent research efforts have been directed towards providing guidance on ground motion selection and scaling (Goulet et al., 2008) – the ground motion database utilized in those studies is generally the NGA database described by Chiou et al. (2008). In Italy, dynamic analysis and design using accelerograms has been allowed for civil infrastructure since 2003

6

(OPCM 3274, 2003), although a recent seismic code (NTC, 2007) specifically requires the use of natural recordings in lieu of synthetic motions for geotechnical applications. There is an urgent need for a database/databank to facilitate such ground motion selection in Italy.

In this chapter, we critically examine the data resources available for the Italian region with respect to the above three attributes: ground motion, site, and source. We also describe the results of recent work to enhance the breadth, quality, and consistency of the strong motion database and site and source databanks. Our focus is the database itself, not the development or validation of GMPEs for Italy nor ground motion selection and scaling procedures.

2.2   STRONG MOTION DATABASE

The first large Italian accelerometer network was installed starting from the mid-1970s by ENEL (Ente Nazionale Energia Elettrica). The array, acquired and developed by the Civil Protection Department (DPC: www.protezionecivile.it) since 1998, is now defined as RAN (Rete Accelerometrica Italiana). Of the 298 RAN accelerometers, 130 are analogue (i.e., Kinemetrics SMA-1 or RFT250) and the others are relatively modern digital instruments (i.e., Kinemetrics Altus ETNA, Altus Everest). Over time, the RAN analogue instruments are being replaced with digital instruments, with the goal being a fully digital network. Other than RAN, additional, relatively small arrays are operated by various agencies including a research institute (Ente Nazionale Energia Ambiente, ENEA) and the University of Trieste.

Despite the increasing prevalence of digital instruments, most of the available strong motion recordings are from older analogue instruments. Noise can significantly affect these recordings (especially analogue) and limit their usable bandwidth, and data processing in the presence of this noise can significantly affect ground motion intensity measures evaluated from waveforms. Potential sources of noise and other errors in analogue recordings include

7

digitization noise, incorrect baseline, instrument resonance, and unknown initial conditions associated with unrecorded first arrivals of seismic waves (e.g., Boore and Bommer, 2005). Many of these noise sources are significantly reduced for digital instruments, but noise is still present and the useable bandwidth is finite. Hence, it is vital that consistent, rational protocols be employed during digitization, filtering, and baseline correction of recordings so that the processed signal is as reliable as possible, at least within a defined frequency range. Lacking such uniform procedures, the resulting signals have unknown, and inconsistent levels of noise affecting the supposedly "corrected" signals.

Italian strong motion recordings can be found from a number of online sources and on compacts disks. Perhaps the most widely recognized source is the European Strong Motion Database ESD (Ambraseys et al., 2004; http://www.isesd.cv.ic.ac.uk/), which includes Italian data from ENEA, University of Trieste, and ENEL. Processed records by ESD are high-pass filtered at corner frequencies that are selected on a record-by-record basis, but a single low-pass corner frequency of 25 Hz is applied to all records. Another unpublished source of data was developed by SSN (Servizio Sismico Nazionale) and ENEA (Paciello et al., 1997) and contains ENEA and ENEL recordings that were processed by filtering using high-pass and low-pass corner frequencies selected on a record-by-record basis so as to optimize signal-to-noise ratio (Rinaldis, 2004). Since the formation of RAN, data from major earthquakes in Italy (namely, 1997-1998 Umbria-Marche and 2002 Molise seismic sequences) are distributed by CDROMs published by SSN (2002) and DPC (2004). All of the available data (except University of Trieste stations) has recently been assembled by INGV and DPC (Working Group S6, 2007), who also re-processed the data according to a procedure that included baseline correction, instrument

correction (for analogue signals), and record-by-record filtering (although a consistent low pass filter was applied at 25-30 Hz for all analogue instruments).

For this study, a total of 509 uncorrected (but digitized) 3-component recordings from 100 earthquakes with magnitude > 3.7 and 160 different recording stations were downloaded in March 2005. Those data are derived from the ESD database for events from 1972 to 1998 (479 three-component recordings) and from DPC (2004) for recordings of the 2002 Molise seismic sequence from the RAN array (30 three-component recordings). Our database is comprised solely of data that was available from the aforementioned sources in March 2005.

The downloaded data were then processed in 2005 by the same seismologists responsible for the NGA data processing (Dr. Walter Silva and colleagues). This was done so that the Italian strong motion data set would be compatible with the NGA data in terms of data quality and in the definitions of usable bandwidth on a record-by-record basis. This processing was performed on uncorrected (Volume 1) data and included filtering (including instrument corrections), integration of accelerograms to velocity and displacement histories, and baseline correction according to procedures described by Darragh et al. (2004). Pseudo-acceleration response spectral ordinates at 5% damping were also computed.

This processing reduced the size of the usable database to 236 recordings from 86 earthquakes and 101 different recording sites. Figure 2.1 shows the distribution of the recording sites. This reduction of the number of recordings (by 52%) relative to the uncorrected data results from delayed triggering of analogue instruments during shaking associated with shear waves (referred to as S-triggers). Figure 2.2 shows an example of an S-triggered record from the 1997 Umbria-Marche earthquake. As shown by Douglas (2003b), such records can have biased response spectral accelerations, and hence it is preferred to exclude such records.

9

Figure 2.1. Spatial distribution of recording stations included in the database
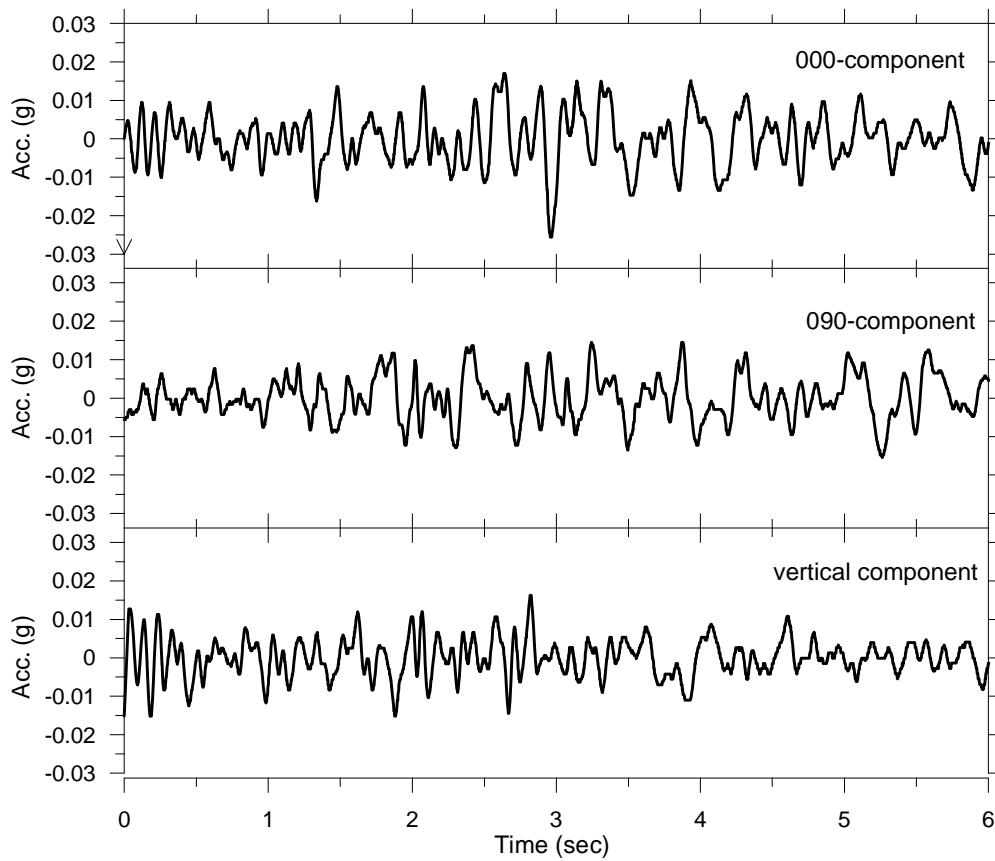
Figure 2.2. Example of S-triggered strong motion recording, Cascia station from 1997 Umbria-Marche earthquake

In Figures 2.3-2.6 we compare several recordings processed as part of this study (labeled as "PEER") to the processed records from the ESD database. Figure 2.3 shows an example of "wobble" of the displacement history from the processed ESD data. The differences in baseline correction do not significantly affect peak acceleration, but produce noticeable differences in peak velocity and displacement, which represent intensity measures sensitive to longer-period components of the waveform. Figure 2.4 shows Fourier amplitude spectra and 5%-damped pseudo acceleration response spectra for these same recordings. The Fourier spectra show similar amplitudes across the frequency range of 1-15 Hz. At higher frequencies, the PEER amplitudes generally exceed those from ESD due to a higher Nyquist frequency (100 Hz for PEER versus 25 Hz for ESD). However, these differences occur at relatively low values of Fourier amplitude ($<$ 10^{-4} g×sec), and do not significantly affect intensity measures of typical engineering interest such as peak quantities (acceleration, velocity, displacement) or spectral accelerations. On the other hand, at lower frequencies, the PEER amplitudes are significantly smaller than ESD due to differences in baseline correction and high-pass filtering, and the effected Fourier amplitudes are relatively large (approximately 10^{-3} g×sec). Those differences in the low frequency components of the waveform result in different values of peak velocity and displacement (Figure 2.3) and spectral acceleration for periods $T > 0.8$ sec. Because the ESD waveform is richer in low-frequency energy, the long-period spectral accelerations are higher for ESD than for PEER processing. Akkar and Bommer (2007) had similar observations regarding ESD data processing to those noted above.
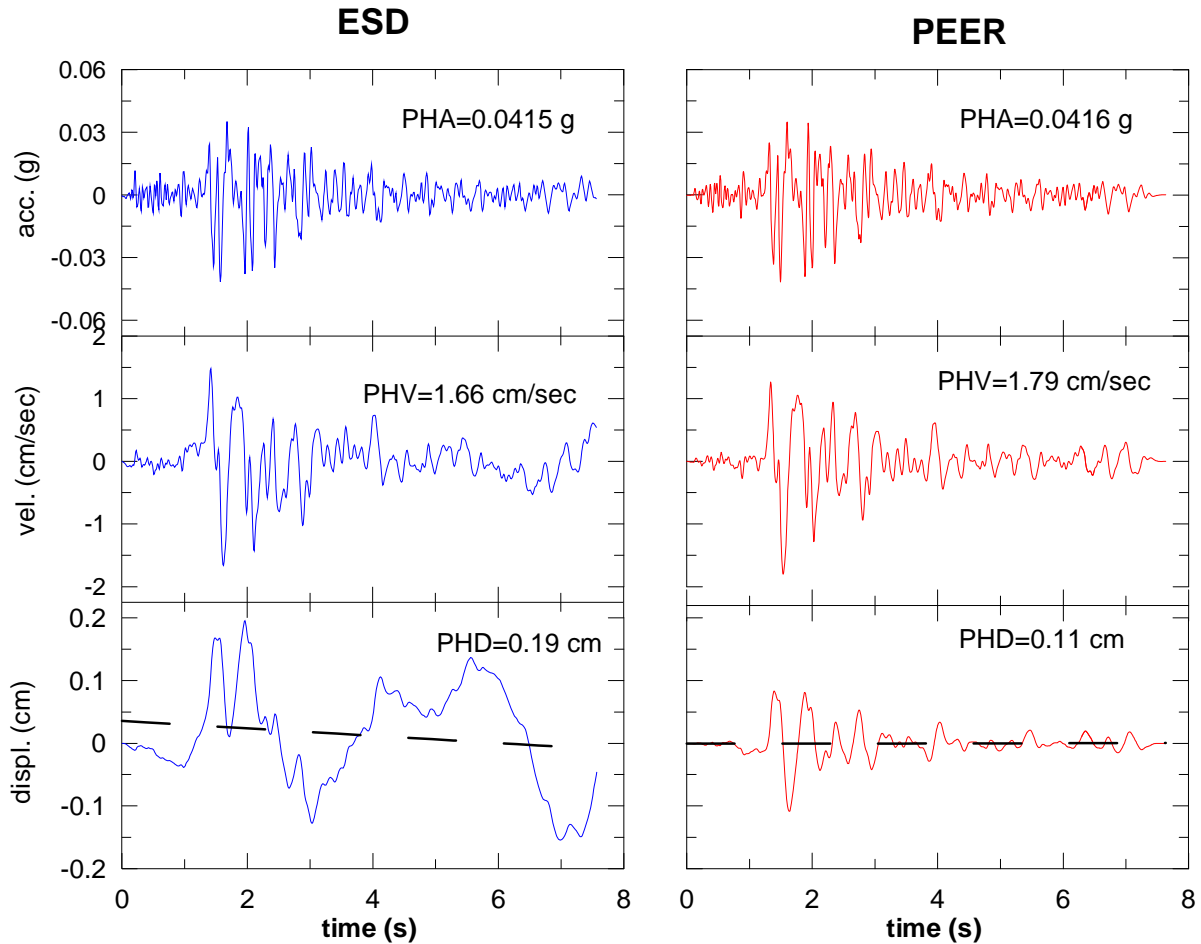
Figure 2.3. Comparison between ESD- and PEER-corrected waveforms using accelerometer recording at the Genio Civile station during the 1972 M_L=4.7 Ancona earthquake

Some of the uncorrected data contain multiple events within the acceleration histories. Waveforms from secondary events were generally removed in the PEER processing but were retained in ESD processing. This situation is evident in recordings of the M_w=6.9 1980 Irpinia Mainshock, as shown in Figure 2.5. It is not clear that the second event in the ESD data affected amplitude-related parameters (PHV, PHD, spectral acceleration) beyond the previously noted effects related to low-frequency energy content. However, the duration is clearly affected.
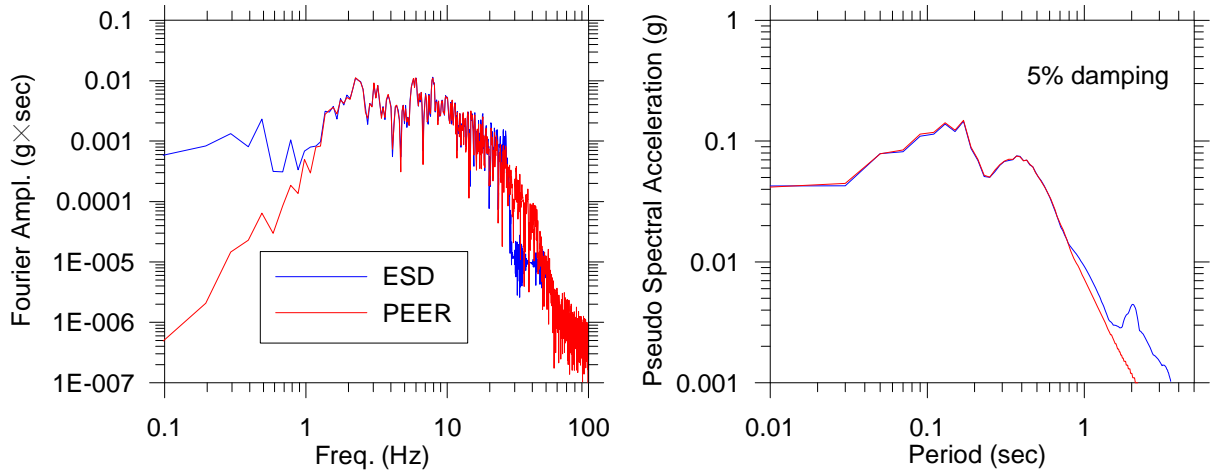
Figure 2.4. Comparison between Fourier and pseudo acceleration response spectra calculated from ESD- and PEER-corrected accelerograms using data from the Genio Civile station during the 1972 M_L=4.7 Ancona earthquake
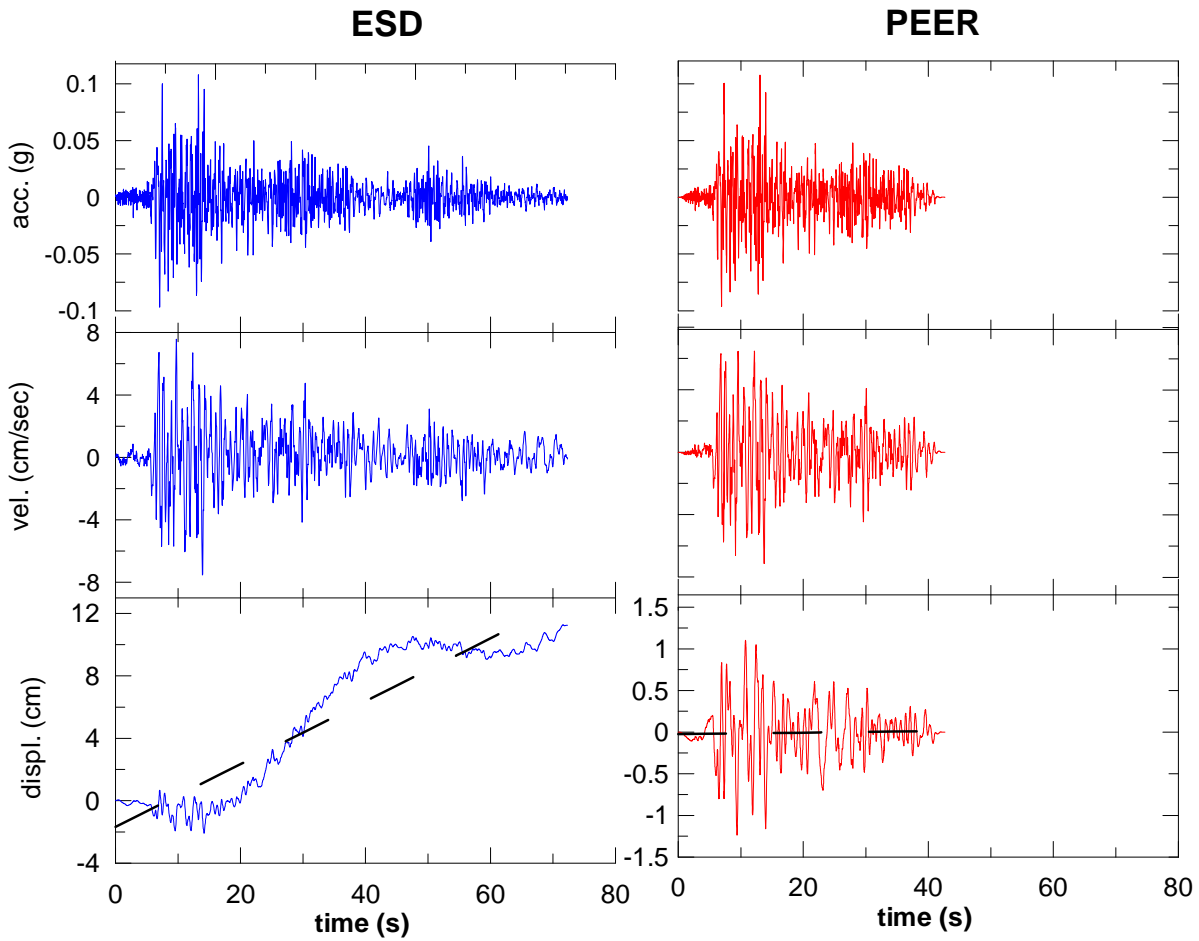
Figure 2.5. Comparison between ESD- and PEER-corrected waveforms using accelerometer recording at the Mercato Sanseverino station during the 1980 M_w=6.9 Irpinia earthquake. The uncorrected data and ESD processed data are interpreted to contain multiple triggering events.
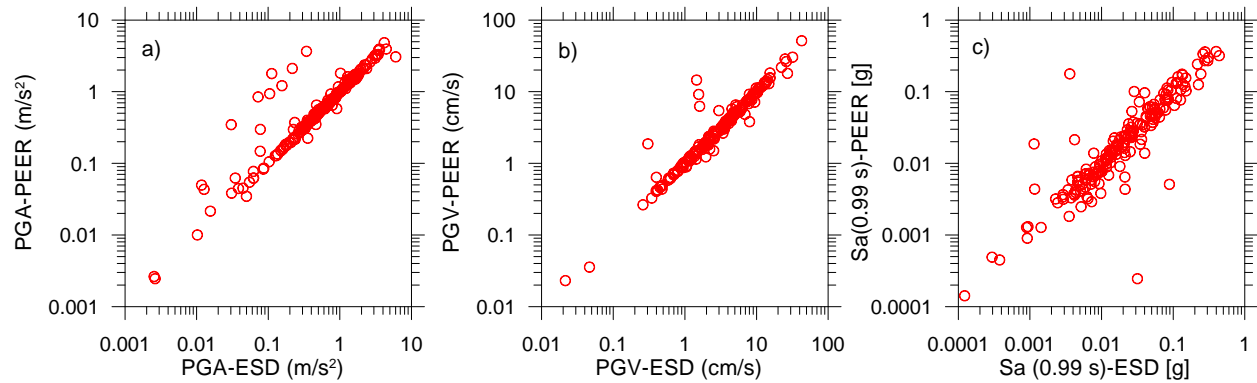
Figure 2.6. Comparison of ground motion intensity measures for corrected records in the ESD and PEER databases. The intensity measures that are compared are (a) peak acceleration, (b) peak velocity, and (c) spectral acceleration at 0.99 sec

To evaluate potential for bias between the two datasets, we compare intensity measures calculated using the ESD and PEER databases in Figure 2.6. Peak accelerations and velocities are generally comparable. The scatter in peak displacements is larger, with values from ESD mostly exceeding those from PEER.

2.3   SITE DATABANK

Attributes of the recording sites that are important for the development of GMPEs and ground motion selection include the geotechnical site conditions and the instrument housing. These attributes are discussed in the following sub-sections. The site databank compiled for this study is for Italian strong motion stations that have produced the 236 recordings referenced in the previous section (98 sites) plus selected additional sites that have been characterized but had s-triggered accelerograms. The total number of sites in the databank is 104.

2.3.1   Geotechnical Site Characterization for GMPEs: General Considerations

Wave propagation theory suggests that ground motion amplitude should depend on the density and shear wave velocity of near-surface media (e.g., Bullen, 1965; Aki and Richards, 1980). Density has relatively little variation with depth, and so shear wave velocity is the logical choice

14

for representing site conditions. Two methods have been proposed for representing depth-dependent velocity profiles with a single representative value. The first takes the velocity over the depth range corresponding to one-quarter wavelength of the period of interest (Joyner et al., 1981), which produces frequency-dependent values. A practical problem with the quarter wavelength V_s parameter is that the associated depths are often deeper than can economically be reached with boreholes. A practical alternative is the average shear wave velocity in the upper 30 m of the site (V_{s30}), which has found widespread application.

Based on empirical studies by Borcherdt and Glassmoyer (1994), Borcherdt (1994) recommended V_{s30} as a means of classifying sites for building codes, and similar site categories were selected for the NEHRP seismic design provisions for new buildings (Dobry et al., 2000). GMPEs have since been developed that incorporate V_{s30} as the site parameter, including each of the NGA GMPEs except Idriss (2008). To develop those GMPEs, each site in the NGA database was assigned a V_{s30} value, with approximately 1/3 coming from on-site measurements and 2/3 coming from correlations with other, more readily available site information.

In the development of the NGA database, protocols were followed for estimating V_{s30} when on-site measurements (extending to a depth of at least 20 m) are not available. Those protocols are as follows (Borcherdt, 2002):

1. Velocity estimated based on nearby measurements on same geologic formation (site conditions verified based on site visit by geologist).

2. Velocity estimated based on measurements on same geologic unit at site judged to have similar characteristics based on site visit by geologist.

3. Velocity estimated based on average shear wave velocity for the local geologic unit; presence of the unit verified based on site visit by geologist.

4. Velocity estimated based on average shear wave velocity for the geologic unit as evaluated from large-scale geologic map (1:24,000 to 1:100,000).

5. Velocity estimated based on average shear wave velocity for the geologic unit as evaluated from small-scale geologic map (1:250,000 to 1:750,000).

We adopt similar procedures for estimation of V_{s30} values at Italian strong motion stations with the results given in Table 2.1. Each site has been assigned V_{s30} value in the table along with an index pertaining to how the value was derived. Those indices are defined as:

- Category A: Velocity measured on-site using cross-hole, down-hole, or spectral analysis of surface wave methods;

- Category B: Velocity estimated based on nearby measurements on same geologic formation (site conditions verified based on site visit by geologist). This is similar to Categories (1)-(2) by Borcherdt (2002).

- Category C: Velocity estimated based on measurements from the same geologic unit as that present at the site (based on local geologic map). This is similar to Categories (2)-(3) by Borcherdt (2002).

- Category D: Velocity estimated based on general (non-local) correlation relationships between mean shear wave velocity and surface geology.

The following three sections describe how velocities were assigned to strong motion sites. As described in the next section, for 36 sites, velocity profiles from the literature and the files of practicing engineers, geologists, and public agencies are used to assign V_{s30} values that are assigned as Categories A, B, or C. We then describe velocity profiling performed for 17 additional sites as part of this study (Category A). Next, we describe how V_{s30} values are assigned on the basis of surface geology for the remaining 51 sites.

Table 2.1. Data on geologic condition, seismic velocity, and instrument housing at selected Italian strong motion recording sites

	Station				Geology					V$_{s30}$ (m/sec)						Housing
#	Name	Agency	Latitude	Longitude	Age	Description	Scale (plan/section)	Wills-Clahan class.	Our class.	Source (1)	Type	Measured	Estimated	Preferred	Reference	(2)
1	Ancona-Palombina	ENEA	43.602	13.474	Pleistocene	clay with silt and sand	1:50000 / 1:2000	QT		A	CH	256	455	256	Woking group (1981)	SB
2	Ancona-Rocca	ENEA	43.621	13.513	Miocene	marls	1:50000 / 1:2000		Tm	A	CH	549	600	549	Woking group (1981)	SB
3	Aquilpark-Citta	DPC	42.346	13.401	Pleistocene	coarse alluvium	local	QT		C			455	455		FF
4	Aquilpark-Galleria	DPC	42.346	13.401	Pleistocene	coarse alluvium	local	QT		C			455	455		T
5	Aquilpark-Parcheggio	DPC	42.346	13.401	Pleistocene	coarse alluvium	local	QT		C			455	455		SB
6	Arienzo	DPC	41.027	14.469	Pleistocene	cinerities, piroclastic and conid material (5m), campanian ignimbrite, overlying limstones of campano-lucana platform	1:50000 / 1:2000		Mv	A	CH	905	1000	905	Palazzo (1991)	CA
7	Assergi	DPC	42.42	13.52	Terziario	sandy clay and marls	1:50000 / 1:2000		Tm	C			600	600		CA
8	Assisi-Stallone	DPC	43.075	12.607	Cretacico	limestone and marls	1:50000 / 1:2000		Ml	C			1000	1000		SB
9	Atina	ENEA	41.620	13.801	Giurassico	dolomitic limestone	1:50000 / 1:2000		Ml	C			1000	1000		CA
10	Atina-Pretura Piano Terra	ENEA	41.645	13.783	Miocene	clay and clay with marls with layers of gray and yellow sandstone	1:50000 / 1:2000		Tm	C			600	600		SB
11	Atina-Pretura Terrazza	ENEA	41.645	13.783	Miocene	clay and clay with marls with layers of gray and yellow sandstone	1:50000 / 1:2000		Tm	C			600	600		SB
12	Auletta	DPC	40.556	15.395	Pliocene	lacustrine and deltaic polygenic conglomerate with sandy-clay cement	1:50000 / 1:2000		Pc	A	CH	1156	1000	1156	Palazzo (1991)	CA
13	Avezzano	DPC	42.03	13.43	Quaternario	Alluvium	1:100000	Qal,deep		B	CH	120	280	120	A.G.I. (1991)	CA
14	Bagnoli-Irpino	DPC	40.831	15.068	Cretacico	limestone	1:50000 / 1:2000		Ml	A	CH	1163	1000	1163	Palazzo (1991)	CA
15	Barcis	DPC	46.187	12.554	Olocene	debris on marls	1:50000 / 1:2000	Qal,coarse		D			354	354		CA
16	Barga	DPC	44.068	10.461	Pleistocene	coarse non cemented alluvium deposit on gravel and conglomerate	1:50000 / 1:2000	Qoa		D			387	387		CA
17	Bevagna	DPC	42.932	12.611	Olocene	clay, clay/sand and sand deposit on "bisciaro"	1:50000 / 1:2000	Qal,deep		A	SASW	182	280	182	This study	CA
18	Bisaccia	DPC	41.010	15.376	Pliocene	cemented conglomerate with sandy thin layers	1:50000 / 1:2000		Pc	A	CH	972	1000	972	Palazzo (1991)	CA
19	Borgo-Cerreto Torre	ENEA	42.814	12.915	Terziario	limestone	1:50000 / 1:2000		Ml	C			1000	1000		SB
20	Bovino	DPC	41.249	15.342	Pliocene	sand and sandstone with conglomerate and sandy clay	1:50000 / 1:2000	QT		A	CH	356	455	356	Palazzo (1991)	CA
21	Brienza	DPC	40.472	15.634	Olocene	recent alluvium on red flysch	1:50000 / 1:2000	Qal,coarse		A	CH	516	354	516	Palazzo (1991)	CA
22	Buia	ENEA	46.222	13.090	Olocene	alternance of gravels and pebbles, mix of gravely sand and silty sand	1:50000 / 1:2000	Qal,coarse		A	CH	254	354	254	Fontanive et al. (1985)	CA
23	Cairano 1	DPC	40.890	15.296	Pliocene	marls	1:50000 / 1:2000		Tm	C		625	600	625	Faccioli (1992)	CA
24	Cairano 2	DPC	40.887	15.312	Pliocene	marls	1:50000 / 1:2000		Tm	C		625	600	625	Faccioli (1992)	CA
25	Cairano 3	DPC	40.887	15.334	Pliocene	marls	1:50000 / 1:2000		Tm	C		625	600	625	Faccioli (1992)	CA
26	Cairano 4	DPC	40.886	15.348	Pliocene	marls	1:50000 / 1:2000		Tm	C		625	600	625	Faccioli (1992)	CA
27	Calitri	DPC	40.898	15.439	Pliocene	sandstone, sand with levels of marls	1:50000 / 1:2000	Tss		A	CH	518	515	518	Palazzo (1991)	CA
28	Cascia	DPC	42.719	13.013	Oligocene	marls	1:50000 / 1:2000		Tm	A	SASW	540	600	540	This study	SB
29	Cascia-Cabina Petrucci	DPC	42.755	13.004	Pleistocene	sandly and gravely deposit	1:100000	Qoa		A	SASW	339	387	339	This study	SB
30	Cassino-Sant' Elia	ENEA	41.523	13.864	Miocene	clay and clay with marls with layers of gray and yellow sandstone	1:50000 / 1:2000		Tm	C			600	600		CA
31	Castelnuovo-Assisi	DPC	43.007	12.591	Olocene	recent alluvium of clayely layers on sands an silt	1:50000 / 1:2000	Qal,deep		A	SASW	293	280	293	This study	CA
32	Castiglione Messer Marino	DPC	41.868	14.449	Miocene	marls	1:100000		Tm	C			600	600		CA
33	Catania-Piana	DPC	37.447	15.047	Olocene	alluvium clayely and sandy deposit on Pleistocene clay	1:50000 / 1:2000	Qal,deep		A	CH	261	280	261	Frenna & Maugeri (1993)	CA
34	Chieti	DPC	42.36	14.14	Quaternario	gray clay and marls	1:100000	Qoa		D			387	387		CA
35	Codroipo	DPC	45.959	12.984	Quaternario	coarse grevely alluvium	1:50000 / 1:2000	Qoa		D			387	387		CA
36	Colfiorito	DPC	43.037	12.921	Pleistocene	lacustrium deposit	1:50000 / 1:2000	Qoa		A	SASW	317	387	317	This study	CA
37	Colfiorito-Casermette	DPC	43.028	12.900	Olocene	lacustrium and fluviolacustrum sandy-clayely sediments	1:100000	Qal,coarse		A	SASW	405	354	405	This study	SB
38	Conegliano Veneto	DPC	45.883	12.288	Quaternario	gravely alluvium	1:50000 / 1:2000	Qoa		D			387	387		CA
39	Contrada Fiumicella-Teora	ENEA	40.881	15.255	Pleistocene	alluvium	1:100000	Qoa		D			387	387		FF
40	Conza-Base	DPC	40.875	15.327	Pliocene	marls and clay	1:50000 / 1:2000		Tm	C		625	600	625	Faccioli (1992)	CA
41	Conza-Vetta	DPC	40.872	15.329	Pliocene	gravely and sandy conglomerate on Pliocene clay	1:50000 / 1:2000	QT		D		406	455	406	Faccioli (1992)	CA
42	Cosenza	DPC	39.304	16.247	Pleistocene	gray clays	1:50000 / 1:2000	QT		D			455	455		CA
43	Feltre	DPC	46.019	11.912	Olocene	recent sandy-silty alluvium on Quaternary deposit	1:50000 / 1:2000	Qal,coarse		D			354	354		CA
44	Ferruzzano	DPC	38.051	16.132	Miocene	varicoloured clay	1:100000		Tm	C			600	600		CA
45	Foligno Santa Maria Infraportas-Base	ENEA	42.955	12.704	Olocene	recent alluvium	1:50000 / 1:2000	Qal,deep		A	SASW	395	280	395	This study	SB
46	Forgaria-Cornino	ENEA	46.221	12.997	Pleistocene	Pleistocene alluvium deposit (50 m) on Miocene marls and sandstone	1:50000 / 1:2000	Qoa		A	CH	454	387	454	Fontanive et al. (1985)	CA
47	Garigliano-Centrale Nuc. 1	DPC	41.258	13.833	Olocene	alluvium deposit	1:50000 / 1:2000	Qal,deep		A	CH	187	280	187	Palazzo (1991)	CA
48	Garigliano-Centrale Nuc. 2	DPC	41.258	13.833	Olocene	alluvium deposit	1:50000 / 1:2000	Qal,deep		A	CH	187	280	187	Palazzo (1991)	CA

49	Gemona-Li Furmie	trieste univ	46.267	13.115	Oligocene	gravel, sand and silt	1:50000 / 1:2000	Qal,coarse		D				354	354		n.r.
50	Gemona-Scugelars	trieste univ	46.283	13.142	Oligocene	gravel, sand and silt	1:100000	Qal,coarse		D				354	354		n.r.
51	Genio-Civile	DPC	43.623	13.516	Miocene	marls	local		Tm	B		549	600	549		Woking group (1981)	SB
52	Gubbio	DPC	43.357	12.602	Miocene	marls with levels of sandstone	1:50000 / 1:2000		Tm	A	SASW	922	600	922		This study	CA
53	Gubbio-Piana	DPC	43.313	12.589	Pleistocene	alluvium	1:50000 / 1:2000	Qoa		A	SASW	492	387	492		This study	CA
54	Lab.Gran Sasso	DPC	42.436	13.554	Eocene	limestone	1:100000		MI	C			1000	1000			SB
55	Lauria-Galdo	DPC	40.021	15.89	Giurassico	limestone	1:50000 / 1:2000		MI	C			1000	1000			CA
56	Maiano-Piano Terra	DPC	46.187	13.069	Olocene	gravely alluvium with sand and silt	1:50000 / 1:2000	Qal,coarse		A	CH	344	354	344		Palazzo (1991)	SB
57	Maiano-Prato	DPC	46.187	13.069	Olocene	gravely alluvium with sand and silt	1:100000	Qal,coarse		A	CH	344	354	344		Palazzo (1991)	FF
58	Matelica	DPC	43.249	13.007	Pleistocene	gravely and sandly alluvium	1:50000 / 1:2000	Qoa		A	SASW	437	387	437		This study	CA
59	Mazara del Vallo	DPC	37.653	12.611	Pleistocene	cemented deposit	1:100000		Pc	C			1000	1000			CA
60	Mercato San Severino	DPC	40.789	14.763	Olocene	recent alluvium (20m) on vulcanic rock(20m) on recfent alluvium (20m) on limestone	1:50000 / 1:2000	Qal,thin		A	CH	451	349	451		Palazzo (1991)	CA
61	Messina 1	DPC	38.207	15.516	Pretriassico	vulcanic and metamorfic rock	1:100000		Mg	B	CH	1800	1000	1000		Baldovini et al.(1993)	CA
62	Milazzo	DPC	38.232	15.244	Pretriassico	metamorfic rock	1:50000 / 1:2000		Mg	B	CH	1800	1000	1000		Baldovini et al. (1993)	CA
63	Moggio	trieste univ	46.406	13.189	Triassico	limestone	1:100000		MI	C			1000	1000			CA
64	Naso	DPC	38.119	14.786	Pliocene	clayely sand and conglomerate	1:100000	QT		B	DH	223	455	223		Dott.Copat. Personal com.	CA
65	Nocera Umbra	DPC	43.113	12.785	Miocene	sandstone on marls	1:100000	Tss		A	SASW	428	515	428		This study	CA
66	Nocera Umbra 2	DPC	43.113	12.785	Miocene	sandstone on marls	1:100000	Tss		A	SASW	428	515	428		This study	CA
67	Nocera Umbra-Biscontini	DPC	43.103	12.805	Miocene	sandstone on marls	local	Tss		A	SASW	442	515	442		This study	n.r.
68	Nocera Umbra-Salmata	DPC	43.149	12.797	Olocene	detritus	1:50000 / 1:2000	Qal,coarse		A	SASW	694	354	694		This study	CA
69	Norcia	DPC	42.791	13.096	Pleistocene	sandy and gravely alluvium and detritus	1:50000 / 1:2000	Qoa		A	SASW	678	387	678		This study	CA
70	Norcia-Altavilla	ENEA	42.796	13.089	Quaternario	recent alluvium, palustrium and lacustrum deposit	1:50000 / 1:2000	Qal,thin		A	SASW	218	349	218		This study	SB
71	Norcia-Zona Industriale	ENEA	42.775	13.097	Quaternario	lacustrium and fluvio-lecustrium deposit	1:50000 / 1:2000	Qal,thin		A	SASW	551	349	551		This study	CA
72	Ortucchio	DPC	41.953	13.642	Olocene	sandy-clayely recent alluvium, locally gravely	1:50000 / 1:2000	Qal,coarse		D				354	354		CA
73	Patti-Cabina Prima	DPC	38.134	14.976	Miocene	sandy limestone	1:50000 / 1:2000		Tm	C			600	600			CA
74	Pellaro	DPC	38.024	15.654	Olocene	weak alluvium fixed by vegetation on marls	1:100000	Qal,thin		D				349	349		CA
75	Poggio-Picenze	DPC	42.322	13.54	Pleistocene	alternation of silt and brecce	1:50000 / 1:2000	QT		D				455	455		CA
76	Ponte Corvo	DPC	41.499	13.683	Pleistocene	limestone and sandstone	1:50000 / 1:2000		MI	C			1000	1000			CA
77	Pradis	trieste univ	46.248	12.888	Cretacico	limestone	1:50000 / 1:2000		MI	C			1000	1000			CA
78	Procisa Nuova	ENEA	40.87	15.19	Pleistocene	recent alluvium	1:100000	Qoa		D				387	387		CA
79	Rieti	DPC	42.430	12.821	Olocene	alluvium deposit	1:100000	Qal,deep		D				280	280		CA
80	Rionero in Vulture	DPC	40.927	15.669	Pleistocene	vulcanic silt and gravel	1:50000 / 1:2000	Qoa		A	CH	539	387	539		Palazzo (1991)	CA
81	Roccamonfina	DPC	41.287	13.980	Olocene	weakly cemented detritus (10m) on vulcanic rock	1:100000	Qal, coarse		D				354	354		CA
82	Roggiano-Gravina	DPC	39.619	16.171	Pliocene	sand and conglomerate weakly cemented	1:100000	QT		D				455	455		A
83	San Agapito	DPC	41.567	14.233	Pleistocene	aluvium deposit	local	QT		B	DH	553	455	553		Isernia Adm: Microzonation	CA
84	San Francesco	trieste univ	46.309	12.935	Triassico	limestone	1:100000		MI	C			1000	1000			CA
85	San Marco dei Cavoti	DPC	41.306	14.88	Miocene	yellow sand and sandstone	1:100000	Tss		D				515	515		CA
86	San Rocco	ENEA	46.221	12.997	Cretacico	limestone	1:50000 / 1:2000		MI	C			600	1000	600		Fontanive et al. (1985)	FF
87	Sannicandro	DPC	41.833	15.572	Pleistocene	silty clay	loacal		Tm	A	CH	865	600	865		Palazzo (1991)	CA
88	Sellano Ovest	DPC	42.87	12.92	Miocene	marls	local		Tm	A	SASW	509	600	509		This study	CA
89	Sirolo	DPC	43.517	13.619	Miocene	marls with weak level on top	1:50000 / 1:2000		Tm	C			600	600			CA
90	Sortino	DPC	37.163	15.030	Miocene sup	vulcanic rock (15m) on limestone	1:50000 / 1:2000		Mv	C			1000	1000			CA
91	Spoleto	DPC	42.736	12.737	Pleistocene	cemented conglomerate	borehole		Pc	C			1000	1000			CA
92	Sturno	DPC	41.021	15.115	Oliogocene	clay and marls	1:50000 / 1:2000		Tm	A	CH	1134	600	1134		Palazzo (1991)	CA
93	Tarcento	DPC	46.226	13.210	Olocene	sandly deposit (10m) on marls and sandstone	1:50000 / 1:2000	Qal,coarse		A	CH	843	354	843		Brambati et al (1979)	CA
94	Tolmezzo-Diga Ambiesta	DPC	46.382	12.982	Cretacico	limestone	1:50000 / 1:2000		MI	A	CH	1092	1000	1092		Fontanive et al. (1985)	D
95	Torre del Greco	DPC	40.797	14.383	Olocene	weak vulcanic rock (high voids presence)	1:50000 / 1:2000		Mv	C			1000	1000			CA
96	Tregnago	DPC	45.525	11.134	Cretacico	limestone	1:50000 / 1:2000		MI	C			1000	1000			CA
97	Tricarico	DPC	40.619	16.156	Miocene	fractured limestone and marls	1:50000 / 1:2000		Tm	A	CH	446	600	446		Palazzo (1991)	CA
98	Valle	trieste univ	46.158	13.393	Eocene	marls and sandstone in alternation with limestone brecce	1:100000		Tm	C			600	600			CA
99	Vasto	DPC	42.111	14.71	Pleistocene	yellow sand in alternation with sandy clay	1:100000	Qoa		D				387	387		CA
100	Villa San Giovanni	DPC	38.216	15.647	Pleistocene	conglomerate	1:50000 / 1:2000		Pc	C			1000	1000			CA
101	Villetta Barrea	DPC	41.759	13.989	Cretacico	limestone	1:50000 / 1:2000		MI	C			1000	1000			D

(1) A= direct investigation (Cross-Hole, Down-Hole, SASW)
B= info from investigations on same area and same material
C= info from investigfations on same formation
D = info from literature

(2) FF = Free Field
CA = ENEL/ENEA Cabin (3<H<5 m; 1.5x1.5<A<3x3 m2)
SB = Structure Basement
D = Dam
T = Tunnel

2.3.2   Site Conditions for Italian Strong Motion Stations – Data from Others

Previous site characterization for Italian strong motion stations can be grouped into the following major categories: (1) site investigations at selected instruments that recorded the 1976 Friuli earthquake (Fontanive et al., 1985) and 1980 Irpinia earthquake (Palazzo, 1991a, 1991b; Faccioli, 1992); (2) microzonation and other studies for local municipalities such as Ancona (Working group, 1981), Tarcento (Brambati et al., 1979), and San Agapito (Isernia Administration, 1998); and (3) individual site studies documented in the literature (e.g., Catania-Piana site, Frenna and Maugeri, 1993) and from the files of consulting engineers and geologists with local experience (e.g., Naso station; personal communication, G. Copat, 2007).

The Friuli and Irpinia site investigations were generally performed at the recording sites and are listed in Table 2.1 as Category A. The work in the Friuli region examined seven accelerograph sites. For each site, two boreholes were drilled to 60 m depth and cross-hole measurements were made to evaluate shear wave velocity profiles. Additional on-site tests included seismic refraction measurements to estimate the p-wave profile. The Irpinia investigation examined 16 strong motion stations. Two boreholes were drilled to 100 m depth at each site and cross-hole measurements were made to profile shear wave velocity. Additional in situ and geotechnical laboratory testing was also performed.

The microzonation and individual site studies were used to assign velocities to strong motion stations that are listed as Categories A-C depending on the proximity of the measurement to the strong motion station and the verification (or not) of similar geologic conditions at the two locations from a site visit by a geologist. Most of these velocity profiles are from cross-hole or down-hole measurements.

2.3.3   Velocity Measurements from this Study at Italian Strong Motion Stations

The 1997-98 Umbria-Marche earthquake sequence produced a significant number of recordings, but prior to this study velocity profiles had been evaluated and disseminated for relatively few of the recording sites in that region. Accordingly, on-site measurements were performed at numerous sites using a controlled sine wave source and the spectral analysis of surface waves (SASW) method (Heisey et al., 1982; Nazarian and Stokoe, 1983). The SASW method of testing is a portable, inexpensive, and efficient means of non-invasively estimating the stiffness properties of the ground. The equipment utilized in the present work can typically be used to profile velocities to depths of approximately 100 m. Although the SASW technique is widely known, we describe in some detail here the specific procedures used for this study since it has not been published previously outside of the grey literature.

The testing program investigated 17 sites in Umbria and Marche. Typically, the strong motion recording (SMR) stations are located in residential or light industrial sites outside the town center, in parks, or on private farm land. We located next to the SMR stations, or the GPS location of the site if we could not observe the SMR.

We performed profiling using a surface wave testing system to collect dispersion data. The equipment consists of 1-Hz seismometers, a low frequency spectrum analyzer, two computer controlled electro-mechanical harmonic-wave sources (shakers) and their amplifiers, cables, and approximately 4.0 kW of total electrical output from generators made available in each test region. The 1-Hz Kinemetrics receivers we used are designed for capturing vertical motions and cover the frequency range of interest in the active-source surface-wave test (1 to ~100 Hz). The source consists of two APS Dynamics Model 400 electro-mechanical shakers that produce in-phase continuous harmonic vertical excitation of the ground. The shakers are controlled by the

20

spectrum analyzer, which produces a sine wave signal that is split into a parallel circuit through two separate power amplifiers that interface with the shakers. Two receivers record the waves and in near-real time, the Fourier spectra, cross power spectra, and coherence are computed. The ability to perform near real-time frequency domain calculations and monitor the progress and quality of the test allows us to adjust various aspects of the test to optimize the capture of phase data. These aspects include the source-wave generation, frequency step-size between each sine-wave burst, number of cycles-per-frequency, total frequency range of all the steps, and receiver spacing.

The dual shaker-sources are arrayed orthogonally to the SASW seismometer line. The test steps through a suite of frequencies, and for each frequency phase computations are made. This method of swept-sine surface wave testing sweeps through a broad range of low frequencies in order to capture the surface wave-dispersion characteristics of the ground. This approach is a modification of the Continuous Sine Wave Source Spectral Analysis of Surface Waves (CSS-SASW) test procedure presented by Kayen et al. (2004; 2005).

Spacing of the receivers stepped geometrically from 1-160 m. The two seismometers are separated by a given distance, d, and the source is usually placed at a distance of d from the inner seismometer. Rayleigh wavelengths (λ) are computed by relating the seismometer spacing (d) and the phase angle (θ), in radians determined from peak of the cross-power spectrum) between the seismometer signals:

$$\lambda = 2\pi d / \theta \qquad (2.1)$$

The Rayleigh wave surface wave velocity, V_r, is computed as the product of the frequency and its associated wavelength:

$$V_r = f\lambda \qquad (2.2)$$

Computing the average dispersion curve for a site requires a suite of individual data sets relating Rayleigh wave phase velocities to their corresponding frequencies and wavelengths. Regardless of the array dimensions, we routinely compute phase velocities for phase angles between 120 degrees and 1080 degrees, corresponding to wavelengths of 3*d* and *d*/3 respectively. If the data are noisy, the range is narrowed to 180 degrees and 720 degrees, or 2*d* and *d*/2. For example, if the array separation was 3 m, velocities are inverted for Rayleigh wavelengths of 1-9 m. Low frequencies produce long wavelengths that sound more deeply into the ground, and hence are used to characterize deeper layers. Figure 2.7 presents a plot of a group of eight individual dispersion curves that together cover a range of wavelengths from 0.6-400 m for the Cascia site in Umbria. The averaged dispersion curve from these eight profiles is used to invert the velocity structure.
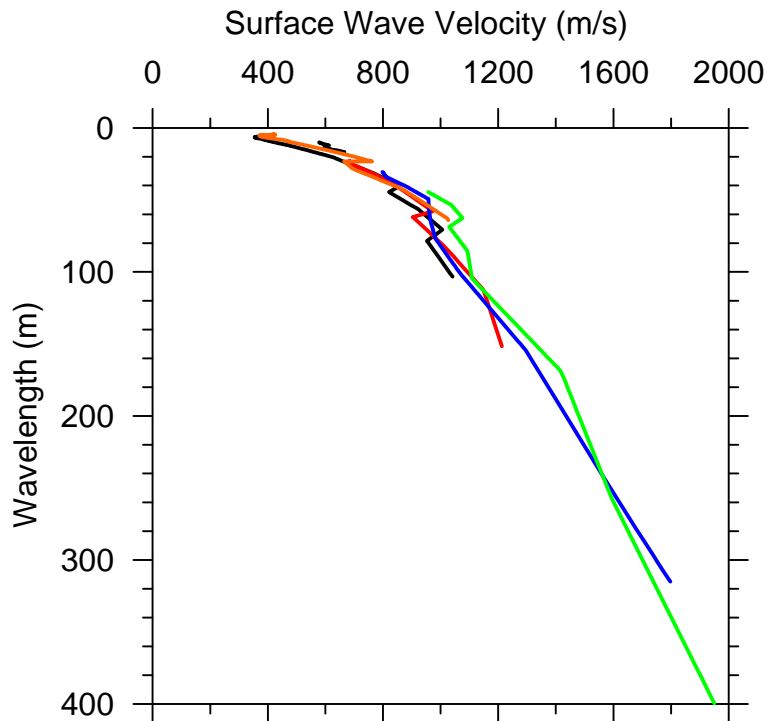
Figure 2.7. A group of eight dispersion curves covering a wavelength range of 1-400 m (Site 267CSC, Cascia, Umbria)

The inversion process is used to estimate a soil velocity model having a *theoretical-* dispersion curve that fits the data. The "best-fit" velocity profile minimizes the sum of the squares of residuals between the theoretical and experimental dispersion curves. The inversion algorithm, WaveEq of OYO Corp. (Hayashi and Kayen, 2003) uses an automated-numerical approach that employs a constrained least-squares fit of the theoretical and experimental dispersion curves. Typically, a 10-15 layer model was used for the inversion, with layer thicknesses geometrically expanding with depth. The increasing layer thicknesses correspond with decreasing dispersion information in the longer wavelength (deeper) portion of the dispersion curve. The profiles generally increase in stiffness with depth, though low velocity layers are present at depth in several profiles. Figure 2.8 shows the inverted shear wave velocity profile for the Cascia, Umbria site, in which velocity rapidly climbs from less than 300 m/s at the surface to >1900 m/s at 40 m. Values of V_{s30}, calculated as 30 m divided by shear wave travel time through the upper 30 m, are given in Table 2.1 and range from 182 to 922 m/s (NEHRP categories B to D).
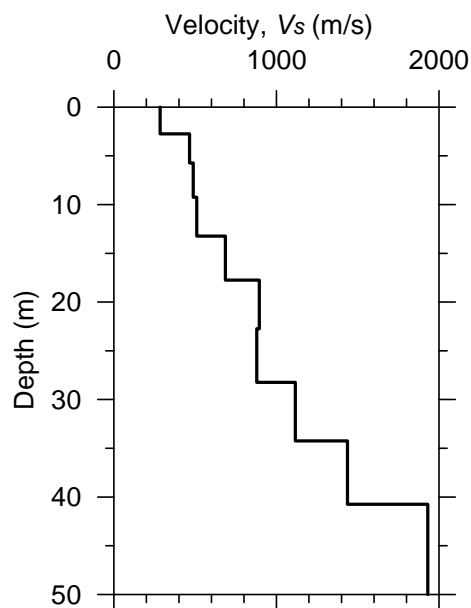
Figure 2.8. Shear wave velocity profile for Cascia, Umbria site 267CSC (V_{s30} = 540 m/s, Site Class C).

2.3.4   Estimating Velocities for Sites without Measurements

For sites for which no local measurements of seismic velocities are available, we estimate V_{s30} values based on correlations with surface geology. Correlations to estimate V_{s30} from surface geology are not available in the literature for geologic units in Italy. Accordingly, we evaluate the effectiveness in Italy of correlations developed for California and develop preliminary additional correlations for geologic units not represented in the California models.

The geology maps available for Italy include large-scale maps (1:100,000) by Servizio Geologico d'Italia (Working Group, 2004) that provide coverage of the entire country (and hence all recording stations) and local geologic maps/sections (typical scale 1:2000) by ENEL. The local maps/sections are derived from a site visit by an ENEL geologist and are available for 77 of 104 strong motion sites. Additional geologic information is available for a few sites from local microzonation reports or geologic reports for individual sites (references given in Table 2.1). The geologic classifications included in Table 2.1 are based on the largest map scale that is available for the site. The map scale from which the classification was taken is indicated in the table, with "local" referring to the aforementioned microzonation studies or geologic reports.

We judge the best available correlations for California to be those of Wills and Clahan (2006). A number of the Wills-Clahan geologic categories are descriptive of conditions encountered at Italian sites. Among these are Quaternary alluvium categories segregated by sediment depth and material texture (Qal,thin; Qal,deep; Qal,coarse), older Quaternary alluvium (Qoa), Quaternary to Tertiary alluvial deposits (QT), and Tertiary sandstone formations (Tss). The relatively firm rock categories used by Wills-Clahan are generally not descriptive of Italian firm rock sites, which are often comprised of limestone, marls, and volcanic rocks.

Wills and Clahan (2006) provide mean and standard deviation values of V_{s30} for each geologic category based on California data. We evaluate the applicability of those estimates to Italian sites by calculating V_{s30} residuals as:

$$R_i = \left(V_{s30}\right)_{m,i} - \left(V_{s30}\right)_{WC} \qquad (2.3)$$

where $R_i = V_{s30}$ residual for site i, $(V_{s30})_{m,i}$ = value of V_{s30} from measurement at Italian site i, and $(V_{s30})_{WC}$ = mean value of V_{s30} from Table 1 of Wills and Clahan (2006). Due to the small number of sites falling in individual categories, we group sites into two general categories for analysis of residuals – Quaternary alluvium (combination of the thin, deep, and coarse sub-categories) and late Quaternary and Tertiary sediments (combination of Qoa, QT and Tss). Figure 2.9 shows histograms of residuals grouped in this manner. Also shown in Figure 2.9 is the range of velocities within ± two standard deviations of zero using average values of standard deviation from Table 2.1 of Wills and Clahan (2006) for the grouped categories (taken as σ_{WC}=85 m/s for the Qal categories and σ_{WC}=170 m/s for the Qoa/QT/Tss categories).
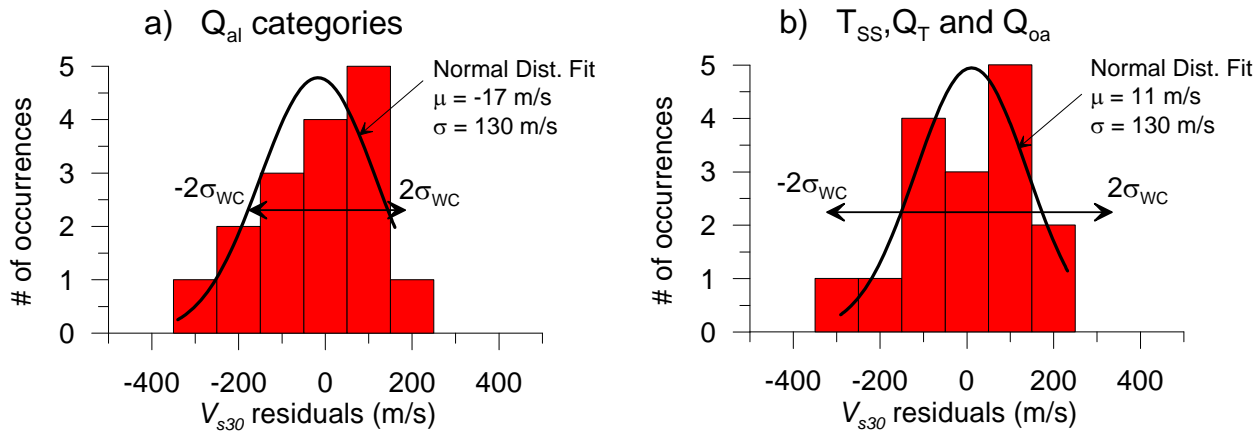
Figure 2.9. Histograms of V_{s30} residuals and normal distribution fits for (a) Quaternary alluvium categories and (b) older Quaternary, Quaternary-Tertiary, and Tertiary sandstone categories. The ±2σ_{WC} limits indicate two standard deviations above and below zero from the Wills and Clahan (2006) correlation.

The histogram for Qal categories (Figure 2.9a) shows that the mean of residuals is nearly zero, but only 78% of the data fall within the $\pm 2\sigma_{WC}$ bands (approximately 95% should fall within this range if the Italian data shared the standard deviation of the California data). The histogram for the Qoa/QT/Tss categories (Figure 2.9b) similarly shows a nearly zero mean, and 85% of the data fall within the $\pm 2\sigma_{WC}$ bands. Similar results are obtained if the grouped categories are broken down to smaller sub-categories (e.g., Qal,deep from Qal). Hence, our preliminary conclusion is that the Wills-Clahan recommendations provide an unbiased estimate of V_{s30} for Italian alluvium sites of Quaternary to Tertiary age. However, the standard deviation of the Italian data is different, being larger for the Qal categories are perhaps slightly smaller for the older alluvium and Tertiary categories.

As mentioned above, many of the rock sites listed in Table 2.1 have conditions geologically dissimilar to California such as limestone, marls, and volcanic rocks. Since we are unaware of existing correlations to V_{s30} for these types of materials, we assembled rock categories descriptive of Italian conditions that seem to generally have similar seismic velocities. These categories are listed in Table 2.1 and are summarized as follows:

- Tm: This category consists of Tertiary Marl, often with surficial overconsolidated clays. It is common along the central-southern Apennines, and 13 sites in our database have this classification. A histogram of the Tm velocities is given in Figure 2.10a, showing a mean $V_{s30} = 670$ m/s and standard deviation = 190 m/s.

- Pc: This category consists of Pleistocene to Pliocene cemented conglomerate. Its occurrence is widespread in Sicily and the Apennines. Five sites in our database have this classification, two of which have velocity measurements with $V_{s30} = 972$ and 1156 m/s. We use $V_{s30} = 1000$ m/s for sites without measurements.

- Ml, Mv, and Mg: This category comprises Mesozoic limestone (Ml), volcanic rocks (Mv), and gneiss (Mg). We group these three together for velocity characterization because the available data is inadequate to justify further discretization and the seismic velocities are generally high (> 1000 m/s). The Ml category includes 14 sites located in the Alps and Apennines. The Mv category applies to three sites located near the active volcanoes of Mt. Etna (Sicily) or Mt. Vesuvio (near Napoli). The Mg category is encountered only at the Messina and Milazzo Station in Sicily. A measured shear velocity of 1800 m/s is reported in Table 1 for Messina, but this measurement was made in a tunnel deep in the ground. Shallow velocities should be slower and hence the preferred V_{s30} value is given as 1000 m/s to be consistent with other the other Mesozoic categories.
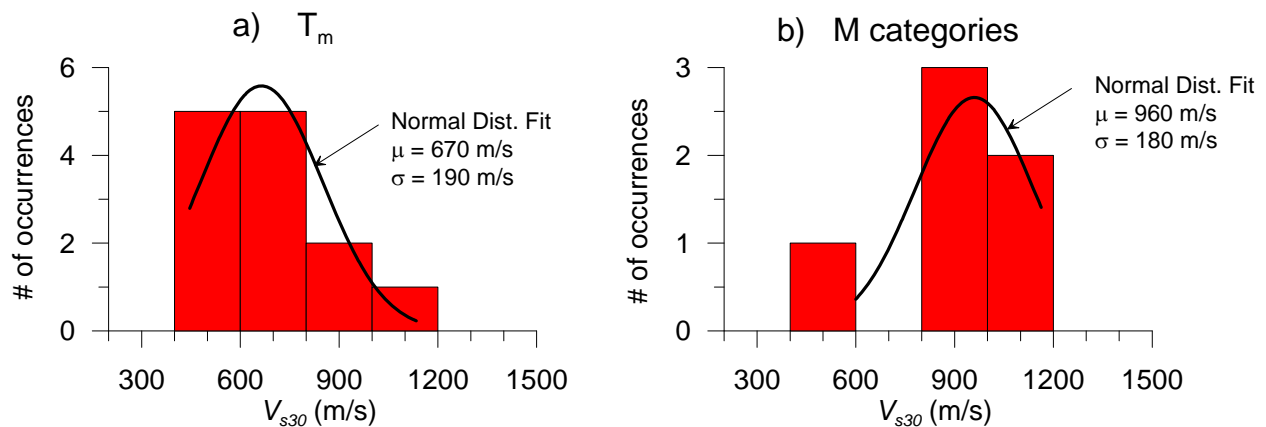
Figure 2.10. Histograms of V_{s30} values and normal distribution fit for (a) Tm category and (b) M categories

2.3.5 Instrument Housing

The characteristics of the structure housing a strong motion accelerometer are an important component of the site databank because soil-foundation-structure interaction (SFSI) affects the recording. Whether the SFSI effect is significant on ground motion intensity measures of engineering interest (e.g., spectral acceleration) depends principally on the embedment of the

foundation, the size (in plan view) of the structure, and the structural mass (Stewart, 2000). Instrument housings considered "free-field" for the NGA project and previous similar work in California have generally consisted of small (1 m square) instrument huts or small 1-2 story structures without basements.

Housing information for the 104 strong motion stations is given in Table 2.1. Most of the buildings (75) are in small cabins (CA), which are described further below. Fifteen stations are at the foundation level of small buildings (typically single story buildings, 3-5 m in height, with footprint areas ranging from 10-30 m^2. Four instruments are on small slabs with no overlying structure, similar to the instrument huts used widely in California – these are denoted as FF in Table 2.1. Remaining instruments have either unknown housing conditions or are located on dams (D) or in tunnels (T).

The small cabins (CA designation) are typical of ENEL instruments. The cabins are electrical substations of masonry construction approximately 3–9 m square in plan view and 3–5 m tall. A typical example is shown in Figure 2.11. The instrument is mounted on a short pillar 20 cm in height above the floor slab and 60 cm in diameter. The pillar extends into the natural ground approximately 0.3-1.0 m and is isolated from the floor slab by a gap (Berardi et al., 1991). Analysis by Berardi et al. (1991) indicates that this configuration would not be expected to introduce any significant modification to the recording from SFSI. Based on those analyses and empirical studies (e.g., Stewart, 2000), we believe that recordings from structures of this type can be assumed to provide a reasonable approximation of free-field conditions.

Figure 2.11. ENEL electrical substation housing a recording instrument in Gubbio-Piana site (Umbria)

2.4 SOURCE DATABANK

Attributes of the seismic source that are important for the development of GMPEs and ground motion selection for response history analysis include magnitude, source location and dimensions, and focal mechanism. We compile in Table 2.2 available source characteristics extracted from publications and internal files of the Istituto Nazionale di Geofisica e Vulcanologia (INGV; F. Mele and B. Castello, personal communication, 2007).

Point source information such as seismic moment and hypocenter location is extracted from a web site (INGV, 2007a) that reports the results of an INGV study termed "Project S6." As described by Pondrelli et al. (2006), the Project S6 source parameters are available for most events between 1972 and 2004. Pondrelli et al. take CMT solutions from the Harvard moment tensor catalogue (e.g., Elkström et al., 2005) where available, which is for $M_w > 5.5$. For events since 1977, Pondrelli et al. (2002, 2006) extend the Harvard dataset with the European-Mediterranean Regional CMT (RCMT) catalogue for $4.5 < M_w < 5.5$. Both Harvard CMT and RCMT solutions are based on model fits to medium and long period seismograms. Moment

29

magnitudes are taken in Project S6 based on CMT and RCMT solutions. As explained by Pondrelli et al. (2006), additional magnitudes are obtained as follows: surface wave magnitude (M_s) is from the IRIS data management center (IRIS, 2007); body wave (m_b) and local magnitude are taken from the USGS National Earthquake Information Center (http://wwwneic.cr.usgs.gov/neis/epic/) with some modifications by INGV.

For events not characterized by Project S6, hypocenter locations and magnitudes were taken, in order of preference, from the Parametric Catalogue of Italian Events (Working Group CPTI04, 2004) or from the ESD database (Ambraseys et al., 2004).

The finite fault parameters shown in Table 2.2 (strike, dip, rake, along-strike length, down-dip width, depth to top of rupture) have been compiled by INGV into the Database of Individual Seismogenic Sources (DISS; INGV, 2007b, Basili et al., 2007). Those finite source parameters were compiled from the literature, and hence were developed using a variety of techniques (surface faulting, geologic investigations, magnitude-area scaling relationships, etc.).

Table 2.2. Source parameters for selected Italian earthquakes

Earthquake Name	Date dd/mm/yyyy	Time (UTC)	Mw	Ms	ML	Mb	lat	long	Focal Mech.	Focal Depth (km)	ref.	center lat	center long	strike	dip	L (km)	W (km)	z-top (ikm)	rake	slip	ref.
Ancona	25/01/1972	23:22:17		4.0	4.0	4.8	43.70	13.41	normal	10	ESD										
Ancona	2/4/1972	2:42:18	5.2	4.8	4.6	4.5	43.63	13.55	oblique	8	CPTI04										
Ancona	2/4/1972	9:18:30		4.3	4.4	4.3	43.73	13.38	oblique	8	ESD										
Ancona	2/4/1972	18:17:25		4.0	4.1	4.8	43.70	13.40	normal	10	ESD										
Ancona	2/5/1972	1:26:30		4.2	4.3	4.3	43.72	13.40	oblique	10	ESD										
Ancona	2/6/1972	1:34:19		4.1	4.3	4.6	43.70	13.43	oblique	5	ESD										
Ancona	2/6/1972	21:44:45			3.0		43.70	13.40	normal	10	S6_D5										
Ancona	2/8/1972	12:19:10			3.9		43.68	13.40	normal	12	S6_D5										
Ancona	14/06/1972	18:55:53	4.8	5.2	4.7	4.9	43.65	13.60	strike slip	8	S6_D5										
Ancona	14/06/1972	21:01:02			4.2		43.67	13.42	normal	8	S6_D5										
Ancona	21/06/1972	15:06:53			4.0		43.82	13.60	normal	4	S6_D5										
Friuli	5/6/1976	20:00:13	6.4	6.5	6.4	5.9	46.35	13.26	thrust	7	S6_D5	46.25	13.14	290	30	16	9	2	105	1.32	DISS-IS
Friuli (aftershock)	5/7/1976	0:23:49	4.9		4.9		46.24	13.27	thrust	9	S6_D5										
Friuli (aftershock)	5/11/1976	22:44:01	5.0		5.3	4.9	46.29	12.99	thrust	6	S6_D5										
Friuli (aftershock)	18/05/1976	1:30:09	4.1		4.1		46.25	12.867	thrust	7	S6_D5										
Friuli (aftershock)	9/6/1976	18:48:17	4.3		4.1		46.35	13.067	thrust	13	S6_D5										
Friuli (aftershock)	6/11/1976	17:16:36	4.5		4.3		46.267	12.967	thrust	9	S6_D5										
Friuli (aftershock)	17/06/1976	14:28:51	4.7		4.5		46.177	12.798	oblique	15	S6_D5										
Friuli (aftershock)	9/7/1976	11:08:16	4.2		4.1		46.3	12.983	thrust	5	S6_D5										
Friuli (aftershock)	9/11/1976	16:31:11	5.3	5.5	5.5	5.0	46.29	13.18	thrust	3	S6_D5										
Friuli (aftershock)	9/11/1976	16:35:03	5.6	5.4	5.8	5.3	46.3	13.317	thrust	12	S6_D5										
Friuli (aftershock)	13/09/1976	18:54:47	4.6		4.3		46.283	13.2	thrust	8	S6_D5										
Friuli (aftershock)	15/09/1976	3:15:19	5.9	6.0	6.1	5.7	46.30	13.19	thrust	15	S6_D5	46.27	13.22	274	35	8	5.5	2	90	0.83	DISS-IS
Friuli (aftershock)	15/09/1976	4:38:53	4.9		4.8	4.8	46.27	13.17	normal	21	S6_D5										
Friuli (aftershock)	15/09/1976	9:21:18	5.9	5.9	6.0	5.4	46.28	13.20	thrust	21	S6_D5	46.28	13.20	276	35	10	6.4	6.5	110	0.75	DISS-IS
Friuli (aftershock)	16/09/1977	23:48:07	5.3	5.1	5.3	5.1	46.28	12.98	thrust	21	S6_D5										
Calabria	3/11/1978	19:20:48	5.2	5.1	5.3		37.98	16.18	normal	15	S6_D5	38.01	15.98	86	45	6.4	4				DISS-MSw
Basso Tirreno	15/04/1978	23:33:48	6.0	5.8	5.5	5.5	38.27	15.11	strike slip	15	S6_D5	38.26	15.05	147	83	12.1	8.6	1.5	180	0.6	DISS-IS
Marche	21/05/1979	14:34:19			3.6		43.05	12.96	n.r.	4	S6_D5										
Valnerina	19/09/1979	21:35:37	5.8	5.9	5.5	5.8	42.80	13.04	normal	4	S6_D5	42.71	13.07	156	45	9.7	5				DISS-MSw
Umbria	21/09/1979	0:52:45			4.2		42.73	13.03	normal	10	S6_D5										
Umbria	28/09/1979	4:41:21			3.6		42.73	13.10	normal	5	S6_D5										
Toscana	6/7/1980	18:35:01	4.6	4.1	4.3		44.05	10.60	normal	30	S6_D5										
Campano Lucano	23/11/1980	18:34:52	6.9	6.8	6.5	6.0	40.76	15.31	normal	16	S6_D5	40.80	15.29	310	60	28	15	1	270	1.65	DISS-IS
Campano Lucano (aftershock)	24/11/1980	3:03:56	5.0		4.5		40.86	15.37	normal	21	S6_D5										
Campano Lucano (aftershock)	25/11/1980	21:53:37			3.8		40.99	15.22	normal	32	S6_D5										
Campano Lucano (aftershock)	26/11/1980	14:55:43			4.3		40.94	15.27	normal	24	S6_D5										
Campano Lucano (aftershock)	12/1/1980	19:04:31			4.6	4.3	40.89	15.31	normal	9	S6_D5										
Campano Lucano (aftershock)	16/01/1981	0:37:47	5.2	5.3	4.6	5.0	40.84	15.44	normal	5	S6_D5										
Campano Lucano (aftershock)	16/01/1981	4:36:51			3.9		40.78	15.35	normal	5	S6_D5										
Campano Lucano (aftershock)	16/01/1981	6:31:26			3.8		40.83	15.50	normal	4	S6_D5										
Campano Lucano (aftershock)	14/02/1981	17:27:46	4.9	4.8	4.7		41.06	14.79	normal	10	S6_D5										
Arpiola	3/22/1984	0:16:25			3.5		44.27	9.91	n.r.	22	S6_D5										
Umbria	29/04/1984	5:02:59	5.6	5.2	5.2	5.1	43.21	12.57	normal	9	S6_D5	43.23	12.57	140	21	10	7	4	270	0.5	DISS-IS
Lazio Abruzzo	5/7/1984	17:49:42	5.9	5.8	5.9	5.4	41.70	13.86	normal	11	S6_D5	41.70	13.95	152	50	10	7.5	5	264	0.27	DISS-IS
Lazio Abruzzo (aftershock)	5/11/1984	10:41:50	5.5	5.2	5.7	5.2	41.71	13.89	normal	8	S6_D5										
Lazio Abruzzo (aftershock)	5/11/1984	13:14:56	4.8		4.6		41.75	13.92	normal	11	S6_D5										
Lazio Abruzzo (aftershock)	5/11/1984	16:39:18			4.4		41.68	13.88	normal	10	S6_D5										
Umbria Marche	26/09/1997	9:40:30	6.0	6.1	5.8	5.7	43.01	12.85	normal	6	S6_D5	43.09	12.84	152	40	12	7.5	4	280	0.37	DISS-IS
Umbria Marche	26/09/1997	0:33:16	5.7	5.6	5.6	5.5	43.02	12.89	normal	7	S6_D5	43.00	12.93	148	40	9	6	4	277	0.38	DISS-IS

Location	Date	Time					Lat	Lon	Mechanism	Depth	Ref										Ref
Umbria Marche (aftershock)	10/6/1997	23:24:00	5.4		5.4		43.03	12.85	normal	7	S6_D5										
Umbria Marche (aftershock)	14/10/1997	15:23:00	5.6	5.6	5.5	5.3	42.90	12.90	normal	7	S6_D5	42.91	12.93	144	40	6	6	2.5	260	0.28	DISS-IS
Umbria Marche (aftershock)	10/3/1997	8:55:22	5.2		5.0		43.04	12.82	normal	6	S6_D5										
Umbria Marche (aftershock)	10/4/1997	16:13:33	4.7		4.5		42.92	12.91	normal	2	S6_D5										
Umbria Marche (aftershock)	10/7/1997	1:24:34	4.2		4.1		43.04	12.85	normal	10	S6_D5										
Umbria Marche (aftershock)	10/7/1997	5:09:57	4.5		4.3		43.04	12.86	strike slip	3	S6_D5										
Umbria Marche (aftershock)	10/11/1997	3:20:56			3.7		43.10	12.79	normal	10	S6_D5										
Umbria Marche (aftershock)	10/12/1997	11:08:36	5.2		5.1		42.91	12.92	normal	6	S6_D5										
Umbria Marche (aftershock)	10/12/1997	20:15:29			4.0		n.r	n.r.	normal	10	ESD										
Umbria Marche (aftershock)	14/10/1997	23:23:28			4.1		42.96	12.87	normal	10	S6_D5										
Umbria Marche (aftershock)	16/10/1997	12:00:31	4.3		4.5		43.04	12.88	strike slip	2	S6_D5										
Umbria Marche (aftershock)	11/8/1997	15:31:54			4.1		42.86	12.97	normal	10	S6_D5										
Umbria Marche (aftershock)	11/9/1997	19:07:33	4.9		4.5		42.85	12.99	normal	2	S6_D5										
Umbria Marche (aftershock)	12/1/1997	22:37:05			3.5		42.86	12.98	normal	10	S6_D5										
Umbria Marche (aftershock)	21/03/1998	16:45:10	5.0		4.4		42.95	12.91	normal	10	S6_D5										
Umbria Marche (aftershock)	26/03/1998	16:26:18	5.3	4.8			43.15	12.81	normal	41	S6_D5										
Umbria Marche (aftershock)	4/3/1998	7:26:00	5.1		5.3		43.19	12.76	normal	6	S6_D5										
Umbria Marche (aftershock)	4/5/1998	15:52:20	4.8		4.5		43.19	12.77	normal	10	S6_D5										
Umbria Marche (aftershock)	13/10/1997	13:09:21	4.4		4.1		42.86	12.94	normal	10	S6_D5										
Norcia	11/8/1979	18:44:43			4.1		42.81	13.04	n.r.	4	ESD										
W of Cosenza	20/02/1980	2:34:01	4.4		4.2		39.29	16.15	oblique	12	S6_D5										
Norcia	3/5/1980	6:23:37			3.4		42.79	13.09	n.r.	21	S6_D5										
Norcia	3/11/1980	5:20:08			3.4		42.81	13.09	n.r.	13	S6_D5										
Norcia	24/05/1980	20:16:05			4.3		42.82	13.13	n.r.	15	S6_D5										
Campano Lucano (aftershock)	24/11/1980	0:24:02	5.0		4.9		40.81	15.27	normal	18	S6_D5										
Campano Lucano (aftershock)	30/11/1980	7:41:59			4.5		40.76	15.32	normal	19	S6_D5										
SW of Campobello di Mazara	6/7/1981	13:01:00	4.9		4.8		37.63	12.72	thrust	45	S6_D5										
Near coast of Scalea	21/03/1982	9:44:02			5.0		39.70	15.64	n.r.	17	S6_D5										
N of Reggio di Calabria	14/05/1985	5:44:36			3.8		38.23	15.67	n.r.	10	S6_D5										
Casamaina	20/05/1985	10:00:28			4.2		42.27	13.37	n.r.	5	S6_D5										
Off coast of Numana	22/06/1986	14:07:51			3.7		43.57	13.75	n.r.	7	S6_D5										
Potenza	5/5/1990	7:21:17	5.8	5.6	5.2	5.2	40.64	15.86	strike slip	8	S6_D5	40.68	15.85	95	88	7.9	6.2	14.8	175	0.26	DISS-IS
Sicilia-Orientale	13/12/1990	0:24:26	5.6	5.2	5.4	5.3	37.27	15.32	strike slip	5	S6_D5										
Colle	17/06/1979	4:49:38			3.8		43.15	12.88	n.r.	1	S6_D5										
Campano Lucano (aftershock)	26/11/1980	15:56:44					40.86	15.71	normal	n.r.	ESD										
Trasaghis-Friuli	28/05/1998	9:39:19			4.1		46.30	13.05	n.r.	11	ESD										
Molise	11/1/2002	15.08	5.7	5.6	5.3	5.5	41.74	14.84	strike slip	10	S6_D5	41.70	14.81	261	86	9.4	8	12	195		DISS-IS
Molise	10/31/2002	10.32	5.7	5.6	5.4	5.2	41.7167	14.893	strike slip	10	S6_D5	41.69	14.94	267	82	10.5	8	12	203		DISS-IS

Reference Legend:
ESD= European Strongmotion Database
CPTI04 = Parametric Catalogue of Italian Earthquakes
DISS = Database of Individual Seismogenic Sources (*IS = Individual Seismogenic Sources Method; MSw = Macroseimic Sources-well constrained*)
S6_D5 = Working Group, 2007. Project 6: Database of Italian accelerometric data related to the 1972-2004 period -Deliverable 6. INGV-Milano, DPC-USSN

2.5 SUMMARY AND CONCLUSIONS

In this chapter, we describe the development of a strong motion database as well as site and source databanks for strong motion studies utilizing Italian data. Our intent was to assemble and disseminate Italian data in a format that is similar to that used in the Next Generation Attenuation project, which applies to world-wide active tectonic regions (but which only sparsely sampled Italian data). The principal users of these data resources are expected to be researchers performing empirical ground motion studies and engineers selecting ground motions for dynamic analyses of structural and geotechnical systems in Italy.

The ground motion database developed here includes only about half of the available recordings due to various issues such as s-triggers that can bias ground motion intensity measures evaluated from the data. We document these biases, which affect principally long-period measures of ground motion as well as duration-related parameters.

A databank of site conditions at Italian ground motion recording stations is compiled that includes geologic characteristics and seismic velocities at 104 sites with strong motion recordings. Geologic characterization is derived principally from local geologic investigations by ENEL that include detailed mapping and cross sections. For sites lacking such detailed study, geologic characterization is from 1:100,000 scale maps by Servizio Geologico d'Italia. Seismic velocities are extracted from the literature for 22 sites with on-site measurements and 14 additional sites with local measurements on similar geology. Data sources utilized include post earthquake site investigations (Friuli and Irpinia events), microzonation studies, and miscellaneous investigations performed by researchers or consulting engineers/geologists. Additional seismic velocities are measured using a spectral analysis of surface wave (SASW) technique for 17 sites that recorded the 1997-1998 Umbria-Marche earthquake sequence. The

compiled velocity measurements provide data for 53 of the 104 sites. For the remaining sites, we estimate average seismic velocities in the upper 30 m (V_{s30}) using a hybrid approach as follows (1) for sites on Quaternary alluvium and Quaternary-Tertiary sediments, we assign V_{s30}-values based on regional correlations for California validated against the available Italian data; and (2) for sites on Tertiary Limestone, conglomerate, and Mesozoic-age rocks, we assign V_{s30}-values based on average velocities from similar units elsewhere in Italy.

A source databank is compiled from the results of recent projects by INGV. Moment tensor solutions derived from instrumental recordings are available for most events, providing estimates of source location, seismic moment, and moment magnitude. For earthquakes with M_w $> \sim 5.5$, finite source parameters include fault strike, dip, rake, along-strike rupture length, down-dip width, and depth to top of rupture.

3 Distribution of Strong Motion and Site Data Via the Web

3.1 INTRODUCTION

Two important web sites for accessing strong motion data online are maintained by COSMOS and PEER. The COSMOS web site (http://db.cosmos-eq.org) contains more than 4,000 records from around the world, although most are derived from the western US, Japan and New Zealand. The PEER database (http://peer.berkeley.edu/smcat) includes 1557 records from 143 shallow crustal earthquakes in active tectonic regions. However, few accelerograms from Europe are currently available in the PEER and COSMOS sites. The most important source of European records is the ESD (European Strong Motion Database) website (http://www.isesd.cv.ic.ac.uk) which includes more than 3,000 strong motions accelerograms recorded in Europe and Middle East along with associated earthquake-, station- and waveform-parameters. Those records have not been uniformly processed and generally lack the source and site metadata that is typical of records in the PEER database.

In Italy, interest has recently been generated in the development of a national database of strong motion accelerograms. This interest is derived from the fact that recent seismic codes in Italy allow the use of natural accelerograms for the design of structural and geotechnical systems. To meet this need, two web databases have recently been developed. One of these databases was developed for strong motion data only and is of a format and quality that is compatible with the

35

NGA database. The development of this database was described in Chapter 2. The second was developed in parallel to the database described in Chapter 2. That database was developed in the framework of the 2004-2006 DPC -INGV agreement, project S6. The resulting database is referred to as the ITACA (Italian Accelerometric Archive) website (http://itaca.mi.ingv.it). ITACA contains 2182 waveforms from 1004 earthquakes with magnitude ranging from very low values up to 6.9.

In this chapter we describe the website generated in this project to disseminate the database described in Chapter 2. The website is called SISMA, i.e. Site of Italian Strong Motion Accelerograms (http://sisma.dsg.uniroma1.it). It is expected that the same data will subsequently be archived at the PEER web site. Unlike ITACA, the database developed in this study does not include a large number of weak records of limited engineering interest (M<4) and all data are processed according to PEER/NGA standards.

The principal objective of the SISMA website is to provide high quality Italian strong motion records whose associated parameters are consistent and reliable and can be used for most engineering applications. This chapter mainly focuses on the principal search criteria in SISMA for the selection of records according to seismological, ground motion and site parameters.

3.2   SEARCHING, DISPLAYING AND DOWNLOADING DATA

The design of SISMA allows records to be located according to three different search criteria: "Search Eqk", "Search Station" and "Search Recording."

3.2.1 Earthquake Search

Clicking on the button "Search Eqk" will display the page shown in Figure 3.1, which currently includes six search options: earthquake name, year of occurr36ence, region, fault mechanism,

local magnitude and focal depth. Other magnitude values (M_W, M_S, m_b) are also provided, where available, in a detailed information page for a given earthquake.
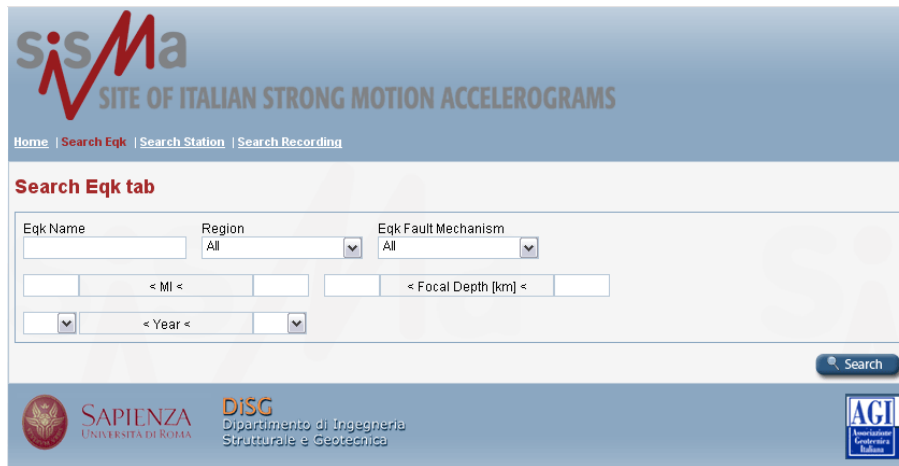

Figure 3.1. SISMA: "Search earthquake" screenshot

Once chosen values are inserted in the *Search Eqk Tab* window, the list related to that selection will appear by clicking on the Search button on the left-downer corner of the page, with the typical results shown in Figure 3.2.

The table can be exported in various formats as indicated at the bottom of the list in Figure 3.2. Details on each event are provided in a dedicated page accessed by clicking the "More Info" button on the right-end of the subject earthquake row in the list. The earthquake information page is saveable in pdf format, with a typical result shown in Figure 3.3. Information provided includes epicenter location ( ), locations of recording stations ( ), and locations of local cultural objects. This feature makes use of the GoogleMap web service (http://www.google.com/apis/maps). Recording stations on the map are listed in the end of the form with their identification code.

37

Figure 3.2. SISMA: "Search earthquake Result Tab" screenshot

Figure 3.3. SISMA: "Earthquake details" screenshot

3.2.2 Station Search

Station information can be searched in a manner similar to that for the seismic sources. By clicking on the button "Search Station", the window shown in Figure 3.4 is displayed. In this case the searchable station parameters are station name and region, instrument type and housing, agency, and site classification according to EC8 or V_{s30}.
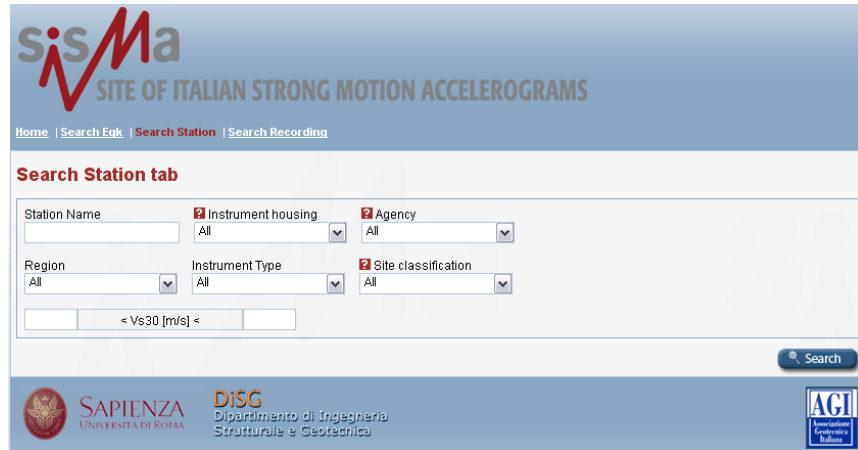
Figure 3.4. SISMA: "Search Station" screenshot

Figure 3.5 shows of the window recovered after writing "Ancona" in the *Station Name* tab. The window shows basic information on stations associated with this text string. The table can be exported in several formats.
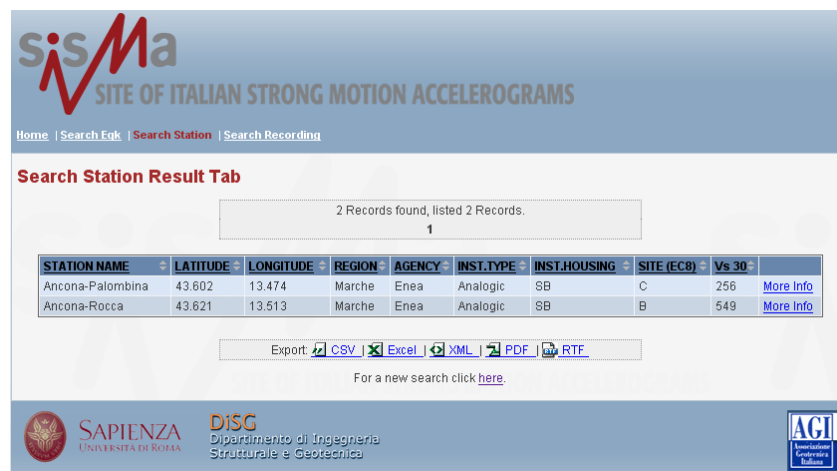
Figure 3.5. SISMA: "Search station results table" screenshot

Clicking on the button "more info" at the right side of the table, a pop-up window appears containing more detailed information about the station, the instrument and the main geological and geotechnical data. An example of this information is given in Figure 3.6. Note that a link to the V_s profile is given on this page.

Figure 3.6. SISMA: "Station details" screenshot

A list of all recordings made at the station is available from the page shown in Figure 3.6 along with a link to the details about the recordings. A map of earthquake epicentres near the station can also be accessed, as shown in Figure 3.7 for the Ancona Palombina station.

Figure 3.7. Map showing location of the earthquakes recorded by Ancona Palombina station

3.2.3 Recording Search

In the "Search recording" window, the search parameters can be a combination of earthquake, fault mechanism, distance, site classification and ground motion parameters, as displayed in Figure 3.8. SISMA offers a large number of searchable strong motion parameters such as peak ground acceleration (PGA), peak ground velocity (PGV), peak ground displacement (PGD), significant duration, Arias intensity (I_a), mean period (T_m), predominant periods (T_p), spectral acceleration at T=1s and Housner Intensity (SI).

An example search result is shown in Figure 3.9, the search criteria being all the records having PGA=0.1-0.3g on type C soil according to EC8. Figure 3.9 lists all the records identified

by this criteria grouped by earthquake in ascending magnitude order along with additional basic information.
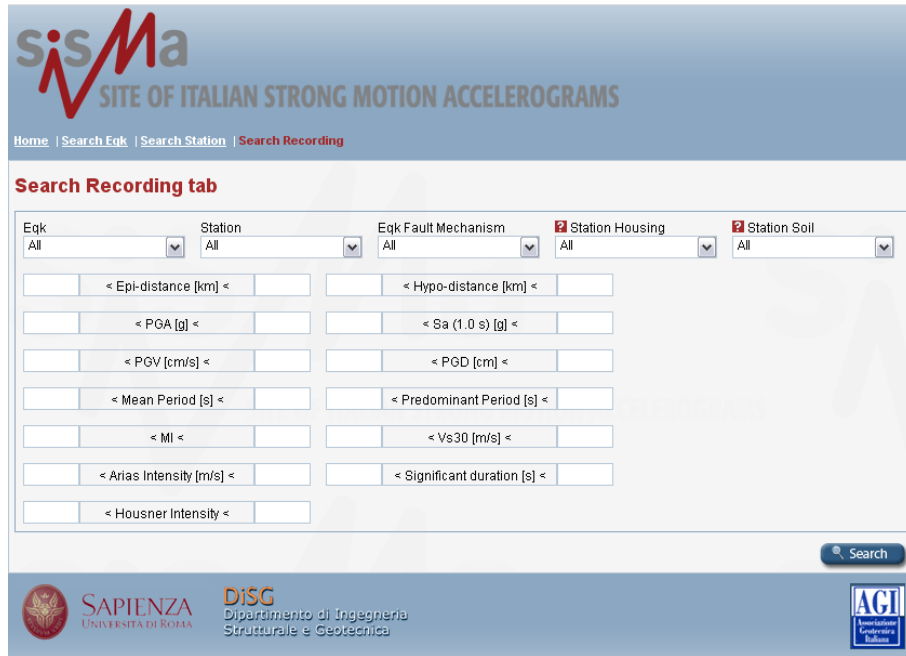
Figure 3.8. SISMA: "Search recording" screenshot

Figure 3.9. Table listing records having PGA=0.1-0.3g on type C soil according to EC8

For a given recording, clicking on "more info" produces the pop-up window shown in Figure 3.10, which contains details concerning the earthquake, station, and strong motion parameters. Acceleration, displacement, and velocity histories can be plotted along with Fourier and pseudo-acceleration response spectra (5% damping) by clicking on the button located at the lower right of the window. This information is also downloadable as a two-page pdf file including recording details and plots. An example is shown in Figure 6.11. Acceleration histories and pseudo-acceleration response spectra for the three components can be downloaded as an ASCII format in a zip file (button at the lower right in the window).

sisMa
http://sisma.dsg.uniroma1.it
SITE OF ITALIAN STRONG MOTION ACCELEROGRAMS

General Data

Eqk Name	Ancona	Station Name	Ancona-Palombina	
Eqk Date	06/02/1972	Epicentral Distance [km]	12.43	
Eqk Time	21:44:45	J&B Distance [km]	0.0	
Ml	3.0	Hypocentral Distance [km]	12.7	
Local Intensity	6.0	Closest Distance [km]	0.0	
		Azimuth	151	

Ground Motion Parameter Values

	NS	WE	NS-WE Mean	UP
PGA [g]	0.044	0.035	0.039	0.014
PGV [cm/s]	1.139	1.39	1.259	0.378
PGD [cm]	0.1	0.103	0.101	0.021
Sa (1.0 s) [g]	0.0050	0.0050	0.0050	0.0010
Predominant Period [s]	0.1	0.18	0.13	0.06
Mean Period [s]	0.17	0.25	0.2	0.16
Arias Intensity [m/s]	0.0045	0.0043	0.0043969	9.238E-4
Housner Intensity	0.0	0.0	0.0	0.0
Uniform Duration [s]	4.21	5.4	4.77	6.41
Significant Duration [s]	4.93	5.18	5.05	5.9

SAPIENZA
Università di Roma

DiSG
Dipartimento di Ingegneria
Strutturale e Geotecnica

UCLA

AGI
Associazione
Geotecnica
Italiana

Figure 3.10. Recording details for one of the Ancona Palombina station records

45
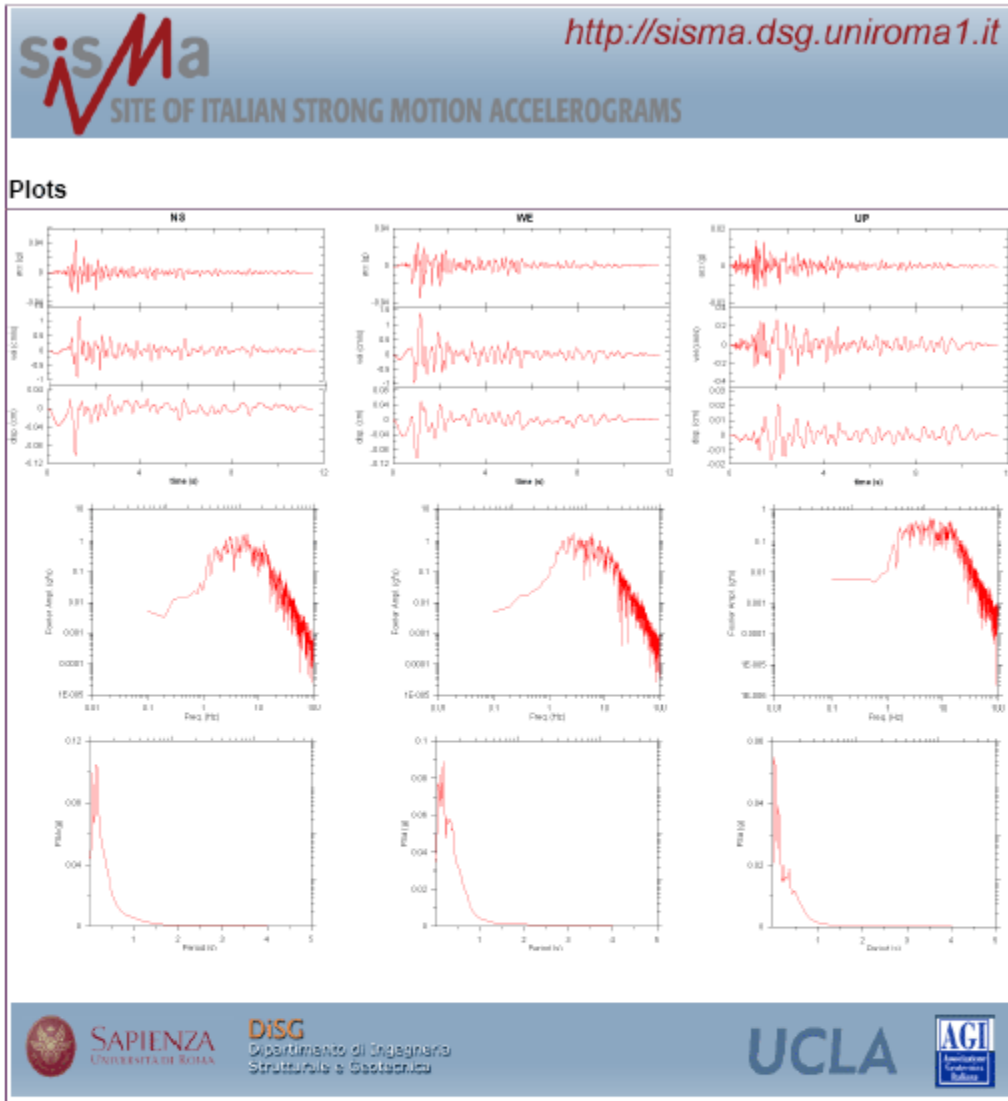
Figure 3.11. Ground motion records and spectra for one of the Ancona Palombina station recordings

46

4   Comparison of Italian data to Ground Motion Prediction Equations

4.1   INTRODUCTION

The characterization of earthquake ground motions for engineering applications generally involves the use of empirical models referred to as ground motion prediction equations (GMPEs). GMPEs describe the variation of the median and lognormal standard deviation of particular intensity measures (such as peak acceleration, spectral acceleration, or duration) conditional on magnitude, site-source distance, site condition, and other parameters. A review of GMPEs for peak acceleration and spectral acceleration published prior to 2006 is given by Douglas (2003a, 2006).

A number of GMPEs have been introduced in recent years that are re-defining the state of practice for probabilistic seismic hazard analysis (PSHA) in many earthquake-prone regions world-wide. For European applications, Ambraseys et al. (2005) and Akkar and Bommer (2007a, b) have introduced GMPEs that are considerably more sophisticated than previous relations that have seen widespread use in Europe such as Ambraseys et al. (1996) and Sabetta and Pugliese (1996). A series of GMPEs have been developed as part of the Next Generation Attenuation (NGA) project that are intended to be applicable to geographically diverse regions – the only constraint being that the region is tectonically active and earthquakes occur in the shallow crust. The NGA GMPEs are presented by Abrahamson and Silva (2008), Boore and Atkinson (2008),

Campbell and Bozorgnia (2008), Chiou and Youngs (2008), and Idriss (2008). These are referred to subsequently as AS, BA, CB, CY, and I.

An important issue for many practical applications is whether ground motions or GMPEs for one region can be applied to another. For example, this issue prompted considerable study for the SSHAC Level 4 PSHA (Budnitz et al., 1997) performed for the PEGASOS project in Switzerland (Abrahamson et al., 2002). The region of the PEGASOS project site has relatively few ground motion recordings, and hence GMPEs are borrowed from other areas for use in PSHA. Cotton et al. (2006) describe how source characteristics, path effects related to geometric spreading and anelastic attenuation, and site effects can vary from region-to-region. Those underlying physics ideally should be manifest in how a GMPE represents the scaling of a particular ground motion intensity measure (IM) with respect to magnitude, distance, and site condition. Those issues are explored subsequently in this chapter.

The database used to develop the NGA models is large (3551 recordings from 173 earthquakes) relative to those developed for relatively local regions, as is common in Europe. As mentioned previously, the NGA database is international, with most recordings derived from Taiwan, California, and Europe/Turkey (Chiou et al., 2008). As noted by Stafford et al. (2008), because of the large size and high quality of the NGA database, certain effects are well resolved in some of the NGA GMPEs that could not be evaluated using the Italian (or European) data. Examples include the effects of depth to top of rupture and nonlinear site response. The NGA data also provides the opportunity to constrain relatively complex functional forms for magnitude and distance scaling as compared to models typically used in Europe, as described further subsequently in the paper.

Because the NGA models represent a major advancement in GMPEs for PSHA due to the quality and size of the database coupled with the relative sophistication of some of the functional forms, it is naturally of interest to determine if the NGA models can be applied in specific geographic regions such as Italy. This issue has been examined in a number of previous studies, the results of which are summarized in the next section. The objective of this paper is to examine this issue by specifically testing the ability of the NGA models to capture the magnitude-scaling, distance-scaling, and site effects represented in the Italian dataset. This testing is of interest for two principal reasons (1) possible application of NGA GMPEs for PSHA in Italy and elsewhere in Europe and (2) testing the NGA models against a dataset principally populated by extensional (normal fault) earthquakes, which are poorly represented in the NGA database.

As shown in the following section, previous studies have not specifically tested the ability of NGA models to capture the magnitude-, distance-, and site-scaling represented by the European data (at least in a statistically robust way). In the subsequent section, we perform analysis of residuals to investigate the magnitude-scaling, distance-scaling and site effects issues. Components of the NGA models that are compatible or inadequate relative to the Italian data are identified. We then modify components of the NGA models judged to be inadequate, retaining the other features. The paper ends with an interpretation of the results and conclusions.

Our focus on Italian data is a matter of convenience and does not reflect an opinion on the part of the authors that ground motions should be examined on the basis of political boundaries. Our focus on Italy is predicated on the re-evaluation of the Italian dataset according to standards similar to those utilized for the NGA database, as presented in Chapter 2. As improvements in the European dataset are made elsewhere, work of this type should be undertaken for broader regions without regard to political boundaries. In that vein, the work

presented in this article should be viewed as a progress report on the broader question of application of world-wide shallow crustal GMPEs in Europe.

4.2 RECENT STUDIES COMPARING EUROPEAN AND CALIFORNIA STRONG GROUND MOTIONS

There are three general approaches that have been used to compare ground motions or GMPEs between regions: (1) direct comparison of median predictions of particular IMs from GMPEs for different regions (Campbell and Bozorgnia, 2006; Stafford et al., 2008); (2) analysis of variance (Douglas, 2004a,b); and (3) evaluation of the consistency of the data distribution with respect to the GMPE model (Scherbaum et al., 2004; Stafford et al., 2008) using a maximum likelihood approach.

4.2.1 Comparison of Medians from GMPEs

Figure 4.1 shows an example of the first approach. Estimates of peak horizontal acceleration (PHA) and 5%-damped pseudo spectral acceleration from the Akkar and Bommer (2007a) and Ambraseys et al. (2005) models are compared to those from the NGA models of AS, BA, CB, and CY. As shown by Campbell and Bozorgnia (2006) and Stafford et al. (2008), the European and NGA predicted medians generally compare well over the range of distances and magnitudes well constrained by the data. The bands of results for the two magnitudes generally show reasonably consistent vertical offsets from model-to-model (e.g., the difference between M7 and M5 PGA at R_{jb} = 30 km is reasonably consistent across models). This suggests generally consistent levels of magnitude scaling. The slopes of the median curves for a given magnitude are generally steeper for the European relations than the NGA relations for PGA, suggesting faster distance attenuation of this parameter. This potential difference in the distance attenuation was not noted by Campbell and Bozorgnia (2006) or Stafford et al. (2008).
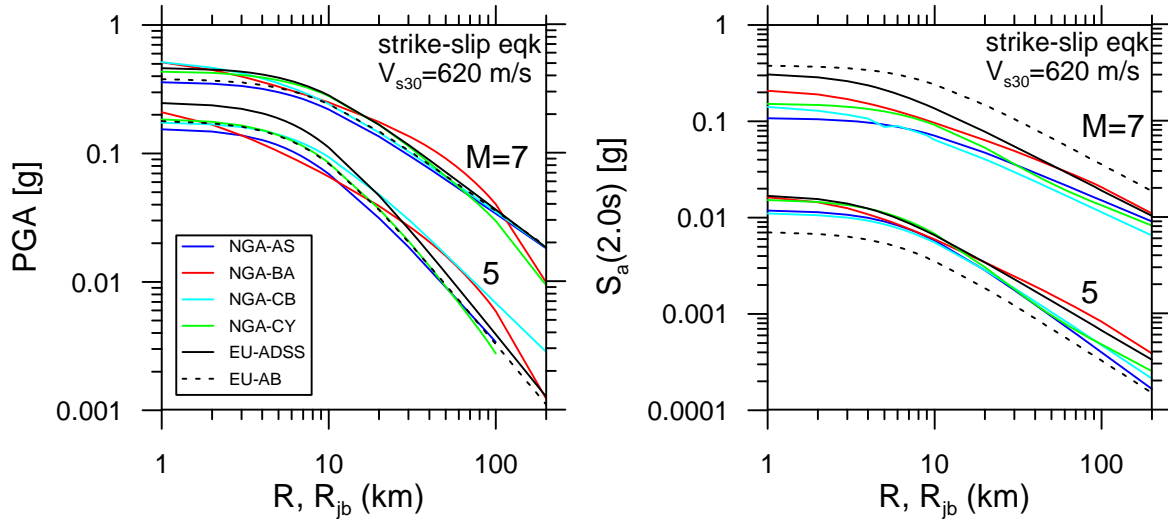
Figure 4.1. Comparison of median predictions of PGA and 2.0 s pseudo spectral acceleration for strike slip earthquakes and soft rock site conditions from NGA and European GMPEs. AS=Abrahamson and Silva (2008); BA=Boore and Atkinson (2008); CB=Campbell and Bozorgnia (2008); CY=Chiou and Youngs (2008); ADSS = Ambraseys et al. (2005); AB = Akkar and Bommer (2007)

4.2.2 Analysis of Variance

The approach termed "analysis of variance" was applied by Douglas (2004a) to compare ground motions for five local regions within Europe and Douglas (2004b) to compare ground motions from Europe, New Zealand, and California. The procedure involves calculating the mean (μ) and variance (σ^2) of the log of the data inside of particular magnitude and distance bins (*M-R* bins) for two different regions (e.g., Europe and California) and combinations of regions. Individual data points are adjusted for a linear site factor from Ambraseys et al. (1996) before the calculation of mean and variance. These results are then used in two ways. First, for a given *M-R* bin and pair of regions, the variance across regions [termed $(\sigma^2)_{inter\text{-}region}$] is compared to the within-region variance [termed $(\sigma^2)_{intra\text{-}region}$] using statistical tests that evaluate whether the data sets are significantly distinct. If $(\sigma^2)_{inter\text{-}region} > (\sigma^2)_{intra\text{-}region}$ in a statistically significant way, there

is likely to be significantly different medians between regions. The second use of the binned results is to plot medians for each *M-R* bin together for pairs of regions.

Using the above approach, Douglas (2004a) found similar variances for the various regions in Europe, indicating a lack of regional variations. Accordingly, Douglas (2004b) combined all of the European data into a single category for comparison to New Zealand and California data. The Europe-California comparisons indicate that approximately half of the *M-R* bins demonstrate significantly different inter- and intra-region variances. The distinction was towards larger ground motions in California (Douglas, 2004b). Careful analysis of Figure 4.1 of Douglas (2004b) indicates that the California and European means for most *M-R* bins have similar amplitudes in short distance bins (< 20 km), whereas California amplitudes are larger at larger distances (> 30 km). Thus, Douglas' (2004b) finding of larger California ground motions could be alternatively expressed as more rapid distance attenuation in Europe. Offsets between California and European means within a given well-populated distance category (e.g., 10-15 km) do not vary significantly across magnitude bins, suggesting similar levels of magnitude scaling.

4.2.3 Overall Goodness-of-Fit of Model to Data

This approach, developed by Scherbaum et al. (2004), provides an overall evaluation of goodness-of-fit of a GMPE to a dataset. A normalized residual is calculated for recording *j* from event *i* in a dataset as:

$$Z_{T,ij} = \frac{\ln\left(IM_{obs,ij}\right) - \ln\left(IM_{mod,ij}\right)}{\sigma_T}$$

(4.1)

where $\ln\left(IM_{obs,ij}\right)$ represents the IM value from the record, $\ln\left(IM_{mod,ij}\right)$ represents the median model prediction for the same magnitude, site-source distance, and site conditions of the record, and σ_T represents the total standard deviation of the model (combination of inter- and intra-event

standard deviations). If the data is unbiased with respect to the model and has the same dispersion, the normalized residuals (Z_T) should have zero mean and standard deviation of one – i.e., the properties of the standard normal variate. Accordingly, in simple terms, the procedure of Scherbaum et al. (2004) consists of comparing the actual Z_T distribution to that of the standard normal variate. Note that this procedure tests both misfit of the median and standard deviation.

Stafford et al. (2008) extended this method to consider both inter- and intra-event variability. They compared European data to the NGA relation of Boore and Atkinson (2008) and the European models of Ambraseys et al. (2005) and Akkar and Bommer (2007a,b). The Boore and Atkinson (2008) relation was shown to match the median of the European data nearly as well as European GMPEs. The Boore and Atkinson standard deviation, however, is lower than values from the European relations. This discrepancy was attributed to the magnitude-dependence of the European GMPE standard deviation models whereas the Boore and Atkinson standard deviation is homoscedastic (constant with respect to magnitude).

4.2.4 Interpretation

It should be emphasized that the Scherbaum et al. (2004) approach assesses model performance in an overall sense – i.e., all aspects of the model (magnitude-scaling, distance-scaling, site effects) are evaluated in a lumped manner. If one of these model components was in error, that effect could be obscured through compensating errors in the analysis of normalized residuals. Accordingly, while the results of Stafford et al. (2008) are certainly promising with respect to the application of NGA relations in Europe, they do not specifically address whether individual components of the NGA models are adequate with respect to European data. Because there is some evidence of faster distance attenuation of European data relative to California data (Douglas, 2004b) and active regions generally (Figure 4.1), a formal analysis of the adequacy of

the NGA relations with respect to magnitude-scaling, distance-scaling, and site effects is needed. We address these issues in the remainder of this article.

4.3 ATTRIBUTES OF NGA AND EUROPEAN GROUND MOTION PREDICTION EQUATIONS

Ground motion prediction equations are formulated with varying degrees of complexity in their functional form as a result of author preference and the size and completeness of the database used in the analysis. The NGA models include two relatively simplified models (BA and I) and three more complex models (AS, CB, and CY). Attributes of the NGA models and several European relations with respect to magnitude-, distance, and V_{s30}-scaling are summarized below. The European models considered here are Ambraseys et al. (2005) and Akkar and Bommer (2007a), which are referred to subsequently as ADSS and AB, respectively.

Table 4.1. Magnitude scaling attributes of NGA and recent European GMPEs

	GMPE	M-scaling[1]	Notes[2]	Parameters[3]
NGA	AS 2008	2nd-order polynomial	Separate style of faulting term	M_w; F
NGA	BA 2008	M≤M_h: 2nd-order polynomial M>M_h: Linear	Coefficients depend on focal mech; M_h set by regression	M_w; F
NGA	CB 2008	Multiple connected line segments, slope depending on M_w	Separate style of faulting term	M_w; F
NGA	CY 2008	sum of linear term & c' × ln(1-exp{c''-c'''M})	Separate style of faulting term, main shocks only	M_w; F
NGA	I 2008	Linear	Separate style of faulting term	M_w; F
Eur.	AB 2007	2nd-order polynomial	Separate style of faulting term	M_w; F
Eur.	ADSS 2005	Linear	Separate style of faulting term	M_w; F

[1] c', c'', etc. indicate coefficients or combinations of coefficients determined by regression
[2] In each case, magnitude also affects distance scaling
[3] M_w=Moment magnitude; F=focal mechanism

Table 4.1 summarizes the principal attributes of the magnitude-scaling in the GMPEs considered here. Magnitude scaling varies from linear (I, ADSS) to nonlinear functions expressed as 2nd order polynomials (AS, BA, AB), piecewise linear relations (CB), and more complex forms (CY). Figure 4.2 shows the variation with magnitude of PGA and T=2 sec 5%-

damped spectral acceleration for a strike-slip, surface rupture earthquake at $R=R_{jb}=30$ km and rock site conditions. The slopes of the curves at a given period are generally similar.
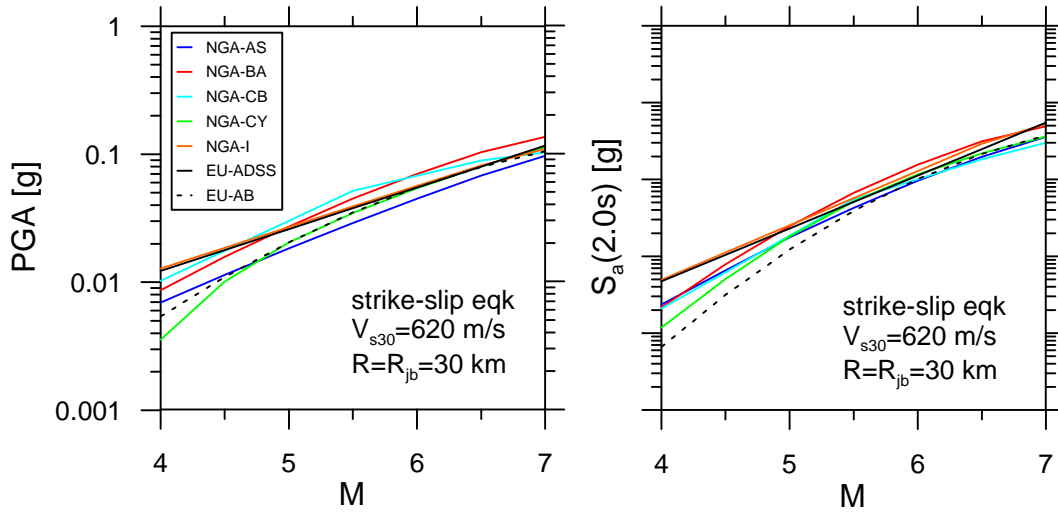
Figure 4.2. Comparison of magnitude scaling of PGA and 2.0 s S_a for strike slip earthquakes and soft rock site conditions from NGA and European GMPEs.

Table 4.2 shows the forms of the distance attenuation functions in the GMPEs used here. Many of the models (AS, CB, AB, ADSS) utilize a relatively simple form consisting of the product of a linear function of magnitude and the natural log of the SRSS (square root of sum of squares) of distance and a source depth term (denoted h in Table 4.2). The linear term accounts for the decrease of attenuation with increasing magnitude (the intercept is negative and the coefficient for the change of slope with magnitude is positive). The BA and CY models account for the variation of distance attenuation with distance to capture the dominant effects of body waves at distances < 40-70 km and surface waves at larger distances. Additional anelastic attenuation terms (represented by $\gamma(M)$) are included by CY and I. Figure 4.1 compares the distance attenuation of NGA and European models. As noted previously, the slopes from

European models are slightly greater. Among the NGA models, the steepening of the slope of the median curve for PGA at distances exceeding about 70 km is apparent in Figure 4.1 from the BA and CY models whereas the AS and CB slopes are constant. Also noteworthy is the relative slopes in the 10-70 km distance range, where much of the data lies. In this range, the steepest slope is CY, the flattest is BA, and AS and CB are intermediate. These differences have implications with respect to the Italian data, as discussed further below.

Table 4.2. Distance scaling functions used in NGA and recent European GMPEs

GMPE		R-scaling[1]	Notes	Parameters[2]
NGA	AS 2008	$\left[a_2 + a_3\left(M - M_r\right)\right] \times \ln\left(\sqrt{R^2 + h^2}\right)$	Additional hanging wall, depth to top of rupture, and large distance scaling terms	R, R_{jb}, R_x, Z_{tor}, W, δ
NGA	BA 2008	$\left[c_1 + c_2\left(M - M_r\right)\right] \times \ln\left(\dfrac{\sqrt{R_{jb}^2 + h^2}}{R_{ref}}\right) + c_3\left(\sqrt{R_{jb}^2 + h^2} - R_{ref}\right)$ None		R_{jb}
NGA	CB 2008	$\left[c_4 + c_5 M\right] \times \ln\left(\sqrt{R^2 + h^2}\right)$	Additional hanging wall term with functional dependence on δ and Z_{tor}	R, R_{jb}, Z_{tor}, δ
NGA	CY 2008	$c_4 \ln\left[R + c_5 \cosh\left\{c_6 \max\left(M - M_r, 0\right)\right\}\right] + \left(c_{4a} - c_4\right) \ln\left(\sqrt{R^2 + c_{RB}^2}\right) + \gamma(M) \times R$ Additional hanging wall terms with functional dependence on δ and Z_{tor}		R, R_{jb}, R_x, Z_{tor}, δ
NGA	I 2008	$-\left[\beta_1 + \beta_2 M\right] \times \ln\left(R + 10\right) + \gamma(T)R$	None	R
Eur.	AB 2007	$\left[b_4 + b_5 M\right] \times \ln\left(\sqrt{R_{jb}^2 + h^2}\right)$	None	R_{jb}
Eur.	ADSS 2005	$\left[a_3 + a_4 M\right] \times \ln\left(\sqrt{R_{jb}^2 + h^2}\right)$	Separate style of faulting term	R_{jb}

[1] a, c, and β terms format retained from original model; h and M_r variables used here to show compatibility across models, these terms do not necessarily match those in the source publications. R_{ref} is specific to BA (2008)

[2] R=rupture distance; R_{jb}=closest distance to horizontal projection of rupture plane; R_x defined in Figure 3; Z_{tor}=depth to top of rupture; W=fault width; δ=dip angle

The models by AS, CB, and CY include hanging wall terms, which account for the larger ground motions observed on the hanging wall of dipping faults. As shown in Table 4.2, a distance parameter used to define this effect for the AS and CY models is R_x, which is defined in Figure 4.3. Additional terms used to define hanging wall effects include depth to top of rupture (Z_{tor}), dip angle (δ), and down-dip fault width (W).
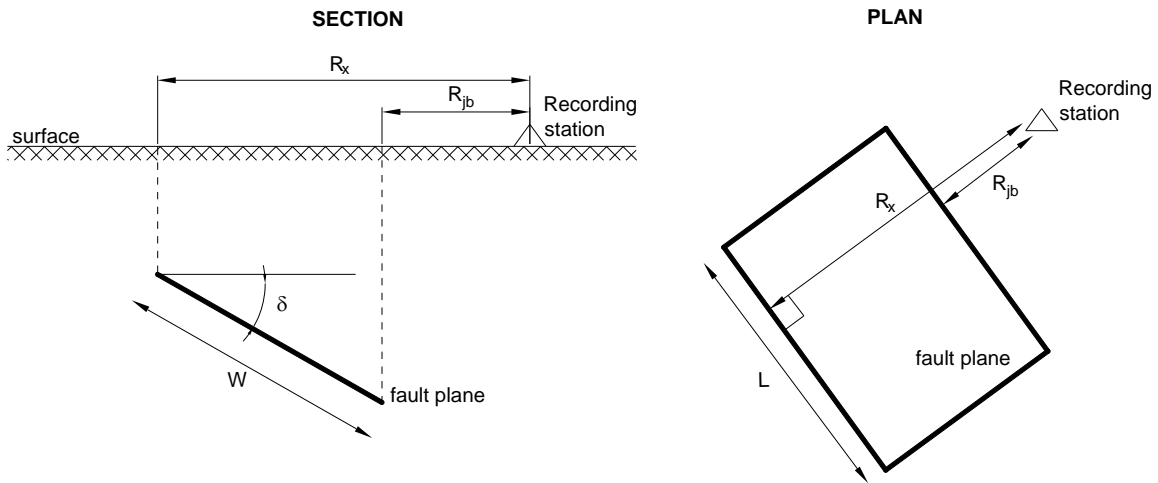
Figure 4.3. Schematic illustration of dipping fault and measurement of R_x parameter used in hanging wall terms for the AS and CY GMPEs.

The site terms utilized in the GMPEs vary significantly in complexity. All NGA models except Idriss (2008) utilize V_{s30} as a site term. As shown in Figure 4.4, the level of amplification for weak input motions (corresponding to nearly elastic conditions) increases with decreasing V_{s30}. In the AS, BA, CB, and CY GMPEs, the reference rock parameter used with the nonlinear components of the site terms is $\widehat{PGA}_{1100}$, which is the median peak acceleration on rock with V_{s30}=1100 m/s. As shown in Figure 4.4, the slope of the amplification function relative to $\widehat{PGA}_{1100}$ flattens with increasing V_{s30}. While the NGA site terms were developed using different procedures (simulation-based, empirical, etc.), Figure 4.4 shows that the resulting models from AS, BA, CB, and CY are generally similar. The Idriss (2008) model does not have a site term. The ADSS and AB site terms are linear and constant for qualitative site descriptors (soft soil, stiff soil, rock). In addition to V_{s30}, the AS, CB, and CY site models include a basin depth term, which is taken as the depth to a particular shear wave velocity isosurface. AS and CY take this depth as $Z_{1.0}$ (depth to V_s=1.0 km/s) whereas CB take this depth as $Z_{2.5}$ (depth to V_s=2.5 km/s).
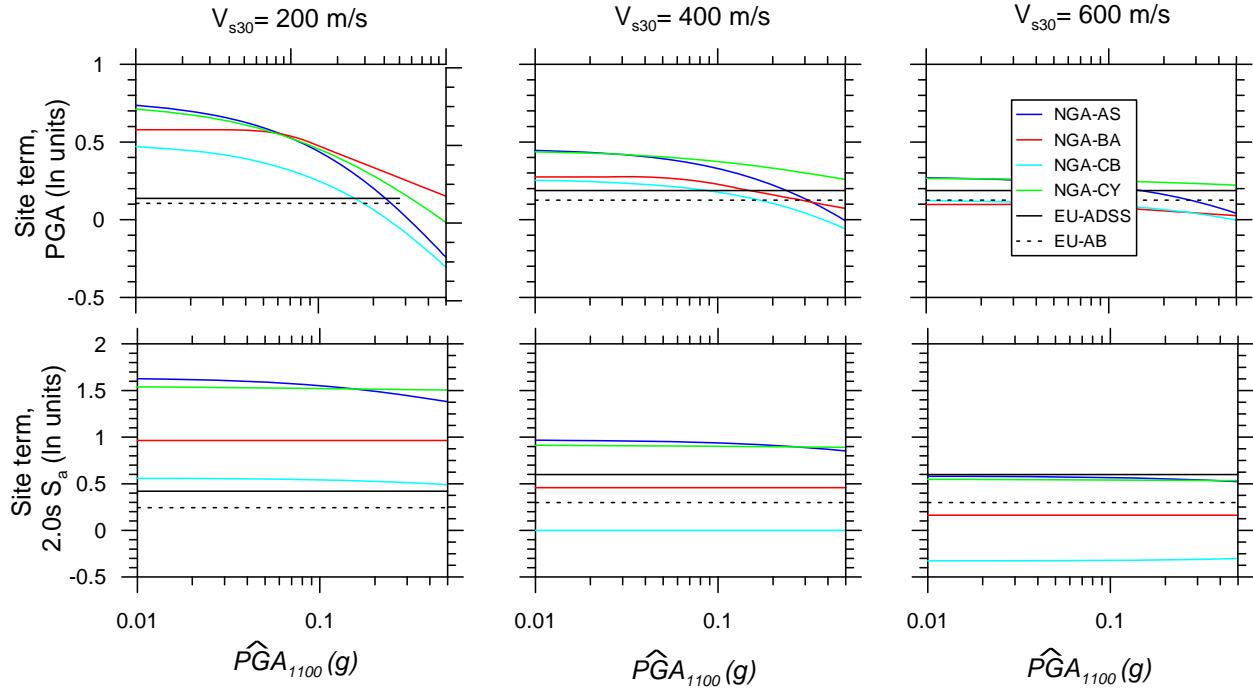
Figure 4.4. Comparison of site terms for PGA and 2.0 s pseudo spectral acceleration from NGA and European GMPEs

For the analyses conducted in this report, we consider each of the GMPEs listed in Tables 4.1 and 4.2 except Idriss (2008). That model is excluded due its lack of a site term. A significant fraction of the Italian data are on soil site conditions and hence require the use of a site term.

4.4   DATABASE

The database used in this study is presented in Chapter 2. The strong motion data were corrected and uniformly processed by the same seismologists (Walter Silva and Robert Darragh) who prepared the data for NGA. During this process, about 50% of the Italian motions were screened out because of s-triggers and other problems. Figure 4.5 shows the number of available recordings with M > 4 as a function of the maximum usable period, taken as the inverse of $1.25 \times f_{HP}$, where f_{HP} is the high-pass corner frequency used in the data processing, which varies from record-to-record according to signal characteristics. Note that there is a significant drop off

in the data for periods > 2-3 sec and results obtained from the data should not be considered useful at those long periods.
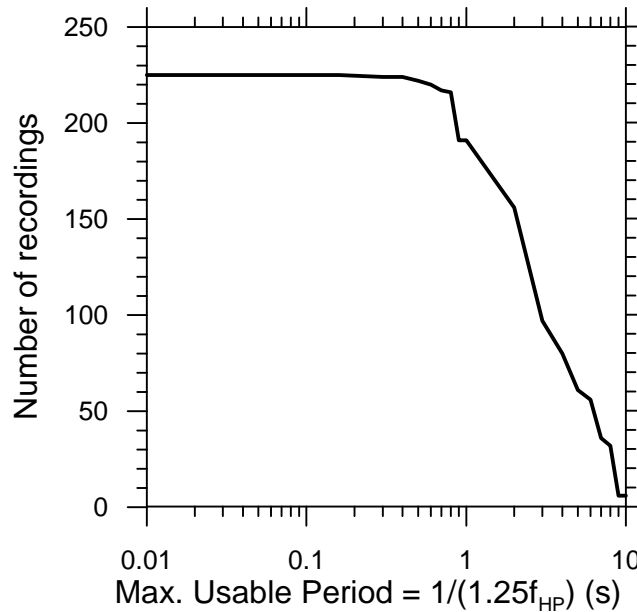
Figure 4.5. Variation of number of available recordings with M > 4 in Italian database with the maximum usable period, which is taken as the inverse of 1.25×f_{HP} (f_{HP} = high pass corner frequency used in data processing)

Source parameters were compiled from databanks maintained by the Italian Institute of Geology and Vulcanology (www.ingv.it) and include moment magnitude, focal mechanism, and hypocenter location for 52 of the 89 events. The other 37 events are small magnitude (M_l=3-5), and for those events M_l is taken as an estimate of M_w. For events with magnitudes > ~ 5.5 finite source parameters were compiled from INGV. Closest distance (R), Joyner-Boore distance (R_{jb}) and a hanging wall index were evaluated by Brian Chiou (personal communication, 2008) using the source parameters and site locations in the database. Distances R and R_{jb} are taken to the fault rupture plane where available. For small magnitude earthquakes without a finite fault model, R is taken as the hypocentral distance and R_{jb} is taken as the epicentral distance. Since the only events without finite fault models are small in magnitude and hence have small fault dimensions, this

approximation was considered to be reasonable. For events with unknown hypocentral depth and focal mechanism, those parameters were estimated based on available data from the local region.

The hanging wall index compiled by Chiou indicates whether a site is located n the hanging wall, footwall, or in a neutral (side) position relative to a dipping fault. For hanging wall sites, parameter R_x is estimated as:

$$R_x \approx R_{jb} + W\cos(\delta)$$

(4.2)

where W = fault width and δ = dip angle. Parameters W and δ are compiled in Chapter 2 for earthquakes with finite source models. For other events where these parameters were needed, they were estimate using empirical models for W (Wells and Coppersmith, 1994) and dip angles for nearby faults (for δ). Distance R_x is not needed for footwall or neutral sites. The approximation in Eq. 4.2 is because R_x is strictly measured normal to the fault strike, as shown in Figure 4.3. Since the hanging wall region can extend slightly beyond the ends of the fault, there will be some sites for which the use of Eq. 4.2 is approximate. As indicated in Table 4.2, another parameter needed for some of the NGA hanging wall terms is depth to top of rupture (Z_{top}). As with dip angle, this is taken from the finite fault database where available and otherwise is calculated assuming the hypocenter is at mid-width as follows:

$$Z_{top} \approx Z_{hyp} - \frac{W}{2}\sin(\delta)$$

(4.3)

where Z_{hyp}=hypocentral depth. Additional adjustments are made on a case-by-case basis as needed (i.e., $Z_{top} < 0$, etc.).

Figure 4.6 shows the magnitude-distance distribution relative to that in the NGA database described by Chiou et al. (2008). Relative to the NGA data, the Italian data is generally sparse for $R < 10$ km and M > 6.5. There is a reasonable degree of overlap in the datasets for R=10-70

km and M=4.5-6. The Italian data is richer than NGA for M < 4.5. An important distinction

between the NGA and Italian databases concerns the preponderance of normal fault earthquake

in the Italian data (44 of 89 events). In contrast, the PEER database has only 13 normal fault

earthquakes with 87 recordings. Accordingly, comparison of the PEER NGA relations to Italian

data provides the opportunity to test their applicability for a predominantly extensional region.
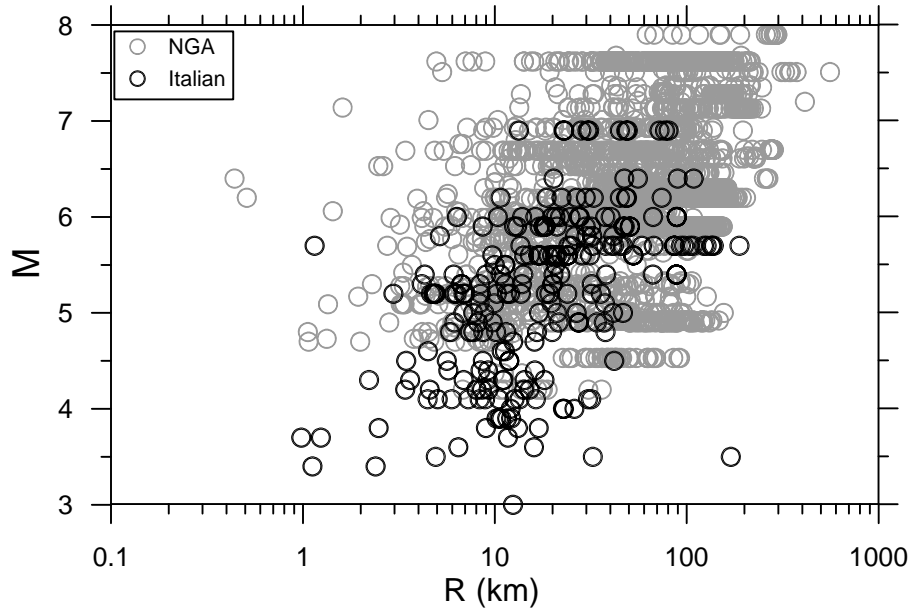
Figure 4.6. Distribution of NGA and Italian data with respect to magnitude and rupture distance

In Chapter 2, we present V_{s30} parameters for all Italian sites utilized in the present

analysis. Basin depth term $Z_{1.0}$ is taken from velocity profiles where available. Otherwise $Z_{1.0}$ is

estimated from V_{s30} using the following function proposed by CY:

$$\ln\left(Z_{1.0}\right) = 28.5 - 0.4775\ln\left(V_{s30}^8 + 387.7^8\right)$$

(4.4)

where $Z_{1.0}$ is in km and V_{s30} is in m/s. Data from approximately 100 sites with measured values

of $Z_{1.0}$ (using the database of Scasserra et al., 2008) suggest that the model in Eq. 4.4

overestimates $Z_{1.0}$ for Italian sites with $V_{s30} < \sim 600$ m/s. However, values of $Z_{1.0}$ are not

available for deep sites due to the lack of sufficiently deep boreholes. Hence, the validation

database is biased towards shallow sites and we cannot reliably evaluate the adequacy of Eq. 4.4 for Italian data. Lacking an alternative, we utilize its estimates of $Z_{1.0}$ for sites lacking data. Depth term $Z_{2.5}$ is evaluated from $Z_{1.0}$ using the following relation similarly derived from the NGA data by Campbell and Bozorgnia (2007):

$$Z_{2.5} = 0.519 + 3.595 Z_{1.0}$$
(4.5)

where both depths are in km. Use of Eq. 4.5 implies similar velocity gradients in rock for California and Italian sites, which may not be the case.

We recognize that the empirical sediment depth estimates described above may not apply to Italy. By using medians that are dependent on V_{s30} for the majority of sites, we are essentially using the average basin effect in the NGA GMPEs. If we are significantly in error, it would be expected to produce bias at long periods, where the basin effects are most pronounced. This is evaluated subsequently in the article.

4.5   DATA ANALYSIS

4.5.1   Overall GMPE Bias and Standard Deviation Relative to Italian Data

We begin by evaluating residuals between the data and a particular GMPE referred to with index k (k=1…6 for the six models from Tables 1 and 2 that are utilized). Residuals are calculated as:

$$\left(R_{i,j}\right)_k = \ln\left(IM_{i,j}\right)_{data} - \ln\left(IM_{i,j}\right)_k$$
(4.6)

Index i refers to the earthquake event and index j refers to the recording within event i. Hence, $\left(R_{i,j}\right)_k$ is the residual of data from recording j in event i as calculated using GMPE k. Term $\ln\left(IM_{i,j}\right)_{data}$ represents the geometric mean of the two horizontal components of the data in

natural log units while term $\ln\left(IM_{i,j}\right)_k$ represents the median calculated using GMPE k in natural log units.

Residuals are calculated using Eq. 4.6 for six GMPEs – AS, BA, CB, CY, AB, and ADSS. The analysis of residuals with respect to magnitude-, distance, and site-scaling requires that event-to-event variations be separated from variations of residuals within events. This is accomplished by performing a mixed effects regression (Abrahamson and Youngs, 1992) of residuals according to the following function:

$$\left(R_{i,j}\right)_k = c_k + \left(\eta_i\right)_k + \left(\varepsilon_{i,j}\right)_k \tag{4.7}$$

where c_k represents a mean offset (or bias) of the data relative to GMPE k, η_i represents the event term for event i (explained below), and $\varepsilon_{i,j}$ represents the intra-event residual for recording j in event i. Event term η_i represents approximately the mean offset of the data for event i from the predictions provided by the GMPE median (after adjusting for mean offset c_k, which is based on all events). Event terms provide a convenient mechanism for testing the ability of a GMPE to track the magnitude scaling of recordings in a dataset, as shown below. Event terms are assumed to be log-normally distributed, and generally have nearly zero mean and standard deviation (in natural log units) denoted as τ. Intra-event error ε is also assumed to be log-normally distributed with nearly zero mean and standard deviation=σ.

Figure 4.7 shows the distribution of event terms from the Italian data as a function of the number of recordings per event. The scatter of event terms is large for sparsely recorded events (1-2 recordings) but is relatively stable for events with three or more recordings. Accordingly, for subsequent analysis we remove from the data set events with only one or two recordings.
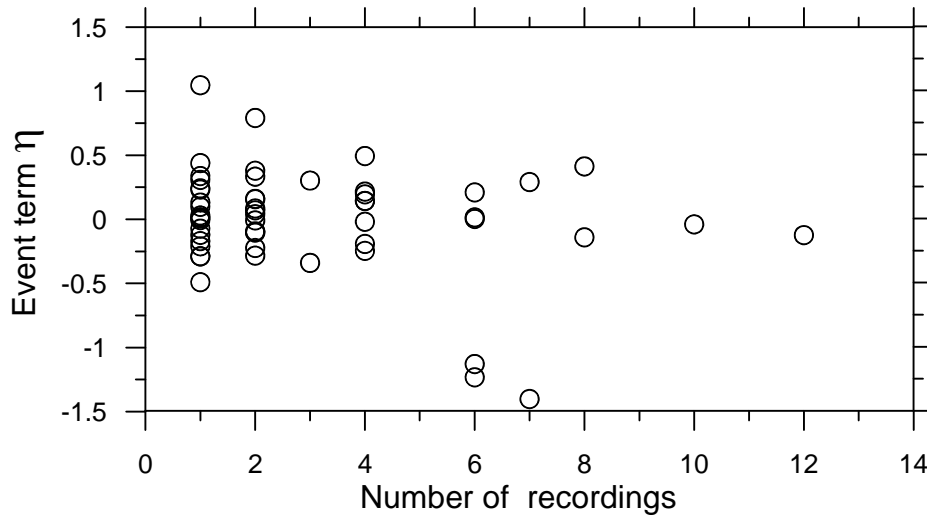
Figure 4.7. Variation of event terms with number of recordings, showing decrease of scatter for events with more recordings. Data from 1- and 2-recording events are not used in this study due to large scatter of event terms.

Using the dataset for earthquakes with three or more recordings, mixed effects regressions were performed using Eq. 4.7 for the aforementioned six GMPEs for five different ground motion intensity measures (IMs): peak acceleration and 5%-damped pseudo spectral acceleration (S_a) at periods of 0.2, 0.5, 1.0 and 2.0 seconds. The results are summarized in Table 4.3, which shows for each GMPE and IM values of c, τ, and σ. Figure 4.8a plots the average misfit of Italian data to the NGA GMPEs as expressed by parameter c, along with ±95% confidence intervals on the estimate of c. Parameter c is not generally significantly offset from zero, nor does it have a significant trend with period. An exception is CB, for which c is consistently and significantly negative for $T>{\sim}0.2$ s. Negative values of c indicate an average over-prediction of the Italian data by the CB GMPE.

Table 4.3. Summary of regression results for NGA GMPEs residuals relative to Italian data

GMPE		Period (s)	c	σ	τ	M-scaling		R-scaling	
						b_M	1-p	b_R	1-p
NGA	AS	PGA	-0.15 ± 0.32	0.71	0.76	-0.16 ± 0.37	0.60	-0.19 ± 0.13	0.99
		0.2	-0.14 ± 0.31	0.80	0.71	0.02 ± 0.36	0.08	-0.16 ± 0.15	0.96
		0.5	-0.23 ± 0.32	0.86	0.57	0.20 ± 0.38	0.68	-0.07 ± 0.14	0.70
		1.0	-0.11 ± 0.30	0.75	0.69	0.31 ± 0.34	0.92	-0.04 ± 0.14	0.46
		2.0	-0.04 ± 0.31	0.86	0.68	0.24 ± 0.32	0.85	0.07 ± 0.16	0.58
NGA	BA	PGA	0.09 ± 0.32	0.73	0.72	-0.36 ± 0.36	0.94	-0.31 ± 0.14	1.00
		0.2	0.10 ± 0.31	0.83	0.68	-0.24 ± 0.34	0.83	-0.34 ± 0.16	1.00
		0.5	-0.08 ± 0.29	0.86	0.64	0.07 ± 0.32	0.32	-0.21 ± 0.14	0.99
		1.0	-0.03 ± 0.28	0.74	0.64	0.21 ± 0.32	0.81	-0.13 ± 0.14	0.93
		2.0	-0.06 ± 0.29	0.86	0.61	0.06 ± 0.30	0.30	-0.05 ± 0.16	0.42
NGA	CB	PGA	-0.17 ± 0.31	0.73	0.70	0.24 ± 0.32	0.85	-0.24 ± 0.14	1.00
		0.2	-0.25 ± 0.28	0.81	0.61	-0.08 ± 0.30	0.38	-0.22 ± 0.16	1.00
		0.5	-0.37 ± 0.28	0.88	0.78	0.19 ± 0.30	0.77	-0.10 ± 0.15	0.81
		1.0	-0.28 ± 0.26	0.75	0.58	0.26 ± 0.28	0.93	-0.06 ± 0.14	0.62
		2.0	-0.26 ± 0.25	0.88	0.50	0.14 ± 0.22	0.77	0.03 ± 0.18	0.24
NGA	CY	PGA	0.08 ± 0.30	0.64	0.69	-0.29 ± 0.35	0.89	-0.08 ± 0.12	0.79
		0.2	0.16 ± 0.28	0.74	0.61	-0.14 ± 0.30	0.65	-0.08 ± 0.14	0.72
		0.5	0.00 ± 0.27	0.91	0.57	0.05 ± 0.28	0.30	-0.04 ± 0.15	0.44
		1.0	-0.02 ± 0.25	0.77	0.52	0.15 ± 0.24	0.78	-0.02 ± 0.14	0.19
		2.0	-0.12 ± 0.27	0.91	0.53	0.06 ± 0.24	0.36	0.12 ± 0.17	0.84
EU	AB	PGA	0.04 ± 0.30	0.68	0.69	-0.29 ± 0.34	0.90	-0.11 ± 0.12	0.90
		0.2	0.04 ± 0.28	0.80	0.58	-0.10 ± 0.28	0.51	-0.14 ± 0.14	0.95
		0.5	-1.02 ± 0.31	0.80	0.69	-0.22 ± 0.34	0.78	-0.24 ± 0.14	0.99
		1.0	0.06 ± 0.25	0.75	0.53	0.06 ± 0.26	0.36	0.02 ± 0.14	0.22
		2.0	0.02 ± 0.25	0.87	0.49	-0.11 ± 0.22	0.67	0.06 ± 0.16	0.54
EU	ADSS	PGA	-0.17 ± 0.28	0.68	0.65	-0.04 ± 0.34	0.21	-0.07 ± 0.13	0.70
		0.2	-0.29 ± 0.28	0.80	0.60	0.10 ± 0.30	0.49	-0.08 ± 0.15	0.72
		0.5	-0.42 ± 0.32	0.76	0.71	0.31 ± 0.34	0.92	0.03 ± 0.14	0.36
		1.0	-0.37 ± 0.29	0.76	0.65	0.39 ± 0.30	0.98	0.05 ± 0.14	0.53
		2.0	-0.55 ± 0.28	0.87	0.57	0.25 ± 0.26	0.94	0.11 ± 0.08	0.80

Figures 4.8b-c plot the inter- and intra-event standard deviations (τ and σ, respectively) versus period as evaluated from the regressions performed using Eq. 4.7. Results are shown for the NGA GMPEs only. Also shown in Figures 4.8b-c are the ranges of τ and σ provided by a representative NGA GMPE (CY) and a European GMPE (AB) for M=5-7. The standard deviation terms from the Italian data are significantly larger than those provided by CY and the other NGA relations. Intra-event standard deviation σ is similar to values obtained previously by AB for Europe, but our τ terms are much larger. This is caused by three events with large

negative event terms (Molise 31-10-2002 and 01-11-2002, Trasaghis-Friuli 28-5-1998), as shown in Figure 4.7. If those events were omitted from the calculation, τ would reduce to values comparable to those from previous studies. Accordingly, we believe the difference in Figure 4.8b is likely a result of the poorly sampled database and a corresponding large impact of these outliers. Differences between the Italian and NGA σ terms are relatively well established by the available data and are discussed further below.
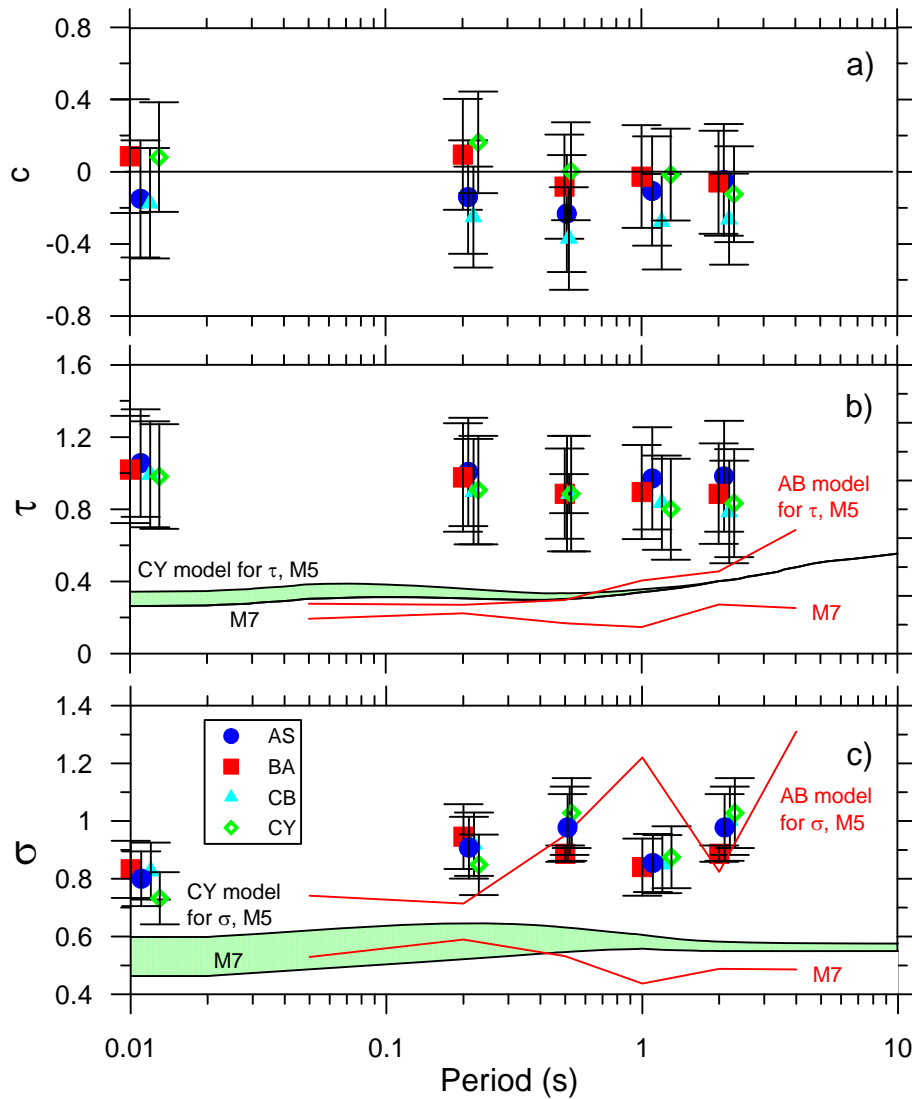
Figure 4.8. Variation with period of mean bias parameter (c), inter-event dispersion (τ), and intra-event dispersion (σ) evaluated from regression of NGA residuals relative to Italian data with Eq. 4.7.

4.5.2 Magnitude Scaling

We next turn to the question of how well the selected GMPEs capture the magnitude scaling of the Italian dataset. The event terms are plotted against magnitude in Figure 4.9 for the IMs of PGA, 0.2 s S_a, and 1.0 s S_a. To help illustrate trends, we also plot a fit line and its ±95% confidence intervals, the fit being made according to:

$$\eta_i = a_M + b_M M_i + \left(\kappa_M\right)_i \tag{4.8}$$

In Eq. 4.8, subscript k has been dropped, but the regressions are performed separately for each GMPE. Parameters a_M and b_M are regression coefficients and $(\kappa_M)_i$ is the residual of the fit for event i. Slope b_M is of interest because if significantly non-zero, it suggests the magnitude scaling in the model does not match the data. The columns with the 'M-scaling' heading in Table 4.3 indicate b_M, its ±95% confidence intervals, and results of hypothesis testing described below.

The statistical significance of the magnitude-dependence of event terms is assessed two ways. The first significance test consists of comparing the absolute value of b_M to its estimation error (taken as the ±95% confidence intervals shown in Table 4.3). When $\left|b_M\right|$ exceeds the estimation error, the nonlinearity is considered significant. Secondly, sample 't' statistics are compiled to test the null hypothesis that b_M=0. This statistical testing provides a significance level = p that the null hypothesis cannot be rejected. For clarity of expression, we show in Table 4.3 and Figure 4.9 values of 1-p, which we refer to as a "rejection confidence for a zero slope model." The rejection confidence levels are consistently small (i.e., < 95%), with only one exception for European GMPE ADSS (at T=1.0 sec). Therefore, while the slope of the trend lines (b_M) in Figure 4.9 are non-zero, we find that they are not statistically significant at the 95% confidence level. On the basis of this result, we conclude that the selected GMPEs adequately capture the magnitude scaling of the Italian dataset.
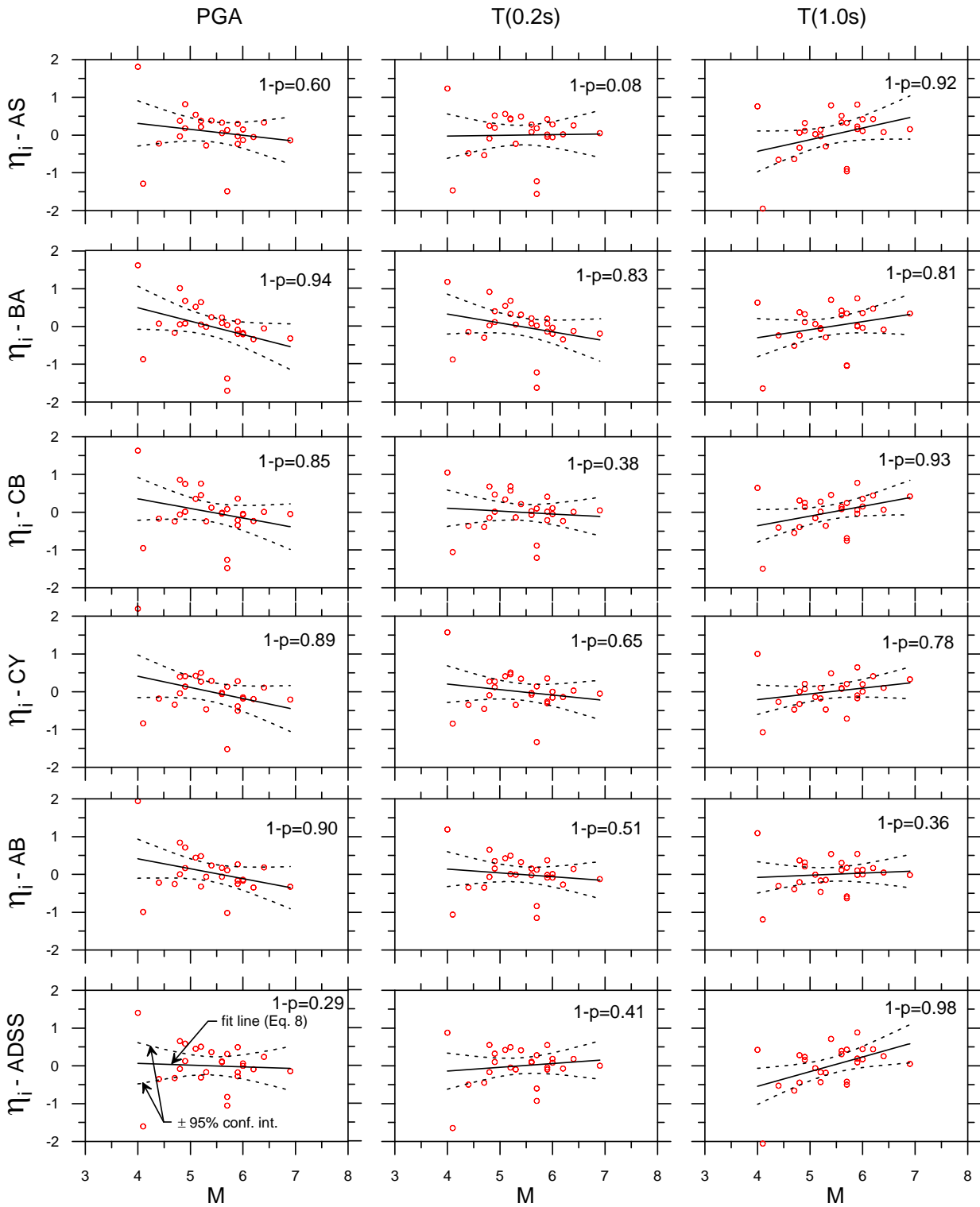
Figure 4.9. Variation of event terms for Italian data with magnitude for PGA, 0.2 s S_a, and 1.0 s S_a.

4.5.3 Distance Scaling

Distance scaling is tested by examining trends of intra-event residuals $\varepsilon_{i,j}$ as a function of distance. Recall that per Eq. 4.7, $\varepsilon_{i,j}$ is the remaining residual after mean error (c) and event term (η_i) are subtracted from the total residual. Figure 4.10 shows $\varepsilon_{i,j}$ for IMs of PGA, 0.2 s S_a, and 1.0 s S_a. To help illustrate trends, we also plot a fit line and its ±95% confidence intervals, the fit being made according to:

$$\varepsilon_{i,j} = a_R + b_R R_{i,j} + \left(\kappa_R \right)_{i,j}$$

(4.9)

Parameters a_R and b_R are regression parameters and κ_R is the residual of the fit for recording j from event i. Subscript k has been dropped in Eq. 4.9, which strictly holds for GMPEs using rupture distance. For BA, AB, and ADSS, R_{jb} replaces R as the distance parameter in Eq. 4.9. The slope parameter (b_R in this case) represents approximately the misfit of the distance scaling in the Italian dataset relative to the selected GMPEs. The columns under the heading 'R-scaling' in Table 4.3 indicate values of b_R, its ±95% confidence intervals, and the rejection confidence for a b_R=0 model (1-p) from hypothesis testing. Figure 4.10 also shows rejection confidence values (1-p) for the zero slope null hypothesis.

The results in Figure 4.10 and Table 4.3 indicate mixed findings with respect to misfits between the NGA distance scaling and the Italian data. The CY GMPE demonstrates no significant misfit across all tested periods, as evidenced by values of b_R that are smaller than their confidence intervals and low rejection confidence for the zero slope null hypothesis (< ~80 %). On the other hand, the AS, BA, and CB models produce statistically significant values of b_R ranging from approximately -0.2 to -0.3 at short periods (PGA and 0.2 s S_a). None of the NGA models show bias in the distance attenuation for long period ($T \geq 1.0$ s). These negative values of b_R at short periods indicate faster distance attenuation of the Italian data relative to these GMPEs.
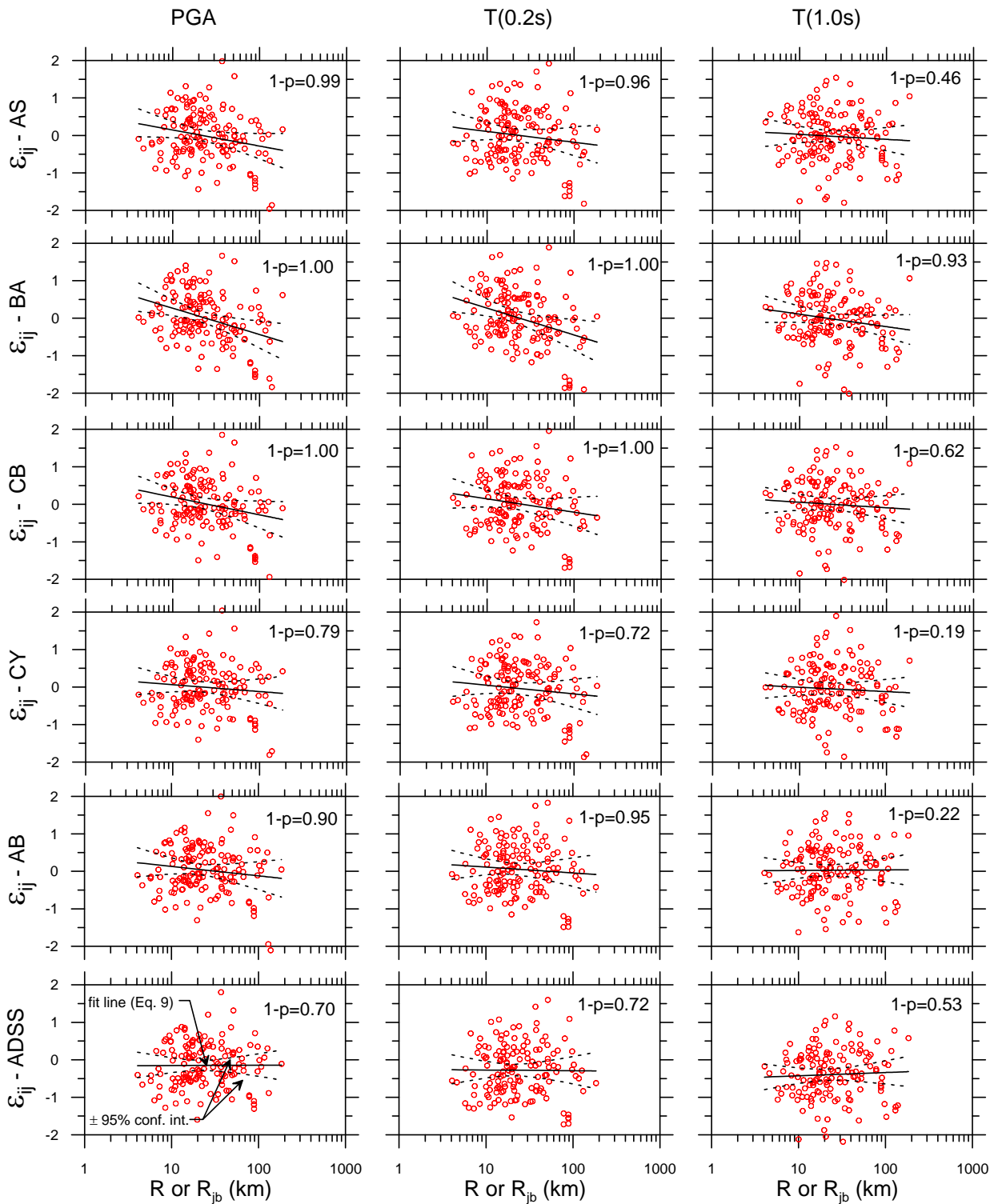
Figure 4.10. Variation of intra-event residuals for Italian data with distance for PGA, 0.2 s S_a, and 1.0 s S_a.

Note that the lack of significant b_R in the CY model is consistent with the relatively fast distance attenuation of this model in the 10-70 km range relative to the other NGA GMPEs, as shown in Figure 4.1. Moreover, the largest b_R values are observed for the BA model, which has the slowest distance attenuation, with AS and CB being intermediate cases.

The European models (ADSS and AB) also indicate mixed results. As shown in Table 4.3, slope parameter b_R is insignificant for short periods (PGA and 0.2 sec) for ADSS but significant (at the 95% level) for AB at 0.2 sec. At T=1.0 sec, AB and ADSS have insignificant values of b_R. Our interpretation of these results is that they are not suggestive of systematic bias in the European GMPEs with respect to the Italian data, which is expected because Italian data was used in the development of those GMPEs.

To further examine the distance attenuation misfit of the NGA models, we regress the Italian data against the AS, BA, and CB functional forms to re-evaluate selected coefficients controlling the distance attenuation, with the results shown in Table 4.4. These regressions are not performed for CY because of the lack of trends in the residuals described above. Recalling the distance attenuation functions given in Table 4.2, the principal coefficient that is re-evaluated is the term expressing the magnitude-independent slope of the distance attenuation (a_2 for AS, c_1 for BA, c_4 for CB). In general, the constant term must also be changed to fit the data (a_1 for AS, c_0 for CB), which is evaluated through regression simultaneously with the distance attenuation term. In the case of BA, the constant term depends on focal mechanism, taking on values of e_1-e_4. The Italian data is not sufficiently voluminous to check the scaling of ground motion with focal mechanism, so we retain the e_1-e_4 values and simply provide an additive term (e_0) that could be applied to each (e.g., the new constant term for strike slip would be e_0+e_1). Finally, we constrain the resulting modified GMPEs to match reasonably closely the original GMPEs at

71

close distance (R or $R_{jb} < 3$ km). This is done because the Italian data cannot constrain ground motions in that range, so we rely on the constraint provided by the NGA models. If the modified NGA models do not provide this match from the regression on the above coefficients, then we enforce the match through adjustment of the fictitious depth term, as shown in Table 4.4. All other coefficients in the GMPEs are fixed at the published values.

Table 4.4. Summary of modified GMPE parameters for constant and distance scaling terms and effect on trends of intra-event residuals with distance. Original coefficients are shown without primes and modified coefficients with primes (').

GMPE	Period (s)	Constant term[a]		Slope Term		h term		$\Delta\sigma$[b]	R-scaling (mod GMPE)	
		a_1	a_1'	a_2	a_2'	c_4	c_4'		$b_{R'}$	1-p
NGA AS	PGA	0.80	1.75 ± 0.34	-0.97	-1.30 ± 0.18	4.5	6.5	0.10	-0.04 ± 0.12	0.49
	0.2	1.69	2.81 ± 0.74	-0.97	-1.34 ± 0.21	4.5	6.5	0.16	-0.06 ± 0.16	0.54
	0.5	1.40	n/c	-0.85	n/c	4.5	n/c	0.17	n/a	
	1	0.92	n/c	-0.81	n/c	4.5	n/c	0.16	n/a	
	2	0.19	n/c	-0.80	n/c	4.5	n/c	0.28	n/a	
		e_0	e_0'	c_1	c_1'	h				
NGA BA	PGA	0.00	0.07 ± 0.60	-0.66	-0.72 ± 0.18	1.35	n/c	0.25	0.00 ± 0.12	0.00
	0.2	0.00	0	-0.58	-0.76 ± 0.10	1.98	n/c	0.22	0.00 ± 0.14	0.03
	0.5	0.00	0	-0.69	-0.75 ± 0.08	2.32	n/c	0.18	-0.01 ± 0.12	0.12
	1	0.00	n/c	-0.82	n/c	2.54	n/c	0.09	n/a	
	2	0.00	n/c	-0.83	n/c	2.73	n/c	0.16	n/a	
		c_0	c_0'	c_4	c_4'	c_6	c_6'			
NGA CB	PGA	-1.72	-0.18	-2.12	-2.48 ± 0.80	5.60	7.14 ± 3.40	0.19	-0.07 ± 0.12	0.73
	0.2	-0.49	0.11	-2.22	-2.46 ± 0.90	7.60	7.6	0.25	-0.12 ± 0.14	0.89
	0.5	-2.57	n/c	-2.04	n/c	4.73	n/c	0.08	n/a	
	1	-6.41	n/c	-2.00	n/c	4.00	n/c	0.18	n/a	
	2	-9.70	n/c	-2.00	n/c	4.00	n/c	0.31	n/a	
		c_1	c_1'	c_4	c_4'	Not used				
NGA CY	PGA	-1.27	n/c	-2.1	n/c			0.10	n/a	
	0.2	-0.64	n/c	-2.1	n/c			0.15	n/a	
	0.5	-1.47	n/c	-2.1	n/c			0.19	n/a	
	1	-2.25	n/c	-2.1	n/c			0.19	n/a	
	2	-3.41	n/c	-2.1	n/c			0.34	n/a	

n/c= no change in recommended coefficient

n/a= not applicable

[a] Modified for AS and CB. Constant term for BA is e_1 to e_4 (dependent on source type); e_0 is an additive term for any focal mechanism

[b] Additive intra-event standard deviation term

The modification of the above parameters was performed using mixed effects procedures with the following equations:

$$\text{AS:} \quad \ln(IM)_{i,j} = a_1' + f_R' + f_{Source} + f_{Site} + \eta_i' + \varepsilon_{i,j}' \tag{4.10}$$

$$\text{BA:} \quad \ln(IM)_{i,j} = F_R' + F_M' + F_S + \eta_i' + \varepsilon_{i,j}' \tag{4.11}$$

$$\text{CB:} \quad \ln(IM)_{i,j} = f'_{mag} + f'_{dis} + f_{flt} + f_{hng} + f_{site} + f_{sed} + \eta'_i + \varepsilon'_{i,j} \tag{4.12}$$

where the prime (′) indicates the function is modified and the lack of prime means the functions are used exactly as given in the published relations. For all models, η'_i and $\varepsilon'_{i,j}$ represent newly determined inter- and intra-event error terms. For AS, a'_1 is a newly regressed constant term; f'_R is the distance term in Table 4.2 with newly estimated coefficients a_2 and a_4 (referred to as and a'_2 and a'_4); f_{Source} indicates the magnitude function in f_1, the focal mechanism flag terms, hanging wall term (f_4), top-of-rupture term (f_6), and large distance model (f_8); f_{Site} indicates the V_{s30} term (f_5) and basin depth term (f_{10}); For BA, F'_R is the distance term in Table 4.2 with c_1 replaced with newly regressed c'_1; F'_M is identical to the BA magnitude term except for the new additive constant term noted above, which we will refer to as e'_0; F_S is the V_{s30}-dependent site term. For CB, f'_{mag} is identical the CB magnitude term except for a new constant term c'_0, f'_{dis} is the distance term in Table 4.2 with c_4 and c_6 replaced with newly regressed c'_4 and c'_6, and the remaining terms are fault type, hanging wall, site, and depth terms that are not modified.

When performing these analyses, we begin with a straightforward mixed effects regression as described above. We then check the prediction of the modified GMPE at short distance to check for compatibility with the original GMPE. As shown in Figure 4.6, the Italian data is sparse at close distance and so cannot constrain short-distance ground motions. Hence, we enforce compatibility of short-distance ground motions between the modified and original GMPE. This compatibility occurred "naturally" (i.e., as a direct outcome of the regression) for the AS model (all periods) and BA (all periods except PGA). For BA (PGA) and CB (all periods), additional adjustments were necessary to establish this compatibility. For BA (PGA), an appropriate value of e'_0 was selected and c'_1 then regressed through an iterative process. A

similar process was used for CB, although the additive distance term (denoted h in Table 4.2 but taken as c_6 in the CB model) is also regressed and constant term c_0' is manually adjusted to achieve compatibility of short-distance IMs.

In Table 4.4, values established thorough regressions are shown with ±95% confidence intervals whereas values that are fixed manually have no confidence intervals. The absolute value of the modified distance-attenuation terms (a_2' for AS, c_1' for BA, c_4' for CB) are consistently larger than the original values, consistent with the faster distance attenuation in the Italian data. This can also be seen in Figure 4.11, which shows the distance attenuation of the original and modified GMPEs for PGA, 0.2 s S_a, and 1.0 s S_a for a soft rock site conditions (V_{s30}=620 m/s) and magnitudes of M=5 and 7. Appendix A of this report (in preparation, June 2008) will provide a full list (across all of the periods in the NGA GMPEs) of the recommended new coefficients.
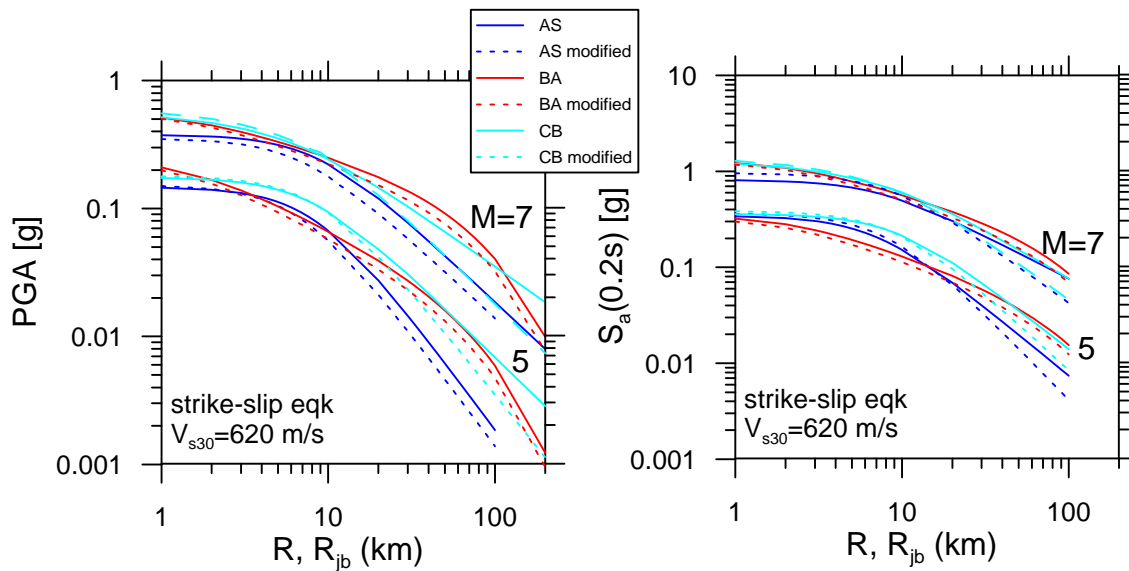
Figure 4.11. Variation of median ground motions with distance and magnitude from NGA and modified NGA relations developed in this study.

After adjusting the constant and distance terms as described above, the magnitude-dependence of event terms (η_i') and the distance dependence of intra-event residuals ($\varepsilon_{i,j}'$) are checked. As shown in Figure 4.12, the magnitude-scaling of the modified GMPEs remains appropriate (results are similar to those shown in Figure 4.9). Figure 4.13 shows that the trends in the distance-scaling observed in Figure 4.10 are removed with the revised coefficients. This is also confirmed by the hypothesis test results in Table 4.4, which show a low confidence (1-p) in rejecting the null hypothesis of zero slope.
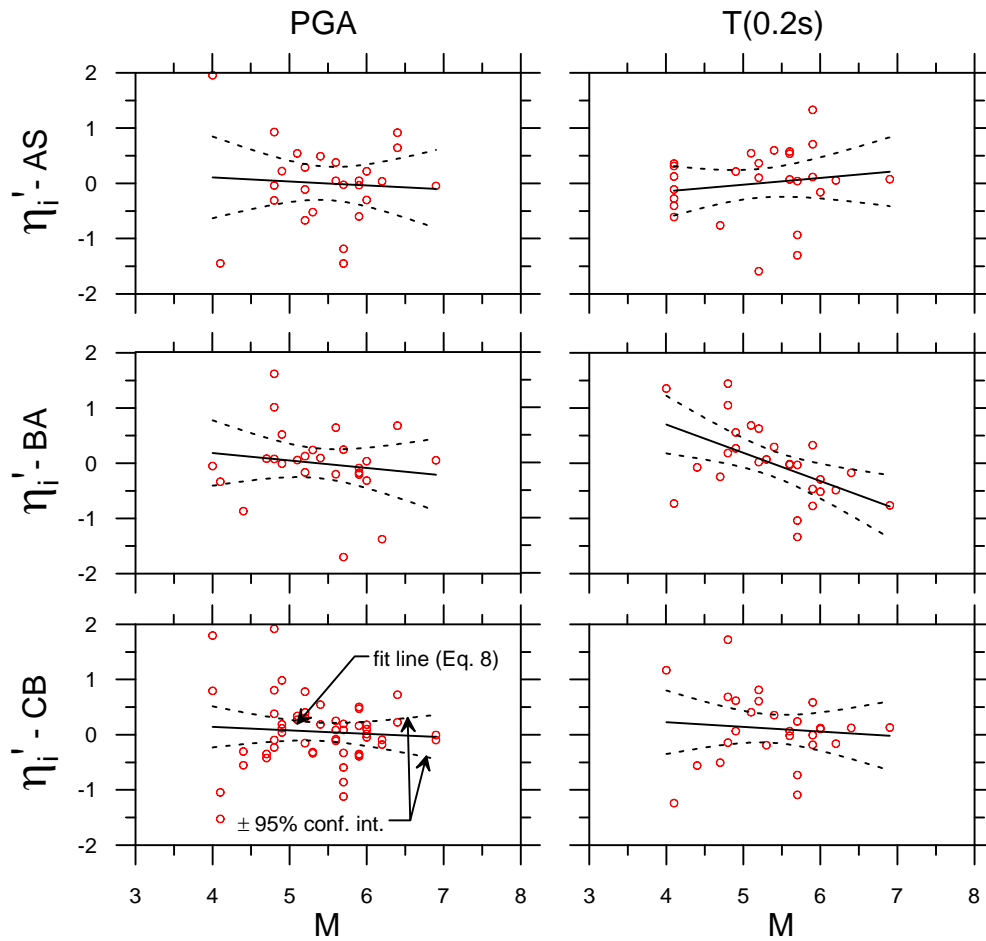
Figure 4.12. Variation of event terms for modified AS, BA, and CB GMPEs with magnitude for PGA and 0.2 s S_a. Magnitude dependence of event terms are similar to the original models presented in Figure 4.9.
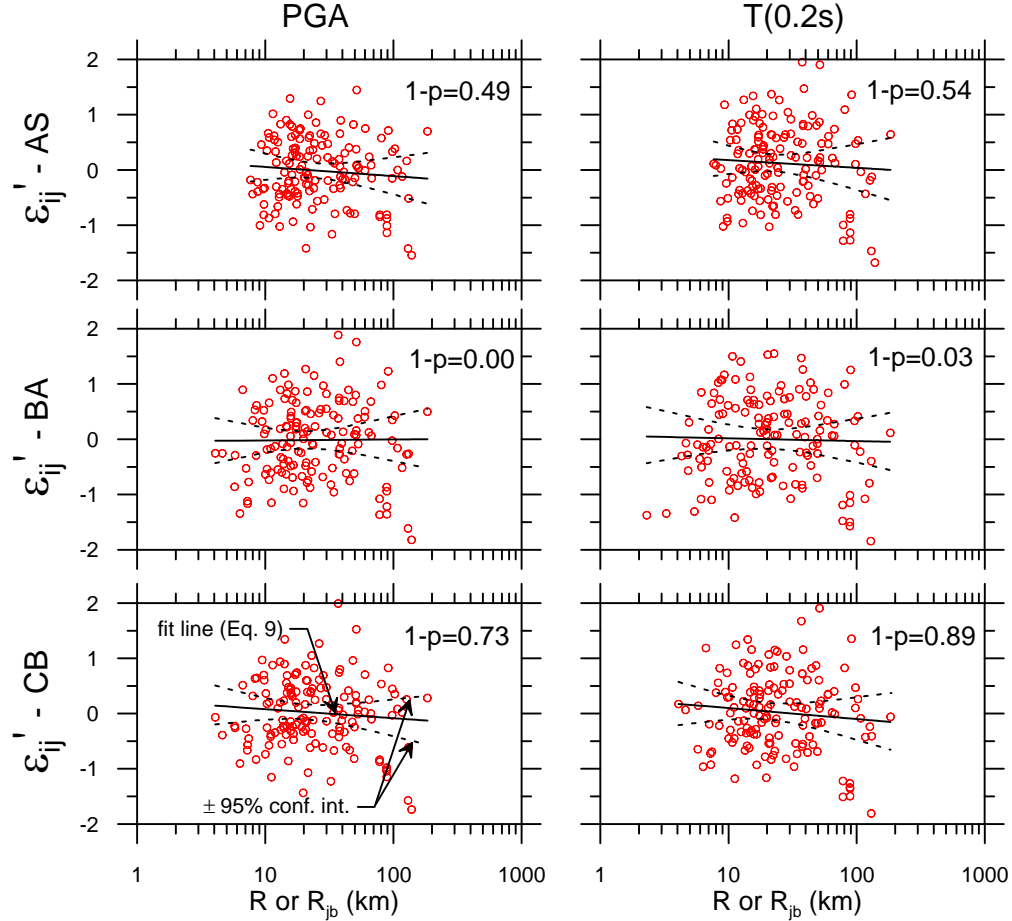
Figure 4.13. Variation of intra-event residuals for modified AS, BA, and CB GMPEs with distance for PGA and 0.2 s S_a. The statistically significant distance-dependence of residuals from the original models presented in Figure 4.10 are removed.

4.5.4 Site Effects

We evaluate the scaling of ground motions with V_{s30} in the NGA GMPEs using versions of the models without distance bias (original CY, modified versions of AS, BA, CB). This is done so that distance-bias is not mapped into the analysis of V_{s30}. We begin by examining in Figure 4.14 trends of intra-event residuals ($\varepsilon_{i,j}$ or $\varepsilon'_{i,j}$) as a function of V_{s30} for the IMs of PGA, 0.2 s S_a, and 1.0 s S_a. Trends are illustrated with a fit line:

$$\varepsilon_{i,j} = a_V + b_V \left(V_{s30} \right)_{i,j} + \left(\kappa_V \right)_{i,j} \tag{13}$$
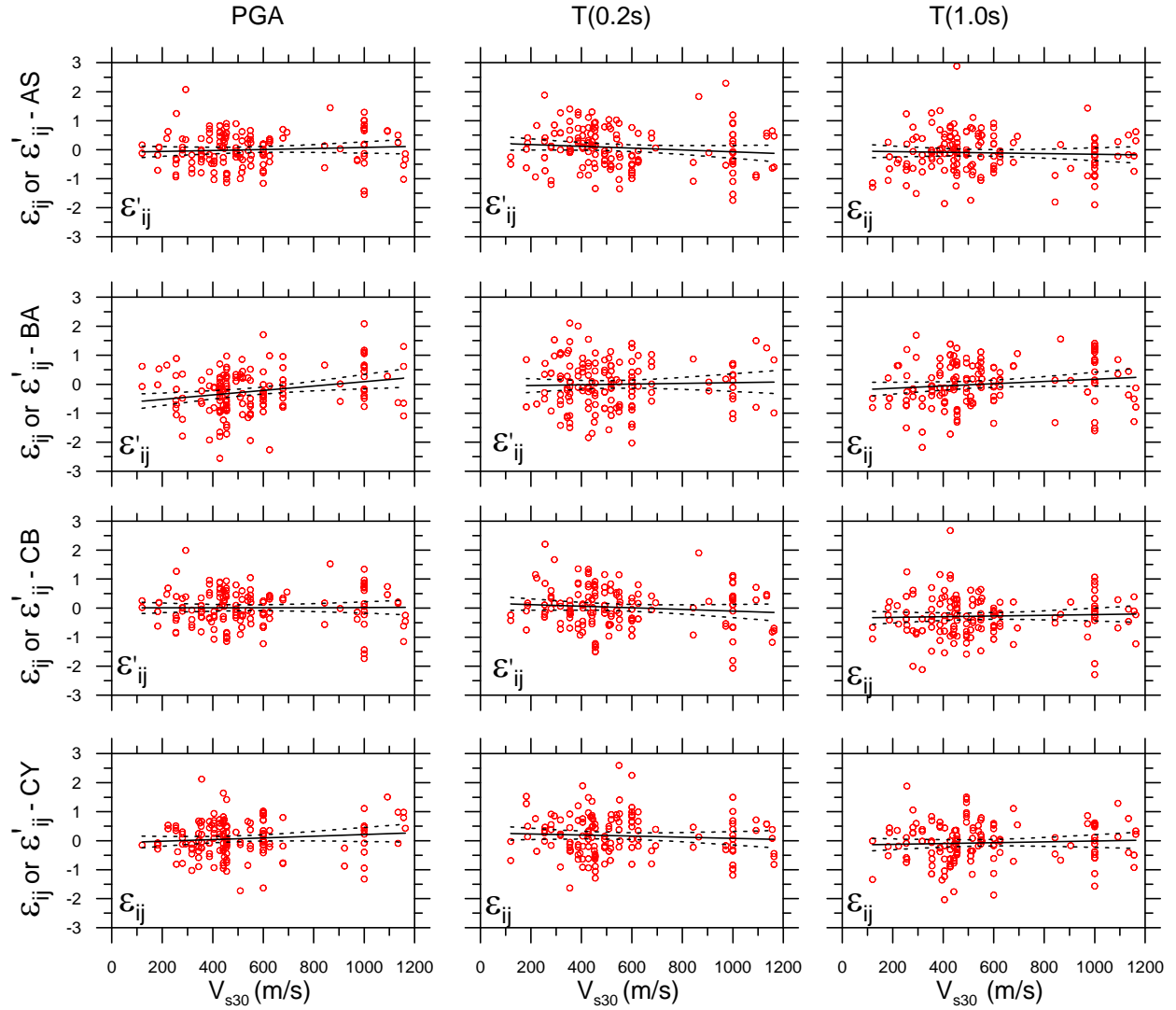
Figure 4.14. Variation of intra-event residuals with average shear wave velocity in upper 30 m (V_{s30}). Residuals shown are for original GMPE when shown without prime (ε_{ij}) and for modified GMPE when shown with prime (ε_{ij}').

Parameters a_V and b_V are regression parameters and κ_V is the residual of the fit for recording j from event i. Eq. 4.13 strictly holds for the CY GMPE; for AS, BA, and CB, $\varepsilon_{i,j}'$ replaces $\varepsilon_{i,j}$ in Eq. 4.13. Slope parameter b_V represents approximately the misfit of the V_{s30}-scaling in the Italian dataset and the selected GMPEs. Table 4.5 shows values of b_V, their ±95% confidence intervals, and the rejection confidence for a b_R=0 model (1-p) from hypothesis testing. The results in

Figure 4.14 and Table 4.5 indicate no statistically significant trends with V_{s30}. This suggests that the V_{s30}-based site terms in the NGA GMPEs may be compatible with the Italian data.

Table 4.5. Summary of modified GMPE parameters for constant and distance scaling terms and effect on trends of intra-event residuals with distance

GMPE	Period (s)	V_{s30}-scaling (mod GMPE)		Rock (V_{s30} = 800-1100 m/s)			Soil (V_{s30} = 180-300 m/s)		
		b_v	1-p	a_{PGA}	b_{PGA}	$(1-p)_b$	a_{PGA}	b_{PGA}	$(1-p)_b$
NGA AS	PGA	0.0002 ± 0.0004	0.58	-0.27	-0.14	0.61	-0.68	-0.34	0.94
	0.2	-0.0002 ± 0.0004	0.50	-0.45	-0.24	0.84	-1.34	-0.75	1.00
	1	-0.0003 ± 0.0004	0.81	-1.16	-0.14	0.58	-1.25	-0.43	0.96
NGA BA	PGA	0.0004 ± 0.0004	0.89	0.77	0.11	0.62	-0.24	-0.23	0.77
	0.2	0.0000 ± 0.0005	0.04	-0.02	-0.10	0.56	-1.18	-0.70	1.00
	1	0.0000 ± 0.0004	0.09	0.11	0.06	0.45	-0.56	-0.36	0.95
NGA CB	PGA	0.0000 ± 0.0004	0.06	-0.17	-0.15	0.71	-0.82	-0.40	0.99
	0.2	-0.0003 ± 0.0004	0.78	-0.57	-0.19	0.80	-1.41	-0.75	1.00
	1	0.0004 ± 0.0005	0.91	-0.24	-0.04	0.26	-0.91	-0.45	0.99
NGA CY	PGA	0.0000 ± 0.0004	0.06	-0.55	-0.34	0.97	-1.11	-0.54	1.00
	0.2	0.0003 ± 0.0004	0.80	-0.35	-0.40	0.99	-1.12	-0.75	1.00
	1	0.0003 ± 0.0004	0.76	-0.59	-0.23	0.91	-0.33	-0.38	0.93

Because of the well established practice of using linear site terms in European GMPEs, we seek to more deeply explore the nonlinearity of site effects implied by the Italian data. This analysis begins by re-evaluating residuals for recordings in the dataset relative to the NGA GMPEs with V_{s30} fixed at the reference value of 1100 m/s, basin depth $Z_{1.0}$ set to zero and $Z_{2.5}$ set to 0.52 km (per Eq. 4.5). Residuals evaluated in this manner are written as $\varepsilon_{i,j}^{1100}$ and are calculated as:

$$\left(\varepsilon_{i,j}^{1100}\right)_k = \ln\left(IM_{i,j}\right)_{data} - \left[\ln\left(IM_{i,j}^{1100}\right)_k + \eta_i\right]$$

(4.14)

where $\left(IM_{i,j}^{1100}\right)_k$ indicates the prediction of GMPE k for the reference rock conditions described above (using modified GMPEs where appropriate) and η_i is the event term evaluated from Eq. 4.7 for CY (which is replaced with η_i' for AS, BA, and CB, per Eq. 4.10-4.12). Those residuals

are then grouped into two categories, one corresponding to recordings made on firm rock site

conditions (V_{s30} = 800 to 1100 m/s) and the other to soft to medium soil conditions (V_{s30} = 180 to

300 m/s). Figure 4.15 shows those residuals plotted as a function of $\widehat{PGA}_{1100}$, which is the

median peak acceleration from the respective GMPEs for the magnitude, distance, and other

parameters associated with the recordings. We illustrate trends in the results with fit lines

regressed according to the following equation for data in each category:

$$\varepsilon_{i,j}^{1100} = a_{PGA} + b_{PGA}P\hat{G}A_{i,j}^{1100} + \left(\kappa_{PGA}\right)_{i,j}$$

(4.15)

where a_{PGA} and b_{PGA} are the regression parameters and $(\kappa_{PGA})_{i,j}$ is the misfit of the line to the

residual for recording j from event i. Those coefficients are given in Table 4.5.

For each of the GMPEs considered, the results show (1) for low values of $\widehat{PGA}_{1100}$, larger

residuals occur for the soil category than the rock category and (2) the slope of the $\varepsilon_{i,j}^{1100}$-

$\widehat{PGA}_{1100}$ relationship (b_{PGA}) is significantly negative, as established by hypothesis test results, for

the soil category but is generally not significantly different from zero for the rock category (CY

is an exception). These results demonstrate a nonlinear site effect for the *IM*s of PGA and S_a for

$T \leq 1.0$ s. Moreover, the difference between the $\varepsilon_{i,j}^{1100}$ fit for soil and rock represents an implied

site effect inherent to the Italian data relative to the V_{s30}=1100 m/s site condition adopted as a

reference in Eq. 4.14. That implied site effect is compared to the V_{s30}-based site term in the AS,

BA, CB, and CY GMPEs in Figure 16. Although the absolute position of the site term varies

somewhat relative the GMPE site term, the slopes are generally similar. In the few cases where

the slopes appear dis-similar (e.g., BA and CB at T=1.0 sec), the slopes of the implied site term

is not significant, as indicated by the wide confidence intervals. This suggests that the NGA site

terms are providing approximately the correct level of nonlinearity for these Italian soil sites.
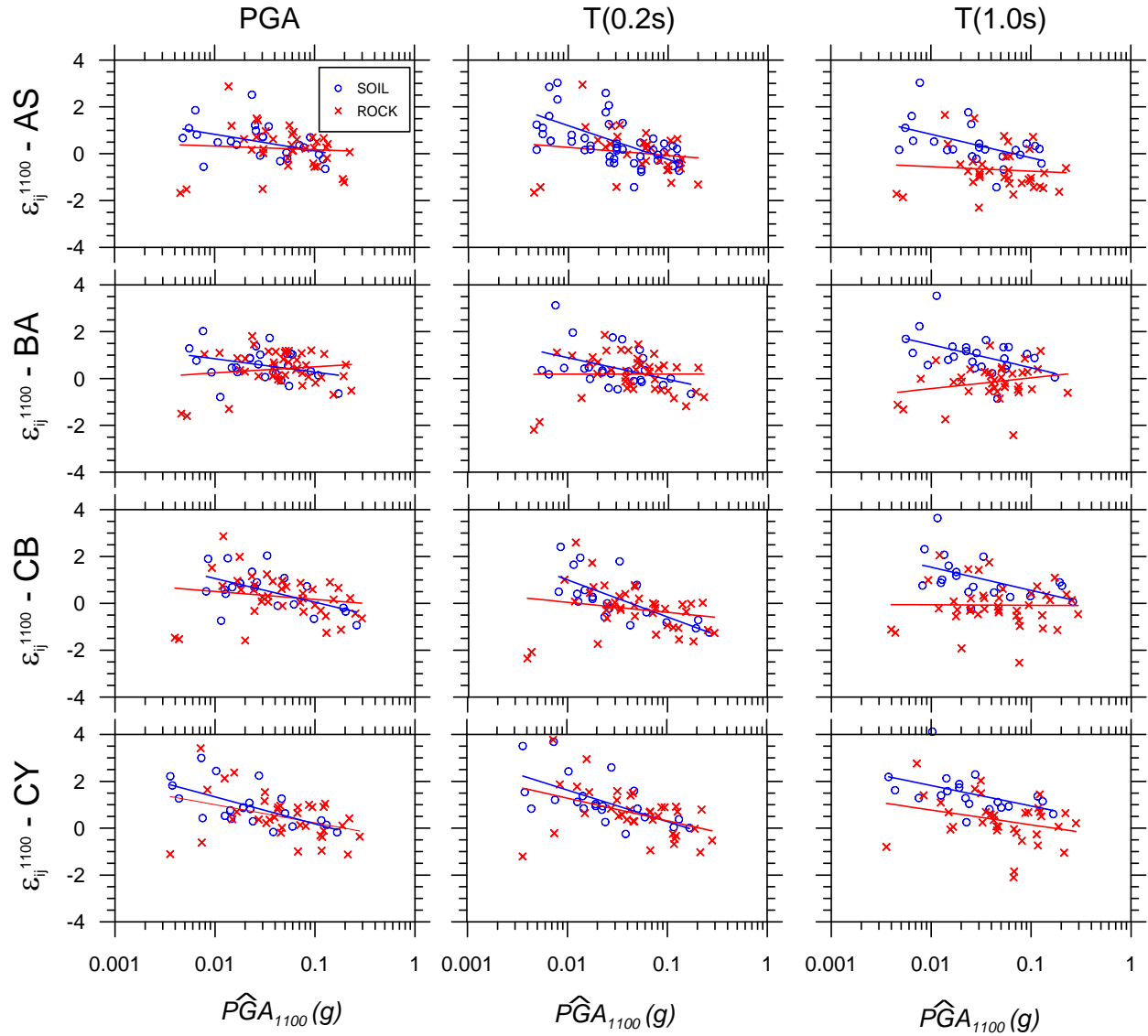
Figure 4.15. Variation of reference-site intra-event residuals (defined using Eq. 4.14) with median anticipated reference site peak acceleration, $\widehat{PGA}_{1100}$. Residuals shown are for original GMPE when shown without prime (ε_{ij}) and for modified GMPE when shown with prime (ε_{ij}').
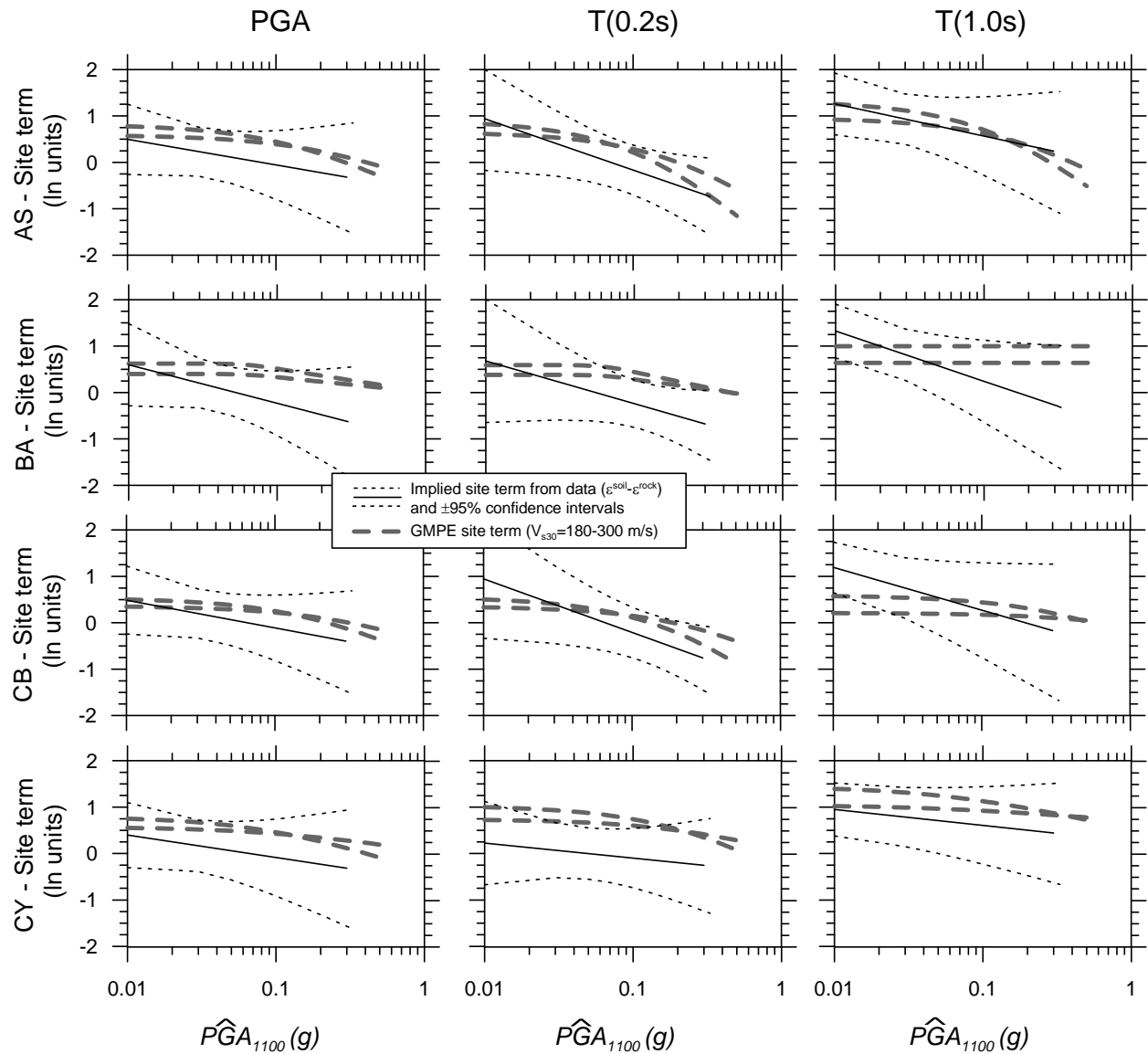
Figure 4.16. Comparison of range of GMPE site terms for V_{s30}=180-300 m/s sites to approximate site effect inferred from Italian data relative to V_{s30}=1100 m/s reference condition.

4.6   INTERPRETATION AND CONCLUSIONS

In this article, we investigate the compatibility of strong motion data in Italy with Ground Motion Prediction Equations (GMPEs) established by the Next Generation Attenuation (NGA) project for shallow crustal earthquakes in active regions. Using a mixed effects procedure, we

evaluate event terms (inter-event residuals) and intra-event residuals of the Italian data relative to the NGA GMPEs. The event terms do not show a statistically significant trend with magnitude, indicating that the magnitude-scaling in the NGA GMPEs is compatible with the Italian data. Two recent European relations are also shown to be compatible with magnitude scaling implied by the Italian data, which is not surprising given that a large fraction of the European dataset was recorded in Italy.

Distance scaling is investigated by examining trends of intra-event residuals with distance. For three of four NGA relations (AS, BA, CB), the residuals demonstrate a statistically significant trend with distance for short periods ($T \leq$ 0.2-0.5 s) that is suggestive of faster attenuation of Italian data. For the fourth NGA GMPE (CY) and the European GMPEs, the residuals do not demonstrate a trend with distance that we consider to be significant. Parameters in the NGA GMPEs that account for distance attenuation are adjusted through regression, which de-trends the residuals. The observed faster attenuation of Italian data relative to many of the NGA GMPEs is consistent with previous work that has shown faster distance attenuation of European data relative to California data (Douglas, 2004b). Moreover, as shown in Figure 4.17, our finding of faster attenuation of Italian data is consistent with higher crustal damping as represented by lower frequency-dependent Q values from the Umbria/Apennines region of Italy (which contributes about 2/3 of the Italian recordings) relative to values for central and southern California (which contributes much of the NGA data).
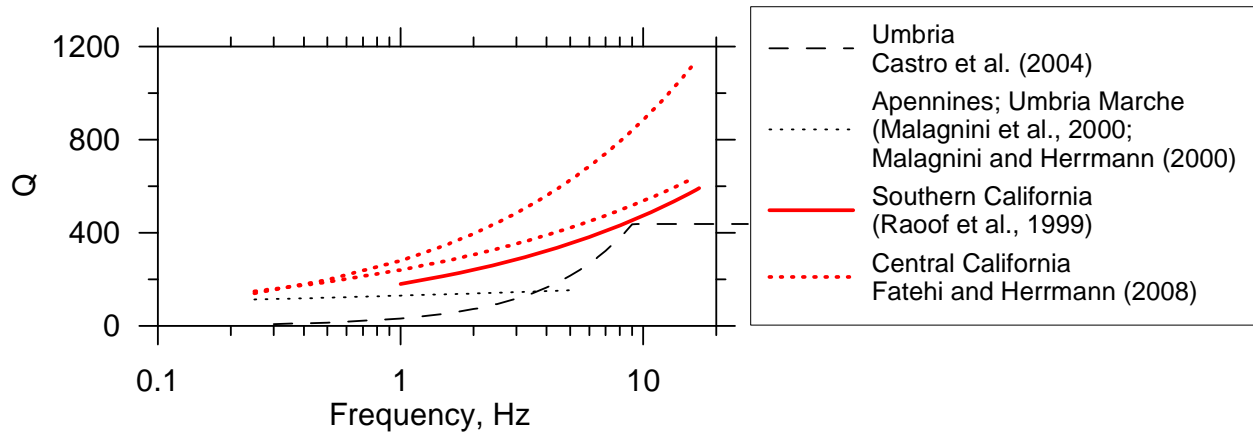
Figure 4.17. Comparison of relatively large Q values from California with smaller values from Apennines region of Italy, indicating higher crustal damping in the Italian region producing most of the recordings in the present database.

Scaling with respect to site condition is investigated by plotting intra-event residuals versus average shear wave velocity in the upper 30 m (V_{s30}). Those residuals are calculated relative to modified NGA GMPEs as applicable (AS, BA, CB). The results indicate no trend with V_{s30}, suggesting that the NGA site terms are compatible with Italian data. Since the NGA site terms are nonlinear, which is inconsistent with past European practice of using linear site terms, we also specifically investigate whether the Italian data support of the use of a nonlinear site term. This is done by examining residuals of Italian data relative to the NGA GMPEs evaluated for a reference firm rock condition. A group of data on firm rock show no trend of residuals with $P\widehat{G}A_{1100}$, which represents the median amplitude of shaking expected on firm rock. However, a group of data from soil sites show a statistically significant trend with $P\widehat{G}A_{1100}$. The differences between these trends for firm rock and soil imply a nonlinear site term having a slope relative to $P\widehat{G}A_{1100}$ that is generally consistent with the NGA site terms. Accordingly, we conclude that nonlinear site response should be incorporated into site terms for GMPEs for Europe.

Whereas many aspects of the NGA GMPEs are compatible with the Italian data, the scatter of the Italian data significantly exceeds that implied by the NGA standard deviation models. In particular, event-to-event variability as expressed by the standard deviation of event terms (τ) exceeds values from NGA by amounts ranging from 0.4 to 0.7 in natural log units. Intra-event standard deviation (σ) is also larger in Italian data than NGA, but by amounts on the order of 0.1 to 0.25. The large τ terms we interpret to be a by-product of the poorly sampled dataset, whereas the larger σ terms we consider to be more reliable.

In summary, we recommend that NGA GMPEs for median ground motions be utilized for hazard analysis in Italy. The CY median NGA relation can be used in its current form except for the increased intra-event error term shown in Table 4.4. The AS, BA, and CB NGA relations can also be used, but we recommend modification of (generally) two or three parameters in the evaluation of median ground motions – one being a constant term, the second representing attenuation from geometric spreading and anelastic attenuation, and the third representing the source depth term. Those parameters and the recommended new coefficients are given in Table 4.4. The associated functional forms for distance attenuation are given in Table 4.2. With respect to standard deviation terms, we recommend the use of the τ terms (representing inter-event variability) in the original NGA equations. We recommend σ (representing intra-event variability) be taken as the sum of the NGA values and the $\Delta\sigma$ values given in Table 4.4.

Finally, while this work has focused on Italy, we believe ground motions know nothing of political boundaries and that the results presented here are likely applicable elsewhere in Europe. We anticipate that future work will formally evaluate data from other regions in a manner similar to what is described here.

5 Conclusions

In this report, we describe work directed towards the enhancement of data resources for strong motion studies in Italy and utilize those resources to critically evaluate and modify state of the art ground motion prediction equations for application in Italy.

The ground motion database developed here includes only about half of the available recordings due to various issues such as s-triggers that can bias ground motion intensity measures evaluated from the data. We document these biases, which affect principally long-period measures of ground motion as well as duration-related parameters.

A databank of site conditions at Italian ground motion recording stations is compiled that includes geologic characteristics and seismic velocities at 104 sites with strong motion recordings. Geologic characterization is derived principally from local geologic investigations that include detailed mapping and cross sections. For sites lacking such detailed study, geologic characterization is from 1:100,000 scale maps. Seismic velocities are extracted from the literature for 22 sites with on-site measurements and 14 additional sites with local measurements on similar geology. Data sources utilized include post earthquake site investigations (Friuli and Irpinia events), microzonation studies, and miscellaneous investigations performed by researchers or consulting engineers/geologists. Additional seismic velocities are measured using a spectral analysis of surface wave (SASW) technique for 17 sites that recorded the 1997-1998 Umbria-Marche earthquake sequence. The compiled velocity measurements provide data for 53

of the 104 sites. For the remaining sites, we estimate average seismic velocities in the upper 30 m (V_{s30}) using a hybrid approach as follows (1) for sites on Quaternary alluvium and Quaternary-Tertiary sediments, we assign V_{s30}-values based on regional correlations for California validated against the available Italian data; and (2) for sites on Tertiary Limestone, conglomerate, and Mesozoic-age rocks, we assign V_{s30}-values based on average velocities from similar units elsewhere in Italy.

A source databank is compiled from the results of recent projects by INGV. Moment tensor solutions derived from instrumental recordings are available for most events, providing estimates of source location, seismic moment, and moment magnitude. For earthquakes with M_w > ~ 5.5, finite source parameters include fault strike, dip, rake, along-strike rupture length, down-dip width, and depth to top of rupture.

Using the compiled strong motion database and site and source databanks, we investigate the compatibility of strong motion data in Italy with Ground Motion Prediction Equations (GMPEs) established by the Next Generation Attenuation (NGA) project for shallow crustal earthquakes in active regions. Using a mixed effects procedure, we evaluate event terms (inter-event residuals) and intra-event residuals of the Italian data relative to the NGA GMPEs. The event terms do not show a statistically significant trend with magnitude, indicating that the magnitude-scaling in the NGA GMPEs is compatible with the Italian data.

Distance scaling is investigated by examining trends of intra-event residuals with distance. For three of four NGA relations (AS, BA, CB), the residuals demonstrate a statistically significant trend with distance for short periods ($T \leq 0.2\text{-}0.5$ s) that is suggestive of faster attenuation of Italian data. For the fourth NGA GMPE (CY), the residuals do not demonstrate a

trend with distance that we consider to be significant. Parameters in the NGA GMPEs that account for distance attenuation are adjusted through regression, which de-trends the residuals.

Scaling with respect to site condition is investigated by plotting intra-event residuals versus average shear wave velocity in the upper 30 m (V_{s30}). Those residuals are calculated relative to modified NGA GMPEs as applicable (AS, BA, CB). The results indicate no trend with V_{s30}, suggesting that the NGA site terms are compatible with Italian data. Since the NGA site terms are nonlinear, which is inconsistent with past European practice of using linear site terms, we also specifically investigate whether the Italian data support of the use of a nonlinear site term. This is done by examining residuals of Italian data relative to the NGA GMPEs evaluated for a reference firm rock condition. A group of data on firm rock show no trend of residuals with $P\widehat{GA}_{1100}$, which represents the median amplitude of shaking expected on firm rock. However, a group of data from soil sites show a statistically significant trend with $P\widehat{GA}_{1100}$. The differences between these trends for firm rock and soil imply a nonlinear site term having a slope relative to $P\widehat{GA}_{1100}$ that is generally consistent with the NGA site terms. Accordingly, we conclude that nonlinear site response should be incorporated into site terms for GMPEs for Europe.

Whereas many aspects of the NGA GMPEs are compatible with the Italian data, the scatter of the Italian data significantly exceeds that implied by the NGA standard deviation models. In particular, event-to-event variability as expressed by the standard deviation of event terms (τ) exceeds values from NGA by amounts ranging from 0.4 to 0.7 in natural log units. Intra-event standard deviation (σ) is also larger in Italian data than NGA, but by amounts on the order of 0.1 to 0.25. The large τ terms we interpret to be a by-product of the poorly sampled dataset, whereas the larger σ terms we consider to be more reliable.

In summary, we recommend that NGA GMPEs for median ground motions be utilized for hazard analysis in Italy. The CY median NGA relation can be used in its current form except for the increased intra-event error term. The AS, BA, and CB NGA relations can also be used, but we recommend modification of (generally) two or three parameters in the evaluation of median ground motions – one being a constant term, the second representing attenuation from geometric spreading and anelastic attenuation, and the third representing the source depth term. Those parameters and the recommended new coefficients are given in Chapter 4. With respect to standard deviation terms, we recommend the use of the τ terms (representing inter-event variability) in the original NGA equations. We recommend σ (representing intra-event variability) be taken as the sum of the NGA values and the $\Delta\sigma$ values given in Chapter 4.

References

Abrahamson, N.A. and Silva, W.J. (2008). "Summary of the Abrahamson and Silva NGA ground motion relations," *Earthquake Spectra*, 24 (S1). accepted for publication.

Abrahamson, N.A., Birkhauser, P., Koller, M., Mayer-Rosa, D., Smit, P.M., Sprecher, C., Tinic, S. and Graf, R. (2002). "PEGASOS- A comprehensive probabilistic seismic hazard assessment for nuclear power plants in Switzerland," Proceedings of the Twelfth European Conference on Earthquake Engineering, Paper no 633, London.

A.G.I.: Associazione Geotecnica Italiana (1991). "Caratteristiche geotecniche dell'argilla del Fucino". *Rivista Italiana di Geotecnica*, 3-4, 145-160.

Aki, K. and Richards, P.G. (1980). *Quantitative seismology*, Vol. 1, W.H. Freeman, San Francisco, CA.

Akkar, S. and Bommer, J.J. (2007a). "Prediction of elastic displacement response spectra in Europe and the Middle East," *Earthq Eng Struct Dyn*, 36, 1275-1301.

Akkar, S. and Bommer, J.J. (2007b). "Empirical prediction equations for peak ground velocity derived from strong motion records from Europe and the Middle East," *Bull Seism Soc Am,* 97(2), 511-530.

Ambraseys, N.N., Simpson, K.A. and Bommer, J.J. (1996). "Prediction of horizontal response spectra in Europe," *Earth. Eng. Struct. Dyn.* 25, 371–400.

Ambraseys, N.N., Douglas, J., Sigbjörnsson, R., Berge-Thierry, C., Suhadolc, P., Costa, G., and Smit, P.M. (2004). "Dissemination of European strong-motion data, Volume 2," *Proc. 13th World Conference on Earthquake Engineering*, Vancouver, B.C., Canada, Paper 32 (electronic file).

Ambraseys, N.N., Douglas, J., Smit, P. and Sarma, S.K. (2005). "Equations for the estimation of strong ground motions from shallow crustal earthquakes using data from Europe and the Middle East: Horizontal peak ground acceleration and spectral acceleration," *Bull. Earthquake Eng.*, 3(1), 1–53.

Baldovini, G., Lavorato, A., Prati, G. (1993). "La galleria ferroviaria dei Peloritani: problemi di progetto."*AGI - XVIII Convegno Nazionale di Geotecnica*, Rimini 11-13 Maggio.

Basili, R., Valensise, G., Vannoli, P., Burrato, P., Fracassi, U., Mariano, S., and Tiberti, M. M. (2007). "The database of individual seismogenic sources (DISS), version 3: summarizing 20 years of research on Italy's earthquake geology," *Tectonophysics*, in press.

Bommer, J.J. (2006). "Empirical estimation of ground motion: advances and issues," *Proc. 3rd Int. Sym. on the Effects of Surface Geology on Seismic Motion*, Grenoble, France, Paper No. KN8 (electronic file).

Boore, D.M. and Bommer, J.J. (2005). "Processing of strong motion accelerograms: needs, options, and consequences," *Soil Dynamics and Earthquake Engrg.*, 25, 93-115.

Boore, D.M. and Atkinson, G.M. (2008). "Ground motion prediction equations for the average horizontal component of PGA, PGV, and 5%-damped PSA at spectral periods between 0.01 and 10.0 s," *Earthquake Spectra*, 24 (S1). accepted for publication.

Borcherdt, R.D. (1994). "Estimates of site-dependent response spectra for design (methodology and justification)," *Earthquake Spectra*, 10(4), 617-653.

Borcherdt, R.D. (2002). "Empirical evidence for acceleration-dependent amplification factors," *Bull. Seism. Soc. Am.*, 92, 761-782.

Borcherdt, R. D. and Glassmoyer, G. (1994). "Influences of local geology on strong and weak ground motions recorded in the San Francisco Bay region and their implications for site-specific building-code provisions" The Loma Prieta, California Earthquake of October 17, 1989--Strong Ground Motion, U. S. Geological Survey Professional Paper 1551-A, A77-A108

Brambati, A., Faccioli E., Carulli G.B., Cucchi F., Onori R., Stefanini S., Ulcigrai F. (1979). "Studio di Microzonizzazione delle'area di Tarcento," Regione autonoma Friuli-Venezia Giulia – Università degli studi di Trieste.

Budnitz, R.J., Apostolakis, G., Boore, D.M., Cluff, L.S., Coppersmith, K.J., Cornell, C.A. and Morris, P.A. (1997). *Recommendations for probabilistic seismic hazard analysis: guidance on uncertainty and use of experts*. Nuclear Regulatory Commission, NUREG/CR–6372.

Bullen, K.E. (1965). *An introduction to the theory of seismology*, Cambridge Univ. Press, Cambridge, U.K.

Campbell, K. W., and Bozorgnia, Y. (2007). "Campbell-Bozorgnia NGA ground motion relations for the geometric mean horizontal component of peak and spectral ground motion parameters," *PEER Report No. 2007/02*, Pacific Earthquake Engineering Research Center, University of California, Berkeley, 238 pp.

Campbell, K.W. and Bozorgnia, Y. (2008). "NGA ground motion model for the geometric mean horizontal component of PGA, PGV, PGD, and 5%-damped linear elastic response spectra for periods ranging from 0.01 to 10 s," *Earthquake Spectra*, 24 (S1). accepted for publication.

Castro, R.R., F. Pacor, D. Bindi, G. Franceschina, and L. Luzi (2004). "Site response of strong motion stations in the umbria, central Italy, region," *Bull. Seism. Soc. Am.*, 94 (2), 576–590.

Chiou, B.S.-J. and Youngs, R.R. (2008). "Chiou and Youngs PEER-NGA empirical ground motion model for the average horizontal component of peak acceleration and pseudo-spectral acceleration for spectral periods of 0.01 to 10 seconds," *Earthquake Spectra*, 24 (S1). accepted for publication.

Chiou, B.S.-J., Darragh, R., Dregor, D., and Silva, W.J. (2008). "NGA project strong-motion database," *Earthquake Spectra*, 24 (S1). accepted for publication.

Choi, Y. and Stewart, J.P. (2005). "Nonlinear site amplification as function of 30 m shear wave velocity," *Earthquake Spectra*, 21 (1), 1-30.

Cotton, F., Scherbaum, F., Bommer, J.J., and Bungum, H. (2006). "Criteria for selecting and adjusting ground-motion models for specific target regions: Application to central Europe and rock sites," *Journal of Seismology*, 10, 137-156.

Darragh, R., Silva, W.J., and Gregor, N. (2004). "Strong motion record processing for the PEER center," Proceedings of Workshop on Strong Motion Record Processing, Richmond, CA, May 26-27, 2004 (http://www.cosmos-eq.org/recordProcessingPapers.html).

Dipartimento della Protezione Civile - Ufficio Servizio Sismico Nazionale - Servizio Sistemi di Monitoraggio, DPC-USSN (2004). "The Strong Motion Records of Molise Sequence (October 2002 - December 2003)" CD-ROM, Rome.

Dobry, R., Borcherdt, R.D., Crouse, C.B., Idriss, I.M., Joyner, W.B., Martin, G.R., Power, M.S., Rinne, E.E., and Seed, R.B. (2000). "New site coefficients and site classification system used in recent building seismic code provisions," *Earthquake Spectra*, 16 (1), 41-67.

Douglas, J. (2003a). "Earthquake ground motion estimation using strong-motion records: a review of equations for the estimation of peak ground acceleration and response spectra ordinates," *Earth Science Review*, 61, 43–104.

Douglas, J. (2003b). "What is a poor quality strong-motion record?" *Bull. Earthquake Engineering*, 1, 141-156.

Douglas, J. (2004a). "An investigation of analysis of variance as a tool for exploring regional differences in strong ground motions," *Journal of Seismology*, 8, 485-496.

Douglas, J. (2004b). "Use of analysis of variance for the investigation of regional dependence of strong ground motion," *Proc. 13th World Conf. Eq. Engrg.*, Vancouver, Canada, Paper 29 (electronic file).

Douglas, J. (2006). "Errata of and additions to 'Ground motion estimation equations 1964-2003'," *Intermediary Report BRGM/RP-54603-FR*, Bureau de recherches géologiques et minières.

Ekström, G., Dziewonski, A.M., Maternovskaya, N.N., Nettles, M. (2005). "Global seismicity of 2003: centroid-moment tensor solutions for 1087 earthquakes." *Physics of the Earth and Planetary Interiors*, 148, 327–351.

Faccioli, E. (1992). "Selected aspects of the characterization of seismic site effects, including some recent European contributions," *Proc. International Symposium on The Effects of Surface Geology on Seismic Motion (ESG1992),* Odaware, Japan, Vol. 1, 65-96.

Fatehi, A. and R.B. Herrmann (2008). "High-frequency ground-motion scaling in the Pacific northwest and in northern and central California," *Bull. Seism. Soc. Am.*, 98 (2), 709–721.

Fontanive, A., Gorelli, V., Zonetti, L. (1985). "Raccolta di informazioni sulle postazioni accelerometriche del Friuli," Commissione ENEA-ENEL per lo studio dei problemi sismici connessi con la realizzazione di impianti nucleari, Rome, Italy.

Frenna, S.M. and Maugeri M. (1993). "Fenomeni di amplificazione sismica sulla piana di Catania durante il terremoto del 13\12\1990". *Atti del VI convegno nazionale L'ingegneria sismica in Italia. 13-15 ott. 1993.* Perugia*,* Italy.

Goulet, C.A., Watson-Lamprey, J., Baker, J., Luco, N., and Yang, T.Y. (2008). "Assessment of ground motion selection and modification (GMSM) methods for non-linear dynamic analyses of structures," in *Geotechnical Earthquake Engineering and Soil Dynamics-IV*, ASCE Geotechnical Special Publication No. 181, D. Zheng, M. Manzari, and D. Hiltunen (eds.) (electronic file).

Hayashi, K. and Kayen, R. (2003) "Comparative test of three surface wave methods at Williams Street Park in San Jose, USA," *2003 Joint Meeting of Japan Earth and Planetary Science*, University of Tokyo, Tokyo, Japan 2003, Paper S051-009.

Heisey, J.S., Stokoe, II K.H., Hudson, W.R., and Meyer, A.H. (1982). "Determination of in situ shear wave velocities from spectral analysis of surface waves," *Research Report 256-2*, Center for Transportation Research, University of Texas at Austin, December, 277 pp.

Idriss, I.M. (2008). "An NGA empirical model for estimating the horizontal spectral values generated by shallow crustal earthquakes," *Earthquake Spectra*, 24 (S1). accepted for publication.

Incorporated Research Institutions for Seismology, IRIS (2007). *IRIS Data Management Center*, http://www.iris.edu/about/DMC/, last accessed November 2007.

Isernia Administration (1998). "Indagini geognostiche prospezioni geofisiche e prove di laboratorio finalizzate all'adozione della variante generale del piano regolatore comunale".

Istituto Nazionale di Geofisica e Vulcanologia, INGV (2007a). *Project S6: Database of Italian accelerometric data from 1972 to 2004*, web site url: http://esse6.mi.ingv.it, last accessed November 2007.

Istituto Nazionale di Geofisica e Vulcanologia, INGV (2007b). *Database of Individual Seismogenic Sources*, web site url: http://legacy.ingv.it/DISS, last accessed November 2007.

Malagnini, L., R. B. Herrmann, and M. Di Bona (2000). "Ground motion scaling in the Apennines (Italy)," *Bull. Seism. Soc. Am.* 90 (4)**,** 1062–1081.

Joyner, W.B., Warrick, R.E., and Fumal, T.E. (1981). "The effect of Quaternary alluvium on strong ground motion in the Coyote Lake, California earthquake of 1979," *Bull. Seism. Soc. Am.*, 71, 1333-1349.

Kayen, R., D. Minasian, R.E.S. Moss, B.D. Collins, N. Sitar, D. Dreger and C. Carver (2004). "Geotechnical reconnaissance of the 2002 Denali Fault, Alaska," *Earthquake Spectra*, 20 (3), 639-667.

Kayen, R., Carkin, B., Minasian, D., and Tinsley, J. (2005). "Shear wave velocity of the ground near southern California TRINET sites using the spectral analysis of surface waves method (SASW) and parallel-arrayed harmonic-wave sources". *Open-File Report 2005-1169*, U.S. Geological Survey, http://pubs.usgs.gov/of/2005/1365/2005.

Malagnini, L. and R. B. Herrmann (2000). "Ground-motion scaling in the region of the 1997 Umbria–Marche earthquake (Italy)," *Bull. Seism. Soc. Am.* 90 (4), 1041–1051.

Malagnini, L. and Montaldo, V. (2004) "Relazioni di attenuazione del moto del suolo App.3 al Rapporto Conclusivo", *Redazione della mappa di pericolosità sismica (Ordinanza PCM 20.03.03, n.3274),* Istituto Nazionale di Geofisica e Vulcanologia.

Nazarian, S. and Stokoe, K. (1984). "In situ shear wave velocities from spectral analysis of surface waves, *Proc. Eighth World Conference on Earthquake Engineering,* San Francisco, California, Vol. III, pp. 31-39.

Norme Tecniche per le Costruzioni, NTC (Draft dated July 27, 2007)

Ordinanza del Presidente del Consiglio dei Ministri, OPCM "Primi elementi in materia di criteri generali per la classificazione sismica del territorio nazionale e di normative tecniche per le costruzioni in zona sismica." 20 marzo 2003, Ordinance No. 3274.

Paciello A., Properzi C., Rinaldis D., Stedile L. (1997) "Database delle registrazioni accelerometriche". ENEA-Servizio Sismico Nazionale.

Palazzo, S. (1991a). "Progetto Irpinia - Elaborazione dei risultati delle indagini geotecniche in sito ed in laboratorio eseguite nelle postazioni accelerometriche di Bagnoli Irpino, Calitri, Auletta, Bisaccia, Bovino, Brienza, Rionero in Vulture, Sturno, Benevento e Mercato S.Severino," Ente Nazionale Energia Elettrica (ENEL), Direzione delle Costruzioni, Rome, Italy.

Palazzo, S. (1991b). "Progetto Irpinia - Elaborazione dei risultati delle indagini geotecniche in sito ed in laboratorio eseguite nelle postazioni accelerometriche di Sannicandro, Tricarico, Vieste, Areinzo, S.Severo e Garigliano," Ente Nazionale Energia Elettrica (ENEL), Direzione delle Costruzioni, Rome, Italy.

Pondrelli, S., Morelli, A., Ekström, G., Mazza, S., Boschi, E., Dziewonski, A.M. (2002). "European-Mediterranean regional centroid-moment tensors: 1997-2000," *Physics of the Earth and Planetary Interiors*, 130, 71-101.

Pondrelli, S., Salimbeni, S., Ekström, G., Morelli, A., Gasperini, P., and Vannucci, G. (2006). "The Italian CMT dataset from 1977 to the present," *Physics of the Earth and Planetary Interiors*, 159, 286-303.

Raoof, M., R. B. Herrmann, and L. Malagnini (1999). "Attenuation and excitation of three-component ground motion in Southern California," *Bull. Seism. Soc. Am.* 89 (4), 888–902.

Rinaldis, D. (2004). "Acquisition and processing of analogue and digital accelerometric records: ENEA methodology and experience from Italian earthquake". *Proc. Workshop on strong-motion record processing*. Consortium of Organizations of Strong-Motion Observation Systems (COSMOS)*,* Richmond, CA.

S.S.N-Monitoring System Group (2002). "The Strong Motion Records of Umbria-Marche Sequence, (September 1997 - June 1998)," CD-ROM, Rome.

Sabetta, F. and Pugliese, A. (1996). "Estimation of response spectra and simulation of nonstationary earthquake ground motion," *Bull. Seism. Soc. Am.*, 86 (2), 337-352.

Scherbaum, F., Cotton, F., and Smit, P. (2004). "On the use of response spectral reference data for the selection and ranking of ground motion models for seismic hazard analysis in regions of moderate seismicity: the case of rock motion," *Bull. Seism. Soc. Am.*, 94 (6), 2164-2185.

Stafford, P.J., Strasser, F.O., and Bommer, J.J. (2008: in press). "An evaluation of the applicability of the NGA models to ground motion prediction in the Euro-Mediterranean region," *Bulletin of Earthquake Engineering*, 6.

Stewart, J.P. (2000). "Variations between foundation-level and free-field earthquake ground motions," *Earthquake Spectra*, 16 (2), 511-532.

Wells, D. L., and Coppersmith, K. J. (1994). "New empirical relationships among magnitude, rupture length, rupture width, rupture area, and surface displacement," *Bull. Seism. Soc. Am.*, 84, 974-1002.

Wills, C.J. and Clahan, K.B. (2006). "Developing a map of geologically defined site-condition categories for California," *Bull. Seism. Soc. Am.*, 96(4a), 1483-1501.

Working group (1981) . "Elementi di Microzonazione sismica dell'area Anconetana." *Consiglio Nazionale delle Ricerce-Progetto Finalizzato Geodinamica,* pub. n.430

Working Group (2004). "Redazione della mappa di pericolosità sismica (Ordinanza PCM 20.03.03, n.3274) All.to 1 Rapporto Conclusivo" *Istituto Nazionale di Geofisica e Vulcanologia*.

Working Group (2007). Project S6-Italian strong motion data base (1972-2004), DPC-INGV Seismological Projects